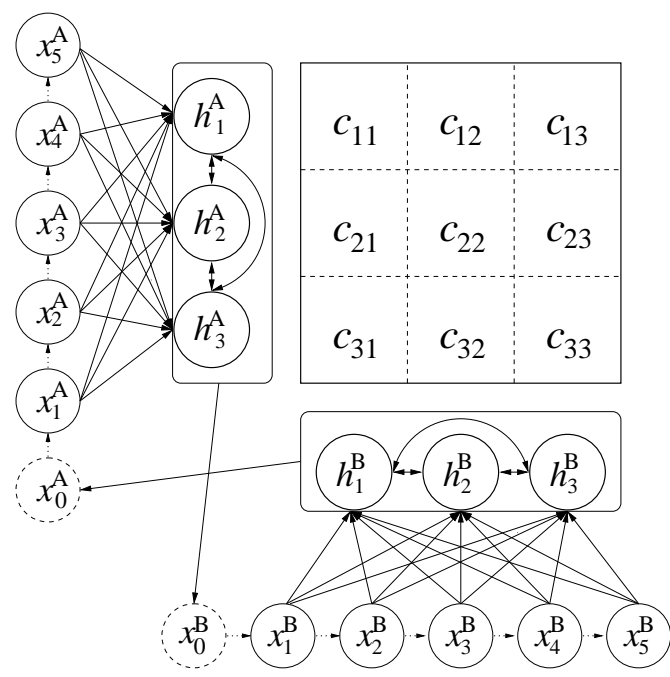


Neural Networks, Game Theory and Time Series Generation



Richard Metzler

Institut für Theoretische Physik und Astrophysik
Bayerische Julius-Maximilians-Universität
Würzburg

2002

Neural Networks, Game Theory and Time Series Generation

Dissertation zur Erlangung des
naturwissenschaftlichen Doktorgrades
der Bayerischen Julius-Maximilians-Universität
Würzburg

vorgelegt von
Richard Metzler
aus Würzburg

Institut für Theoretische Physik und Astrophysik
Bayerische Julius-Maximilians-Universität
Würzburg

September 2002

Eingereicht am 3.9.2002
bei der Fakultät für Physik und Astronomie

Beurteilung der Dissertation:

1. Gutachter: Prof. Dr. W. Kinzel
2. Gutachter: Prof. Dr. G. Reents

Mündliche Prüfung:

1. Prüfer: Prof. Dr. W. Kinzel
2. Prüfer: Prof. Dr. A. Haase

Tag der mündlichen Prüfung: 1.10.2002

Zusammenfassung

Das kollektive Verhalten von Systemen aus vielen wechselwirkenden Komponenten ist traditionell ein Hauptthema der statistischen Physik. In den letzten Jahren sind verstärkt auch ökonomische Systeme wie z.B. Aktienmärkte untersucht worden, deren "Komponenten" (Menschen und Firmen) durch Agenten mit vereinfachten Entscheidungsregeln (beispielsweise durch neuronale Netze) modelliert wurden. Von besonderem Interesse sind dabei auch die Zeitreihen, die durch solche Systeme erzeugt werden, und die Fähigkeit der Agenten, aus den Zeitreihen Informationen zu beziehen.

Kapitel 2 dieser Arbeit widmet sich dem Konzept der antivorhersagbaren Zeitreihen: zu jedem Vorhersagealgorithmus gibt es eine Zeitreihe, für die er völlig versagt. Die Eigenschaften dieser Zeitreihen werden für drei spezielle Algorithmen untersucht und mit denen von gut vorhersagbaren Zeitreihen verglichen. Aspekte von Interesse sind zum Beispiel die Länge von Zyklen bei diskreten Zeitreihen, chaotisches Verhalten bei kontinuierlichen Zeitreihen und die Unterdrückung von Korrelationen, auf die der Algorithmus empfindlich ist, bei antivorhersagbaren Zeitreihen.

Der erste Algorithmus, der untersucht wird, ist das einfache Perzeptron, bei dem die Dynamik des Gewichtsvektors eine Reihe von Aussagen über die Autokorrelationen der erzeugten Zeitreihe zulässt. Eine eventuelle praktische Anwendung zur Erzeugung binärer Zeitreihen mit maßgeschneiderten Autokorrelationsfunktionen wird erläutert.

Der zweite Algorithmus, ein kontinuierliches Perzeptron, stellt sich als komplizierte nichtlineare Abbildung heraus, mit hochdimensionalem Chaos und intermittentem Verhalten. Nach einer Mean-Field-Rechnung zur Ermittlung der statistischen Eigenschaften der erzeugten Zeitreihe wird das Verhalten in Abhängigkeit von Systemgröße und Verstärkungsparameter untersucht und Lyapunov-Exponenten und Attraktordimension ermittelt.

Der dritte Vorhersagealgorithmus benutzt Boolesche Funktionen. Einige Eigenschaften der erzeugten Zeitreihe lassen sich durch graphentheoretische Ansätze beweisen, z.B. die Länge und Anzahl von Zyklen. Die Erfolgsaussichten von gleichartigen Vorhersagealgorithmen mit längerem oder kürzerem Gedächtnis werden untersucht.

Kapitel 3 beschreibt verschiedene Varianten des Minoritätsspiels, bei dem eine grössere Anzahl von Spielern sich unabhängig voneinander für eine von zwei Möglichkeiten entscheiden soll und diejenigen gewinnen, die in der Minderheit sind. Besonderes Augenmerk gilt den Varianten, die von unserer Arbeitsgruppe eingeführt wurden: eine korrekte und vollständigere Betrachtung von neuronalen Netzen im Minoritätsspiel wird angestellt; die stochastische Strategie von Reents und Metzler wird vorgestellt und analytisch gelöst; und es wird gezeigt, dass eine Verallgemeinerung auf mehr als zwei Wahlmöglichkeiten für alle gängigen Strategien möglich ist und qualitativ vergleichbare Ergebnisse bringt.

Eine Verbindung zu Kapitel 2 wird dadurch geschaffen, dass bei vielen Varianten in bestimmten Parameterbereichen die Zeitreihe der Entscheidungen genähert werden kann durch die antivorhersagbare Zeitreihe eines einzelnen Algorithmus, der die Mehrheit der Spieler repräsentiert.

Kapitel 4 beleuchtet eine andere Verbindung zwischen neuronalen Netzen und Spieltheorie: hier versucht ein neuronales Netz, in einem Zwei-Spieler-Nullsummenspiel durch wiederholtes Spielen und Anpassen der Gewichte eine gute Spielstrategie zu entwickeln. Eine Abwandlung von Hebbschem Lernen wird untersucht, die näherungsweise die Nash-Gleichgewichtsstrategie des Spiels finden kann. Die Eigenschaften dieser Regel lassen sich für kleine Auszahlungsmatrizen analytisch angeben, für große Matrizen mit zufälligen Einträgen können Abschätzungen gemacht werden.

Beim Lernen von Mustern mit Vorzugsrichtung (wie zum Beispiel Zeitreihenmustern) muss dieser Algorithmus jedoch modifiziert werden. Die dann naheliegende Variante (die ebenfalls aus Hebbschem Lernen abzuleiten ist), stellt sich als Abwandlung eines bekannten Lernalgorithmus für Matrixspiele heraus.

Contents

1	Introduction	3
1.1	Neural Networks	3
1.2	Time series generation	4
1.3	Game theory	4
1.4	An outline of this work	5
2	Antipredictable time series	6
2.1	Prediction of time series	6
2.2	Simple Perceptrons: the Confused Bit Generator	10
2.2.1	Sequence generation by a static perceptron: the Bit Generator	10
2.2.2	Hebbian Learning: the Confused Bit Generator	11
2.2.3	Dynamics of the weight vector	12
2.2.4	The Bernasconi model	14
2.2.5	Shaping the autocorrelation function	17
2.2.6	Distribution of cycles	18
2.2.7	Summary of the CBG	19
2.3	Continuous Perceptrons: the Confused Sequence Generator	20
2.3.1	Continuous perceptrons with fixed and adaptive weights	20
2.3.2	Mean-field solution	21
2.3.3	Autocorrelation function	23
2.3.4	Cycles and attractors	24
2.3.5	Chaotic dynamics and Lyapunov exponents	25
2.3.6	Summary of the CSG	29
2.4	Decision Tables	29
2.4.1	Decision tables and DeBruijn graphs	29
2.4.2	Static tables	31
2.4.3	Dynamic tables: complete antipersistence	32
2.4.4	Properties of cycles	34
2.4.5	Stochastic antipersistence	38
2.4.6	Summary of antipersistent time series	40

3	The Minority Game and its variations	42
3.1	Introduction	42
3.2	Rules of the Minority Game	43
3.3	The standard Minority Game	44
3.4	Neural Networks in the MG	46
3.4.1	Ensembles of vectors	46
3.4.2	Hebbian Learning	48
3.5	Johnson's evolutionary MG	51
3.6	Reents' and Metzler's stochastic MG	52
3.6.1	Solution for small p	54
3.6.2	Solution for large p	55
3.6.3	Mixed strategy populations & susceptibility to noise	58
3.6.4	Correlations in the time series	61
3.6.5	Relation to the original MG	62
3.7	Multi-choice MGs	64
3.7.1	Random Guessing	64
3.7.2	Neural Networks	66
3.7.3	Decision tables	73
3.7.4	Johnson's evolutionary MG	74
3.7.5	Reents' and Metzler's stochastic strategy	79
3.8	Summary and remarks on the Minority Game	81
4	Neural Networks in Two-Player Games	84
4.1	An overview over game theory	84
4.1.1	Combinatorial game theory	85
4.1.2	Economic game theory	85
4.1.3	Evolutionary game theory	86
4.2	Zero-sum games	87
4.2.1	Nash equilibria	88
4.3	Multi-Choice Perceptrons	89
4.4	Learning from unbiased patterns	91
4.4.1	Generating a probability distribution	91
4.4.2	Learning rule	92
4.4.3	The case of $K = 2$	93
4.4.4	Large K	95
4.5	Learning from biased patterns	104
4.6	Summary	109
5	Conclusion and outlook	111
A	Notation	113

Chapter 1

Introduction

“Neural Networks, Game Theory and Time Series Generation” – the title of this dissertation contains three fields of research that are so broad that bookshelves full of literature have been written on each one of them. Consequently, I will start with a disclaimer: this dissertation is not a textbook, and it cannot give exhaustive accounts of each field. Instead, it is my aim to present several projects which connect the three fields. Although more elaborate introductions to the ideas and formalisms needed to understand the projects will be given in the individual chapters, I will start with a brief overview over the fields and an outline of the dissertation.

1.1 Neural Networks

In an attempt to understand the workings of animal and human nerve systems, simple mathematical models of nerve cells (neurons) have been devised, which can be combined into artificial neural networks of considerable complexity. The simplest building block of these networks, the McCulloch-Pitts neuron [1], is interesting enough when studied in isolation. This network, which is then called a simple perceptron, can perform limited, but nontrivial, feats of storing, classification, and learning of unknown rules [2, 3, 4]. It formalizes two features of biological neurons: they receive signals from other cells via synaptic connections, and they are active if the added input exceeds some threshold, and inactive if it does not.

For increasing complexity and realism, compared to the simple perceptron, two directions suggest themselves: one is to assemble more complex structures out of simple perceptrons, such as multi-layer feed-forward networks, associative memory networks or recurrent networks [3]. This direction tends towards computer science and machine learning. The other direction is to incorporate more details from biological mechanisms [5, 6], such as explicit modeling of cell membrane potential and firing rates. While these models are hard to approach

analytically, they can be used to emulate biological pattern recognition problems realistically [7, 8]. In this dissertation, however, the simplest architectures that are suitable to a given task – namely, simple and continuous perceptrons, and multi-class perceptrons – will be used. Understanding their interaction with themselves or other networks is a sufficient challenge.

1.2 Time series generation

One of the applications that neural networks have been put to is the prediction of time series [9, 10]. The idea here is that many physical systems generate a stream of observables at regular time intervals (such as daily temperature measurements) that exhibit certain regularities. These properties of the time series can be used by a suitable algorithm to predict future values from a finite number of past values. Time series that can be predicted without error by some algorithm are those that can be generated by the same algorithm by feeding the predicted value back into the history that is used to make the next prediction. Therefore, it is helpful to look at the properties of a time series generated by an algorithm to learn about its prediction capacities.

It has been pointed out in Ref. [11] that the success of a prediction algorithm depends completely on the properties of the time series that it is applied to, and that there are always time series for which a given algorithm fails completely. These sequences can again be generated by that algorithm by inverting its output and feeding it back to the history. Comparing these sequences to the ones that are well predictable for the same algorithm sheds more light on the capabilities of the algorithm.

1.3 Game theory

Game theory deals with situation in which two or more players must make decisions, and the payoff which each player receives depends on the combined decisions of all players. In such situations, being able to predict what the others are going to do is extremely useful, whereas making decisions that are predictable for others is not.

Two game-theoretical problems will be treated in detail in this work: in two-player zero-sum games, both players pick one of their available options independently at the same time, and the gain of one player is always the loss of the other. As the groundbreaking studies of v. Neumann showed [12], this type of game has a unique equilibrium set of strategies for both players, which can be determined by rational calculations and beyond which no improvements for either player are possible. This allows to quantify the success of a given learning algorithm that develops a strategy from repeated playing, by comparing the achieved strategy

to the equilibrium strategy.

In the second scenario that will be presented, the Minority Game [13], a large number of players pick one of two options, and those in the majority lose. Although randomly choosing one option would be the rational strategy, other prescriptions (collectively labeled “bounded rationality”) where players try to predict the majority decision can lead to coordination among players, and thus improved average gains, compared to random guessing. On the other hand, attempts to avoid the predicted majority can lead to over-reactions, which result in herding behavior and dramatically reduced average gains.

1.4 An outline of this work

As mentioned, to understand the properties of prediction algorithms, it is helpful to study the properties of sequences that can be predicted well by them and especially those are predicted wrongly every time. In Chapter 2, I will do this for three prediction algorithms: simple and continuous perceptrons, and Boolean functions. Aspects of interest are properties of cycles (for discrete time series) and attractors (for continuous ones), and especially the suppression of correlations that the prediction algorithm is sensitive to in antipredictable time series.

Chapter 3 will present different aspects of the Minority Game, focusing on the variations of the game that were introduced by our research group, such as neural networks (Sec. 3.4 – this is a first link between neural networks and game theory) and the stochastic strategy presented in Sec. 3.6 (where, if a memory is included, the players can behave like a Boolean function with a learning algorithm). It will be shown that in Sec. 3.7 all presented strategies can be generalized to more than two options.

I will point out, where applicable, under what circumstances the dynamics of the Minority Game generate a time series that is partly antipredictable for the individual players, and completely antipredictable for a predictor that represents the ensemble of players, thus combining game theory and time series generation.

Chapter 4 presents a different aspect of connecting game theory and neural networks: there, a simple neural network tries to learn a two-player zero-sum game by adapting its weights and learning from experience. If random patterns are presented to the network, a modified Hebbian learning rule can lead to a good strategy and, under some circumstances, even converge to the equilibrium strategy.

If biased patterns are used, the learning rule has to be modified. The modified rule turns out to be a stochastic variation of a well-known learning algorithm for matrix games.

Chapter 2

Antipredictable time series

2.1 Prediction of time series

A time series is a sequence of values x^{t_1}, x^{t_2}, \dots with $t_1 < t_2 < \dots$. Often, the values are taken at regular time intervals, and the times t_1, t_2, \dots can be denoted by integer numbers $1, 2, \dots$. In most cases that are of interest to physicists, time series are observables of a physical system or variables of a mathematical model, and one tries to characterize the system by studying the statistical properties of the time series. However, in many cases it is of practical interest to *predict* the time series, i.e., make good guesses about the future values x^{t+1}, x^{t+2}, \dots from knowledge about a finite number of past values x^{t-M+1}, \dots, x^t [9, 14]. For example, considerable effort goes into the prediction of the weather (temperature, rainfall etc.), and many amateur and pro stock brokers would love to be able to predict the future of stock prices.

In the absence of information on external factors which might influence the time series (like new economic data that allow guesses about stock prices, or ecological events that influence the climate), a prediction algorithm can only take a finite stretch of the time series as input data and produce a guess based on this data. In other words, a prediction algorithm is a function $g(\mathbf{x}, \mathbf{w})$ that maps an input vector \mathbf{x} (whose components are the M past values of the time series, which may be binary or discrete) onto a (continuous or discrete) output.¹ The function may depend on internal parameters \mathbf{w} , such as the weight vectors in a neural network.

In the following sections, I will concentrate mainly on discrete time series $x^t \in \{-1, 1\}$, switching to the binary notation $x^t \in \{0, 1\}$ where it is more convenient. For discrete time series, the concept of accuracy is easy to define: the error rate is simply the percentage of predictions that do not agree with the

¹In game theory, “prediction” can mean predicting the probability distribution of possible outputs instead of giving a single most probable value [15]. I will not use this definition, which is difficult to apply to systems where only one of the possible realizations of randomness is observed.

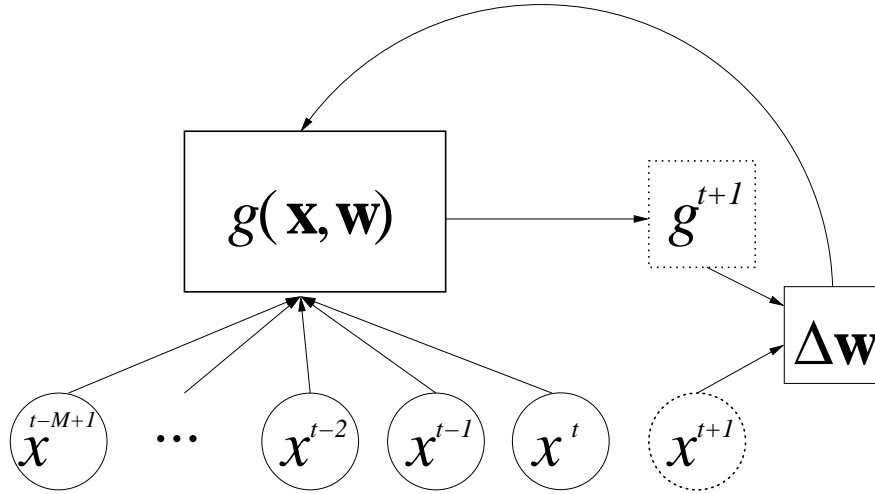


Figure 2.1: A simple representation of a prediction algorithm: external inputs \mathbf{x} are fed into a function $g(\mathbf{x}, \mathbf{w})$. Internal parameters \mathbf{w} are modified after comparing prediction g^{t+1} and reality x^{t+1} .

time series. In some cases, continuous or multi-valued discrete values will be considered as well.

Adaptive prediction algorithms are capable of changing their internal parameters based on a comparison between the time series and their prediction of it. One reasonable demand is that a prediction algorithm does not adapt its parameters as long as it is 100% accurate, and adapts if there are discrepancies between prediction and reality – this is for example realized in gradient-descent-based learning algorithms, where the norm of the update that is added to the parameters is proportional to the error.

Another reasonable assumption is that the predictor is deterministic: even though the model to be predicted may contain noise, adding noise to the predictor is unlikely to make a prediction better (leaving aside concepts like stochastic resonance [16]).

The time series that is to be predicted is generated by some system that can be arbitrarily complex, and can include any amount of randomness. The values of the time series (which represent observables like temperature, stock values etc.) reveal some information about the state of the system. For example, in deterministic chaotic systems with a finite number m of degrees of freedom, the full information about the state of the system is contained in a time series of at most $2m$ values of a suitable observable [17].

The prediction algorithm is then a more or less crude model of the system that generates the time series, as sketched in Fig. 2.1. Adjusting the parameters can improve the fit between the model and reality, or, to speak in the language of neural network theory, the overlap between “student” and the “rule” [18] or “teacher” [19].

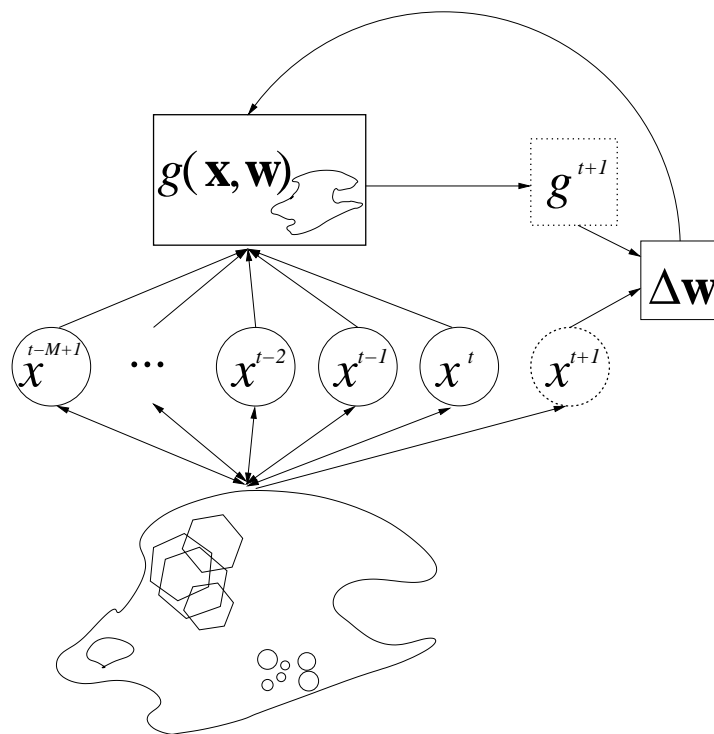


Figure 2.2: The next step: the system that generates the time series is included in the consideration. The predictor models some (hopefully relevant) properties of the system, and tries to improve the fit.

One could assume that, if the prediction algorithm has structural similarity to the generator of the time series, and if the time series is largely deterministic, the algorithm will predict the time series with fair accuracy after some training time. However, it was pointed out in Ref. [11] that for any algorithm that makes a binary prediction, there exists a generator of the same degree of complexity that generates a time series which will make the predictor fail every single time. This generator can be constructed easily: it is an exact copy of the predictor, including the internal parameters, the adaption algorithm and the random number generator, that takes the same input data and inverts the output. As the example of the antipersistent binary time series will show later (see. Sec. 2.4.3), in some cases this scheme will also fool predictors that start with a different set of initial parameters, if they “forget” their initial state quickly enough.

One interesting thing about the antipredictable sequence generated in this fashion is that it is completely deterministic. In the same fashion, deterministic sequences can be designed that make the predictor fail every second, third, etc., prediction [11].

In the framework outlined above, time series that can be predicted without error by an algorithm are those where the output of the algorithm is exactly the next value of the time series. The time series can thus be constructed (without any external information) by feeding the newly generated bit back into the pattern. Analogously, antipredictable sequences are those generated by the algorithm, inverting the bit and feeding it back. In the following, prediction and generation are thus very much interchangeable, and in order to study the properties of time series that are predictable or antipredictable, I will actually study time series *generated* by the algorithm.

The concept of antipredictability may seem highly artificial. However, it can turn out to be relevant if the predictors are part of the system they are trying to predict (see Fig. 2.3). For example, the concept of the Minority Game that is explained in Chapter 3 has a strong element of self-defeating prophecy.

The following sections will compare the properties of predictable and antipredictable sequences for two simple algorithms: a simple neural network, and a Boolean function. Sections 2.2 and 2.3 are based on from Refs. [20] and [21], whereas Sec. 2.4 was presented in Ref. [22]. These differences will shed some light on the considered algorithms themselves, and the features in the time series that they are sensitive to, giving a better intuition about the applicability of an algorithm to a given problem.

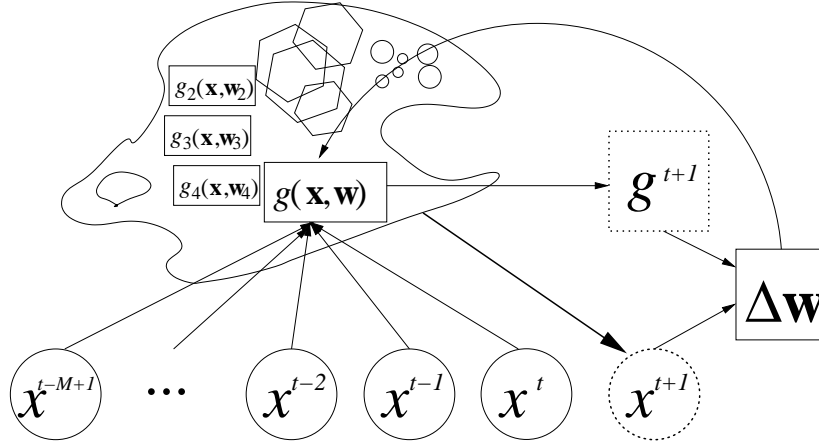


Figure 2.3: Sometimes, the predicting algorithm is part of the system that it is trying to predict, together with other algorithms and a complex environment.

2.2 Simple Perceptrons: the Confused Bit Generator

2.2.1 Sequence generation by a static perceptron: the Bit Generator

The first example of a prediction algorithm that I am going to present is the simplest model of a neural network, the simple perceptron [2, 3]. Inspired by biological neurons [1], this model has received much attention, and in spite of its simplicity, it shows many interesting features (see Ref. [18] for an overview).

In analogy to a biological neuron that receives impulses from other neurons through synaptic links and either starts firing impulses itself or stays passive depending on the received inputs, the perceptron performs a weighted sum over a set of inputs x_i , $i = 1, \dots, M$. Each input is multiplied with a synaptic weight w_i . The output is either $+1$ or -1 , depending on whether the weighted sum of inputs is larger or smaller than 0.

In a geometrical interpretation, both the weights and the input data represent M -dimensional vectors \mathbf{w} and \mathbf{x} , and the output is the sign of the scalar product between the vectors.

One way to generate a time series using a perceptron (or, for that matter, any other feed-forward neural network [23]) is to use an M -bit window of the time series as input and continue the time series with the output on that pattern:

$$x^{t+1} = \text{sign}\left(\sum_{i=1}^M w_i x^{t-i+1}\right). \quad (2.1)$$

For the simple perceptron with binary output (and, correspondingly, a binary

time series) and fixed weights, this system, which was named Bit Generator (BG), was studied in Refs. [24, 25, 26]. It is a deterministic dynamical system with a finite state space: there are only 2^M possible histories. Once a history appears the second time, the system is on a cycle. Simulations show that cycles have a typical length $l < 2M$; their average length $\langle l \rangle$ (averaged over initial conditions) increases polynomially in M [25]. Typically, cycles are dominated by one short sequence that is interrupted by “defects”, such as $+ - + - + - + + - + - + - \dots$. The wavelength of the underlying short sequence usually corresponds to a wavelength that is strongly represented in a Fourier decomposition of the weight vector.

As long as the weight stays fixed, the predictable sequence for a given \mathbf{w} is precisely the anti-predictable sequence for $-\mathbf{w}$. Things get more interesting if the weight vector becomes adaptive.

2.2.2 Hebbian Learning: the Confused Bit Generator

In order to find regularities in a set of data, the weights of a neural network have to adapt to the data. This can occur either offline (all patterns and desired outputs are known and are processed at the same time) or online (patterns are shown to the network one by one and then discarded). Since the patterns and the output to be learned are generated by the predictor, offline learning makes little sense. Therefore, online learning will exclusively be considered from now on.

Online learning algorithms for perceptrons come in many variations, ranging from simple to elaborate [3, 27, 28, 29, 4]. However, most boil down to the same principle: the updated weight vector \mathbf{w}^{t+1} is a linear combination of the previous weight vector \mathbf{w}^t and the pattern \mathbf{x}^t . This seems natural for symmetry reasons, since these two vectors are the only preferred directions in a possibly high-dimensional space.²

The coefficients of the linear combination can depend on the desired output (in our case, the next step of the time series, x^{t+1}), the so-called hidden field $h^t = \mathbf{w}^t \cdot \mathbf{x}^t$, a learning rate η , and a few other quantities, which should be accessible to the neural network. The two most basic learning algorithms are the Hebbian rule

$$\mathbf{w}^{t+1} = \mathbf{w}^t + \frac{\eta}{M} \mathbf{x}^t x^{t+1}, \quad (2.2)$$

and the Rosenblatt rule,

$$\mathbf{w}^{t+1} = \mathbf{w}^t + \frac{\eta}{M} \mathbf{x}^t x^{t+1} \Theta(-x^{t+1} \text{sign}(h^t)). \quad (2.3)$$

In the latter case, the correction step is applied only if the output of the perceptron and the desired output disagree. Since this is always the case for a completely

²The interpretation of the pattern as a time series, however, breaks the symmetry between input dimensions: it may be reasonable to give more weight to the more recent past. Secs. 2.2.4 and 2.2.5 provide examples for this.

antipredictable time series, both rules amount to the same in this case. The perceptron which always learns the opposite of its own output was studied first in Ref. [11], and examined extensively in Refs. [21] and [20], where it was named Confused Bit Generator (CBG). A very similar system was studied in Ref. [30]. The CBG is defined by the equations

$$x^{t+1} = -\text{sign}(\mathbf{x}^t \cdot \mathbf{w}^t); \quad (2.4)$$

$$\mathbf{w}^{t+1} = \mathbf{w}^t + (\eta/M)x^{t+1}\mathbf{x}^t. \quad (2.5)$$

This is a deterministic dynamic system with $2M$ variables, instead of M variables in the BG. Indeed, the dynamics of the weight vector are very helpful in understanding the properties of the generated time series.

2.2.3 Dynamics of the weight vector

Geometrically speaking, \mathbf{w} does a random-walk-like movement on an M -dimensional cubic lattice: in each component of the weight vector, the learning step has a value of $\pm\eta/M$. Although the weight components are real numbers, once an initial state \mathbf{w}^0 has been defined, the components w_i can only take values $w_i^0 \pm n\eta/M$, with $n \in \mathbb{Z}$.

Each learning step has a negative overlap with the current \mathbf{w} . The norm of the weight vector fluctuates around an equilibrium value that can be estimated by taking the square of Eq. (2.5) and applying the usual formalism for online learning [29, 31]. Since the patterns are windows of the time series and are hence generated by a complex dynamical process, the required averages over scalar products between the weight and the pattern cannot be done exactly. However, the generated time series looks sufficiently irregular at first glance (no prominent frequency, no short-term repetitions) that one can try replacing \mathbf{x} with a random vector whose components are independent random variables of mean 0 and variance 1, and see how far that approximation carries:

$$\langle \mathbf{w}^{t+1} \cdot \mathbf{w}^{t+1} - \mathbf{w}^t \cdot \mathbf{w}^t \rangle = -\frac{2\eta}{M} \langle \mathbf{x}^t \cdot \mathbf{w}^t \text{sign}(\mathbf{x}^t \cdot \mathbf{w}^t) \rangle + \frac{\eta^2}{M^2} \langle \mathbf{x}^t \cdot \mathbf{x}^t \rangle. \quad (2.6)$$

Introducing a time scale α with $d\alpha = 1/M$ and averaging over \mathbf{x} , this becomes a deterministic differential equation for the norm $w = |\mathbf{w}|$ in the thermodynamic limit $M \rightarrow \infty$:³

$$\frac{dw}{d\alpha} = -\sqrt{\frac{2}{\pi}}\eta + \frac{\eta^2}{2w}. \quad (2.7)$$

The attractive fixed point of this equation is $w = \sqrt{\pi/8}\eta \approx 0.6267\eta$. The learning rate η thus only sets a length scale, but does not influence the behavior of the system once the weight vector has reached its fixed-point length.

³This limit will be tacitly assumed every time a differential equation is written down; it usually gives good results even for moderate M (on the order of $M \sim 20$.)

However, using the time series generated by the perceptron as patterns, simulations give a slightly different value of $w \approx 0.566\eta$, independent of M (this was already observed in [11]). Two possible mechanisms for this deviation suggest themselves: first, the time series windows generated by the CBG are not isotropically distributed on the M -dimensional hypercube; some patterns are more likely to appear than others (see Ref. [21] for details). Second, correlations between the outputs and the patterns might be the cause of the deviations. This can be checked by using patterns drawn randomly from an anisotropic distribution that resembles the one generated by the CBG. Since this leads to values of w compatible with the result for random vectors, one must conclude that correlations between outputs and patterns are responsible for the deviation.

Using the approximation of random patterns, the autocorrelation of the weight vector can be estimated as well:

$$\langle \mathbf{w}^t \cdot \mathbf{w}^{t+\tau} \rangle = w^2 \exp\left(-\frac{4}{\pi} \frac{\tau}{M}\right). \quad (2.8)$$

Of course, this does not reflect the fact that the CBG is a deterministic system with a bounded number of states, so cycles are inevitable, and the weight vector must return to its original point later (i.e., the autocorrelation of the weights will return to w^2 at multiples of the return time). The dynamics of the weights can be linked to the autocorrelation function C_j^t of the sequence, defined by

$$C_j^t = \sum_{i=1}^t x^i x^{i-j}, \quad (2.9)$$

where t is the number of patterns summed over. Simply add t update steps according to Eq. (2.5):

$$w_j^t = w_j^0 + \sum_{i=1}^t (\eta/M) x^i x^{i-j} = w_j^0 + (\eta/M) C_j^t. \quad (2.10)$$

Each value C_j^t for $1 \leq j \leq M$ corresponds to the distance of the weight vector from its starting point along one axis in the M -dimensional weight space, measured in units of η/M . This point is important and will be exploited in the following paragraphs. Note that Eq. (2.10) holds for any perceptron that learns a time series following the Hebb rule, regardless whether the time series is predictable, antipredictable or anything in between. This means that in the long run, the perceptron is only sensitive to the first M values of the autocorrelation function of the considered time series. The stronger the autocorrelation of a sequence is, the more accurate the prediction will be.

In the CBG, the norm of the weight vector, and therefore the autocorrelation function of the generated sequence, is suppressed: as described, the norm of \mathbf{w} stays bounded. Following Eq. (2.10), each component of the autocorrelation function stays bounded as well, instead of growing with $\sqrt{\alpha}$ as it would for a random sequence.

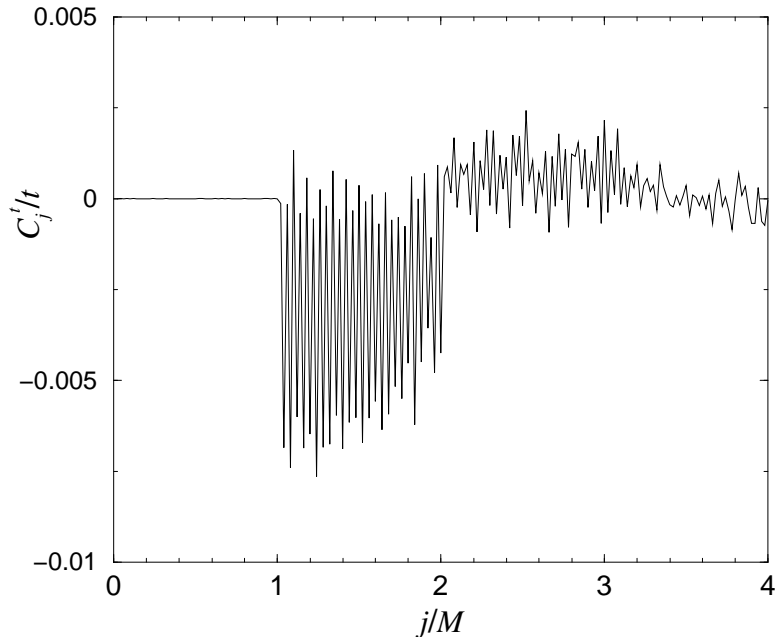


Figure 2.4: Autocorrelation function of the time series generated by the CBG, averaged over $t = 2 \times 10^6$ for $M = 50$ (taken from Ref. [21]). The first M components are suppressed by the dynamics of the weights.

2.2.4 The Bernasconi model

Bit series with low autocorrelations are of interest in mathematics and have applications in signal processing [32]. On one hand, this allows to apply findings on these sequences to the CGB. On the other hand, it is interesting whether the CBG generates sequences with autocorrelations significantly lower than for random series. Two measures that indicate low autocorrelations are commonly used in the literature: for periodic sequences of length l , an energy function (which is studied in the so-called Bernasconi model for periodic boundary conditions [33]) can be defined by

$$H_p = \sum_{j=1}^{l-1} (C_j^l)^2 = \sum_{j=1}^{l-1} \left(\sum_{i=1}^l x^i x^{i+j} \right)^2. \quad (2.11)$$

Results on the ground states of this Hamiltonian can be found in [34]. By trial and error, initial conditions for the CBG can be found which yield cycles slightly larger than $2M$, for which all value of C_j^l except one are 0. However, even for the best sequences we found in long simulation runs, H_p was larger than the known ground state energies by at least a factor of 2.

The original model does not use periodic boundary conditions: in a sequence of length p , only the sum over $p - j$ different terms with a lag of j can be

calculated. The energy for aperiodic sequences is therefore given by

$$H_{ap} = \sum_{j=1}^{p-1} (C_j^{p-j})^2 \quad (2.12)$$

(note the summation limits). The so-called merit factor F introduced by Golay [35] is defined by

$$F = \frac{p^2}{2H_{ap}}. \quad (2.13)$$

A merit factor of 1 is expected for a random sequence; lower autocorrelations yield higher F . The theoretical limit for large p is conjectured to be about $F = 12$ [33, 36], whereas optimization routines such as simulated annealing typically find sequences with $5 < F < 9$ (see [37] and references therein) and exact enumeration for $p < 60$ suggests $\lim_{p \rightarrow \infty} F = 9.3$ for the optimal sequence [38].

To analytically estimate the merit factor of sequences generated by the CBG, one can solve Eq. (2.10) for $C_j^{t^2}$ and use the autocorrelation of the weights given by Eq. (2.8):

$$\langle (C_j^{p-j})^2 \rangle = \frac{M^2}{\eta^2} \langle w_j^{0^2} + w_j^{t^2} - 2w_j^t w_j^0 \rangle = \frac{\pi}{4} M \left(1 - \exp \left(-\frac{4}{\pi} \frac{p-j}{M} \right) \right). \quad (2.14)$$

The energy can be expressed as a sum or approximated by an integral in continuous variables $\alpha = p/M$ and $\beta = j/M$. Since Eq. (2.14) only holds for $1 \leq j \leq M$, $C_j^{p-j^2} = p-j$ must be used for $j > M$. One gets the expression

$$\begin{aligned} H_{ap} &= \sum_{j=1}^{p-1} M \frac{\pi}{4} \left(1 - \exp \left(-\frac{4}{\pi} \frac{p-j}{M} \right) \right) \\ &\approx \int_0^\alpha M^2 \frac{\pi}{4} (1 - \exp(-(4/\pi)(\alpha - \beta))) d\beta \\ &= M^2 \frac{\pi}{4} \left[\alpha - \frac{\pi}{4} \left(1 - \exp \left(-\frac{4}{\pi} \alpha \right) \right) \right] \end{aligned} \quad (2.15)$$

for $j \leq M$ and

$$\begin{aligned} H_{ap} &= M^2 \left[\frac{\pi}{4} \left(1 - \frac{\pi}{4} \left\{ \exp \left(\frac{4}{\pi} (1 - \alpha) \right) - \exp \left(-\frac{4}{\pi} \alpha \right) \right\} \right) + \frac{1}{2} (\alpha - 1)^2 \right] \\ &\quad \text{for } j > M. \end{aligned} \quad (2.16)$$

The corresponding merit factor is compared to simulations in Fig. 2.5: Eqs. (2.15) and (2.16) give qualitatively correct results, but differ from the observed values by roughly 10%. The feedback mechanisms of the CBG cause a faster decay of C_j^t than predicted for random patterns.

A simple extension of the dynamics allows to slightly manipulate this result: if each weight component gets an individual (positive) learning rate, one can write

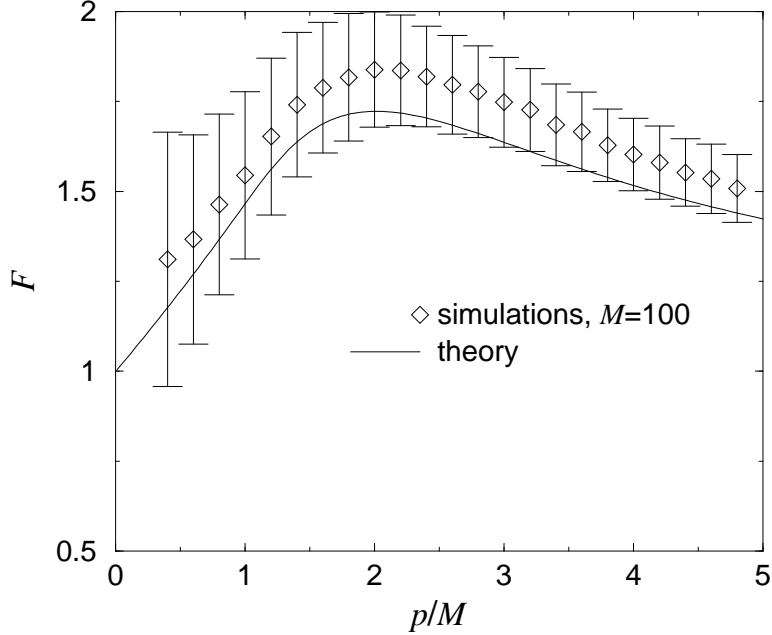


Figure 2.5: Merit factor F of sequences generated by the CBG, as a function of scaled sequence length p/M , compared to Eqs. (2.15) and (2.16). Error bars denote the standard deviation of F for $M = 100$, not the standard error.

down an update equation for each component that separates the influence of that component on the output from all others. A short calculation (again under the assumption of random patterns, which has yielded qualitatively correct predictions so far) then shows that the mean square value of that weight is proportional to its learning rate:

$$\langle w_i^2 \rangle = \sqrt{\frac{\pi}{8}} \frac{\eta_i}{M} \sqrt{\sum_j w_j^2} = \frac{\pi}{8} \frac{\eta_i}{M^2} \left(\sum_j \eta_j \right). \quad (2.17)$$

Although Eq. (2.17) looks like a regular on-line learning equation, it does not carry quite as far: w_i^2 is not a self-averaging quantity [39], i.e., the variance of w_i^2 does not go to zero in the thermodynamic limit, and Eq. (2.17) only makes a statement about the long-time average.

What it does state is that a component with a higher learning rate has, on the average, a larger weight and thus a stronger influence on the output. This also leads to a faster decay of the corresponding segment of the autocorrelation:

$$\langle w_i^t w_i^{t+\tau} \rangle = \frac{\sum_j \eta_j}{\eta_i} \frac{\pi}{4} \exp \left(-\frac{\eta_i}{\sum_j \eta_j} \frac{4}{\pi} \tau \right). \quad (2.18)$$

Returning to the Bernasconi problem, the search for a minimal H_{ap} can be written as an optimization problem in the continuous function $\eta(\beta)$, where $\eta_j = \eta(j/M)$.

Solving this problem with a variational approach, one finds that it is sensible to give the last 41% of the weights a learning rate and norm of zero, and increase the learning rate continuously towards components with smaller indices. Unfortunately, even this optimization does not improve the merit factor beyond $F = 1.74$ in theory and $\langle F \rangle = 1.86$ in simulations. This is still a lot worse than the results of other optimization methods [33, 37], so the CBG is not a competitive generator of low-autocorrelation sequences.

The limited use of the CBG in generating sequences with a high merit factor may be related to phase space arguments: as seen in Sec. 2.2.6, the CBG can still generate exponentially many different time series depending on initial conditions, whereas there are very few sequences with the highest achievable high merit factors (see [40] for the density of states with cyclic boundary conditions). The mechanism of the CBG allows for manipulation of the autocorrelation function only if the constraints on the desired sequence are not too strong, such as suppressing all of the elements of C_j on a short time scale. On the other hand, choosing a given shape for long-time averages of C_j still allows for many realizations of the sequence.

Although it is not very useful in a straight application to the Bernasconi problem, the Confused Bit Generator still has some interesting possibilities:

2.2.5 Shaping the autocorrelation function

In some cases, it may be interesting to generate a time series whose power spectrum has a specific shape in the long-time limit. Using Eqs. (2.17) and (2.10) in the limit where $w^0 \approx 0$ and with non-negative learning rates, one can obtain the inverse relation between the square of the autocorrelation function $C_j^{t^2}$ and the corresponding learning rate η_j

$$\langle C_j^{t^2} \rangle = \frac{\pi \sum_{i=1}^M \eta_i}{8 \eta_j}. \quad (2.19)$$

Thus, just about any desired shape of the square autocorrelation function is achievable by using the appropriate profile for η_j , which can be extracted from Eq.(2.19).

If one is not only interested in the shape, but also the norm of the autocorrelation function, one can influence this by distorting the output with multiplicative noise: if there is a probability of p_f for flipping the output,

$$x^{t+1} = \begin{cases} \text{sign}(\mathbf{x} \cdot \mathbf{w}) & \text{with probability } p_f \\ -\text{sign}(\mathbf{x} \cdot \mathbf{w}) & \text{with probability } 1 - p_f \end{cases}, \quad (2.20)$$

the learning step has a positive overlap with the weight with probability p_f , leading to a larger norm w in the stationary state. For homogeneous learning

rates, Eq. (2.7) now reads

$$\frac{dw}{d\alpha} = \sqrt{\frac{2}{\pi}}\eta(2p_f - 1) + \frac{\eta^2}{2w}, \quad (2.21)$$

and the fixed point (which only exists for $p_f < 1/2$) is correspondingly

$$w = \sqrt{\frac{\pi}{8}} \frac{\eta}{1 - 2p_f}. \quad (2.22)$$

However, Eq.(2.10) still holds – and $\sum C_j^2$ increases accordingly. The same factor of $1/(1 - 2p_f)$ also appears in Eq.(2.19) if the calculation is repeated for individual learning rates.

If it is desired to enhance certain correlations rather than suppress them to a lesser or greater degree, it is possible to give some components a learning rate of 0 and a fixed norm. The sign of that weight component determines whether the correlation is positive or negative, the norm determines the strength of the correlations.

Does all this work in practice? Within certain bounds, it does. However, the autocorrelation function of a sequence cannot be shaped arbitrarily [41], and imposing strong constraints on some components of C leads to a strong violation of the assumption of random patterns that underlies the calculations. The results are not easy to calculate, so some trial-and-error is required to get the desired result.

Furthermore, for each individual set of initial conditions, the autocorrelation function will show significant deviations from the calculated profile, and good agreement is only reached when averaging over sufficiently many initial conditions. Fig. 2.6 shows two examples of autocorrelation functions shaped with exponential and sinusoidal profiles, together with the theoretical profile (the proportionality constant was fitted).

Concludingly, simulations show that with some twiddling, the CBG could be used as an alternative mechanism for generating colored binary sequences using local rules instead of nonlocal mechanisms such as Fourier transforms.

2.2.6 Distribution of cycles

Just like the BG with fixed weights, the CBG is a deterministic system with a finite number of states, and thus has to fall into a cycle eventually. The distribution of cycle lengths l was studied in some detail in my diploma thesis [21]. For completeness, I will repeat the essential results here.

The connection between the autocorrelation function and the weights that was exploited in the previous sections can be used to give a lower bound on cycle lengths of the CBG: since the weight has to return to its original position after l steps, the first M components of the autocorrelation function C_j^l have to

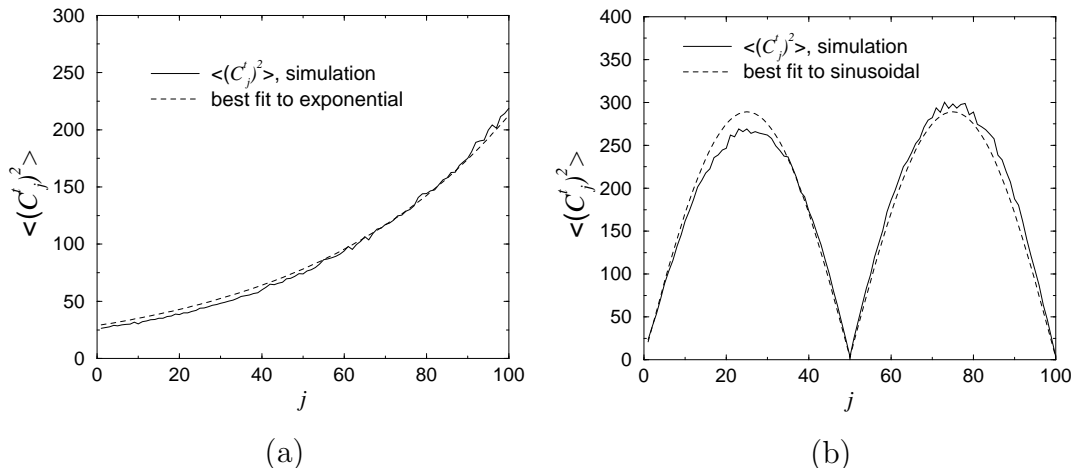


Figure 2.6: Mean square autocorrelation function after $t = 1000$ steps, generated with a CBG with $M = 100$ and the learning rate profiles $\eta_j = \exp(-2j/M)$ (plot (a)) and $\eta_j = 1/(0.01 + |\sin(2\pi j/M)|)$. Dashed lines show the profile predicted from Eq. (2.19), with a proportionality constant fitted to the data. Simulations averaged over 1000 runs.

vanish (see Eq. (2.10)). By renaming the indices, one can see that the last M components C_{i-j}^l must vanish as well. That would mean that for $l \leq 2M$, all components of C_j^l would be zero. There is good mathematical evidence [34] that this is not possible for $M > 3$. Furthermore, to get $C_j^l = 0$ for any j , l must be divisible by 4.

Extensive simulations indeed show that the lower bound $l > 2M$ holds (with the exception of $M = 2$). However, the shortest cycle lengths that are observed are the smallest multiples of 4 larger than $2M$. The average cycle length grows exponentially with M : $\langle l \rangle \propto 2.2^M$.

2.2.7 Summary of the CBG

The Confused Bit Generator generates the time series that is antipredictable for a perceptron, and it is hardly surprising that the properties of that sequence differ from one that is easily predictable: while a perceptron with Hebbian learning is sensitive to the autocorrelation of a time series, the CBG suppresses the first M bits of the autocorrelation function – as many as it can, with a memory of M time steps.

This suppression can be linked directly to the dynamics of the weights. These can in turn be calculated under the assumption of random patterns, which allows to estimate quantities like the merit factor of the generated sequence. Unfortunately, the CBG is not a very good source of low-autocorrelation sequences; however, individual learning rates for different components allow for a manipulation and customized shaping of the autocorrelation function.

The suppression of the autocorrelation function points to another difference between the CBG and the BG: the sequence generated by the CBG no longer has a dominant Fourier component. The Fourier transform of the weight vector is no longer a very meaningful quantity either, since it changes constantly as the vector moves.

The CBG has a significantly larger number of accessible states than the BG with equal M . However, while the average cycle length of the BG grows polynomially in M , and has a typical value of $2M$, $\langle l \rangle$ grows exponentially for the CBG, and has $2M$ as a lower bound.

2.3 Continuous Perceptrons: the Confused Sequence Generator

2.3.1 Continuous perceptrons with fixed and adaptive weights

The perceptron with binary output can readily be generalized to continuous output by replacing the sign function with a sigmoid function, such as the error function. This introduces a new parameter, the amplification β :

$$g(\mathbf{x}, \mathbf{w}) = \operatorname{erf}(\beta \mathbf{x} \cdot \mathbf{w}). \quad (2.23)$$

Just like the simple perceptron, the continuous perceptron can be used to generate a time series:

$$x^{t+1} = \operatorname{erf}\left(\beta \sum_{i=1}^M w_i x^{t-i+1}\right). \quad (2.24)$$

This system (the Sequence Generator or SGen) was studied in Refs. [23, 42, 43]. In the typical case, depending on the amplification, the system either converges to the trivial solution $x_t \equiv 0$ or, after a short chaotic transient, relaxes into a stable limit cycle (see. Fig. 2.7).

A careful investigation shows that there are small areas in parameter space (which is spanned by \mathbf{w} and β) that lead to chaotic behavior. Since these areas are themselves fractals, and the appearance of chaos is therefore sensitive to small variations in the parameters, the term *fragile chaos* was coined to characterize the system [23].

It is not quite obvious how to generalize the Confused Bit Generator to continuous output: there is no unique value of the prediction that is “wrong”, since any value that is different from the actual value of x is more or less wrong. The following simple prescription was chosen to keep the dynamics as close as possible to that of the CBG, and especially to keep the connection between the weight vector and the autocorrelation function of the generated time series. The

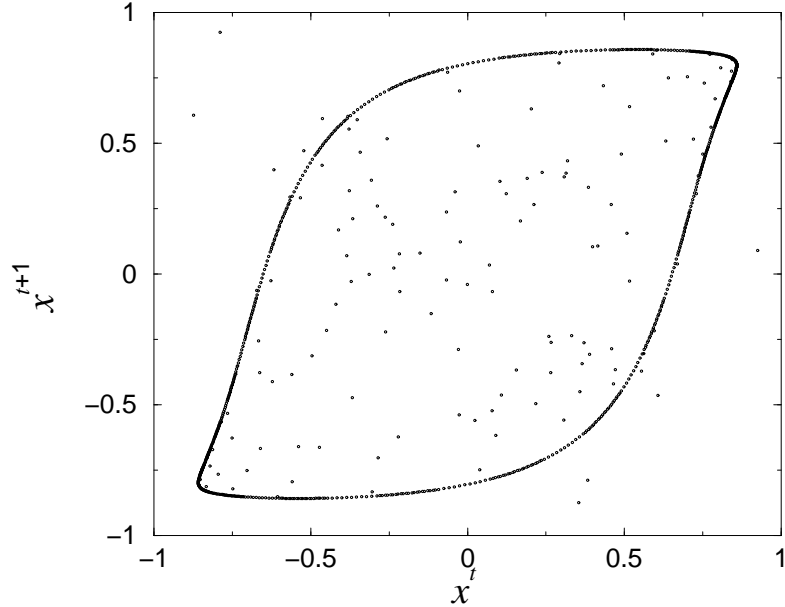


Figure 2.7: Typical return map of an SGen: after a short transient (scattered points) the system enters a quasi-periodic limit cycle.

continuation of the time series is thus simply taken to be the negative of the perceptron’s output, and the learning step is proportional to the desired output (and therefore, to the difference between the desired and the real output):

$$x^{t+1} = -\text{erf}(\beta \mathbf{x}^t \cdot \mathbf{w}^t); \quad (2.25)$$

$$\mathbf{w}^{t+1} = \mathbf{w}^t + (\eta/M)x^{t+1}\mathbf{x}^t. \quad (2.26)$$

This system was introduced in Ref. [20], where it was named Confused Sequence Generator (CSG).

2.3.2 Mean-field solution

Similar to the CBG, the weight vector of the CSG does a directed pseudo-random walk near the surface of a hypersphere of a radius w . Unlike the CBG, the length of the learning steps, which determines w , is not fixed, but depends on the magnitude of the output, which in turn depends on w and the outputs in previous time steps. To find an approximate solution to this self-consistency problem, I will first ignore correlations between patterns and weights and treat the patterns as random and independent.

In this approach, the hidden field $h = \mathbf{w} \cdot \mathbf{x}$ is a Gaussian random variable of mean 0 and variance $w^2 S^2$, where $S^2 = \langle x^{t2} \rangle_t$ is the mean square output of the system.

The norm w is found by taking the square of (2.26):

$$w^{t^2} = w^{t-1^2} - \frac{2\eta}{M} \mathbf{x}^t \cdot \mathbf{w}^t \operatorname{erf}(\beta \mathbf{x}^t \cdot \mathbf{w}^t) + \frac{\eta^2}{M^2} S^{t^2} \mathbf{x}^t \cdot \mathbf{x}^t, \quad (2.27)$$

and averaging over the input patterns. The self-overlap $\mathbf{x} \cdot \mathbf{x}$ is on the average MS^2 , so the fixed point of w is given by

$$2\langle h \operatorname{erf}(\beta h) \rangle = \eta S^4. \quad (2.28)$$

The average on the left hand side can be evaluated and leads to

$$\frac{4}{\sqrt{\pi}} \frac{\beta w^2 S^2}{\sqrt{1 + 2\beta^2 w^2 S^2}} = \eta S^4, \text{ or} \quad (2.29)$$

$$w^2 = \frac{\pi \beta \eta^2 S^6 + \eta S^2 \sqrt{\pi} \sqrt{16 + \pi \beta^2 \eta^2 S^8}}{16\beta}. \quad (2.30)$$

Let us now turn to S^2 . The probability distribution of S itself is rather awkward, since it involves inverse error functions, and its slope diverges at $S = \pm 1$. However, S^2 can be easily calculated by using the distribution of h :

$$\begin{aligned} \langle S^2 \rangle &= \int_{-\infty}^{\infty} \operatorname{erf}^2(\beta h) (2\pi w^2 S^2)^{-1/2} \exp\left(-\frac{h^2}{2w^2 S^2}\right) dh \\ &= \frac{2}{\pi} \arcsin\left(\frac{2\beta^2 w^2 S^2}{1 + 2\beta^2 w^2 S^2}\right). \end{aligned} \quad (2.31)$$

Plugging $w^2(\eta, \beta, S^2)$ from Eqs. (2.30) into (2.31) and solving numerically, one obtains a self-consistent solution for S^2 . A closer look at the equations reveals that if a new quantity $\gamma = \eta\beta$ is introduced, only γ enters into the equation for S^2 , and w^2 is of the form $w^2 = \eta^2 \hat{w}^2(\gamma)$, so only one curve must be considered. This is intuitive, since a higher η eventually leads to a higher w , which has the same effect on S^2 as having a smaller w , but multiplying $\mathbf{w} \cdot \mathbf{x}$ with a higher factor β .

The map defined by Eqs. (2.25) and (2.26) always has the trivial solution $\mathbf{x} = \mathbf{0}$. Only for a sufficiently high $\gamma > \gamma_c$ are the outputs high enough to sustain a non-vanishing solution. Note that $\mathbf{x} = \mathbf{0}$ is always an attractive solution for all $\gamma < \infty$, but its basin of attraction becomes smaller for larger γ .

The numerical solution of Eqs. (2.30) and (2.31) shows that the system undergoes a saddle-node bifurcation at $\gamma_c \approx 5.785$, which is in good agreement with simulations. Above γ_c , two new fixed points exist, only one of which is stable. While for $S^2(\gamma)$ excellent agreement is found between theory and simulation (see Fig. 2.8), $w^2(\gamma)$ shows quantitative differences which are caused by correlations between \mathbf{x} and \mathbf{w} : the mean square overlap $\langle (\mathbf{x} \cdot \mathbf{w})^2 \rangle$ turns out to be $(1.22 \pm 0.01)w^2 S^2$ instead of $w^2 S^2$ as expected for random patterns. This causes

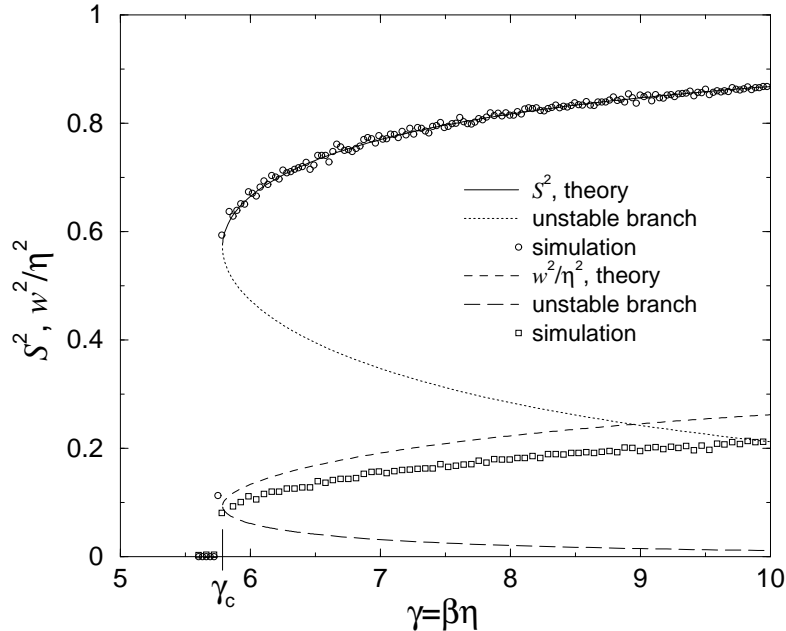


Figure 2.8: Mean-field solution of the CSG (Eqs. (2.30) and (2.31)), compared to simulations with $M = 400$.

a factor of roughly 0.82 between the theoretical and observed value of w^2 , as seen in Fig. 2.8. It is the same factor that is found in the CBG, and likely caused by the same mechanisms.

For large γ , S^2 goes to 1 (as it should, since the system is identical to the CBG if $\gamma = \infty$), and the theoretical prediction for w goes to $\sqrt{\pi/8}\eta$, just like in the CBG.

2.3.3 Autocorrelation function

The relation Eq. (2.10) that links the autocorrelation function to the weights in the CBG still holds for the CSG. Since the weight vector is bounded in the CSG as well, the same argument can be given for the suppression of the first M values of the autocorrelation function. Correspondingly, C_j^P/p is almost indistinguishable from that of the CBG shown in Fig. 2.4.

In principle, this allows to play the same games as in Sec. 2.2.5 to shape the first M components of C_j^P . However, the practical need for a continuous time series with a rather odd probability distribution and a custom-tailored autocorrelation function is probably small.

2.3.4 Cycles and attractors

The CSG can be seen as a nonlinear mapping that maps the vector $\mathbf{x}^t \oplus \mathbf{w}^t$ onto $\mathbf{x}^{t+1} \oplus \mathbf{w}^{t+1}$. Again, this is opposed to the SGen with static weights, where the components of the sequence window are the only dynamic variables, and in analogy to the difference between the Bit Generator and the CBG. The only relevant control parameter of this mapping is γ .

Since both the sequence and the weights now live in a high-dimensional space of real numbers, the CBG can display a wide variety of behaviors, depending on M and γ :

For $\gamma < \gamma_c$, the zero solution is the only attractor, and the system will quickly reach $\mathbf{x}^t = \mathbf{0}$ and stop developing.

For γ slightly above γ_c , an irregular-looking time series with the distribution and variance that were calculated in Section 2.3.2 and displayed in Fig. (2.8) is generated. However, the zero solution is still attractive, and after some time the system will drift close to it and stay there, i.e. the irregular behavior represents a chaotic transient rather than a stable chaotic attractor.

The survival time on the transient increases dramatically with increasing M and γ . It is hard to decide from numerical results whether the average survival time $\langle t_s \rangle$ diverges with a power law ($\langle t_s \rangle \propto |\gamma - \gamma_d|^{-a}$), as one usually finds in scenarios where a chaotic transient becomes a chaotic attractor [44], or whether $\langle t_s \rangle$ increases exponentially with γ . In either case, the system shows chaotic behavior for sufficiently long times to get stable numerical results – for example, for $M = 20$ and $\gamma = 7.0$, the average survival time is on the order of 10^6 steps.

If γ is larger than some critical value that depends on M , the chaotic transient can eventually end in a cycle that is related to a possible cycle of the discrete CBG. “Related” means that x^t in the CSG is very close to ± 1 and that clipping the sequence to the nearest value of ± 1 would give the equivalent attractor of the CBG. More different cycles become stable with higher γ ; however, the cycle lengths are usually of order $2M$ – short cycles are apparently more likely to become stable than ones whose length is of order 2^M . A possible explanation for this is probabilistic: as Sec. 2.3.5 will show, stability is possible only if the transfer function is almost saturated, which only happens if the pattern and weight have a high overlap. It is easier to find a short cycle for which this is fulfilled for every pair of pattern and weight, than a long cycle.

At amplifications γ slightly below the lowest γ for which the first cycle becomes stable for a given M , intermittent behavior is observed: both \mathbf{x}^t and \mathbf{w}^t stay near a cycle for an extended number of steps (typically several thousand steps for $M = 6$) before returning to chaotic behavior for a similar time. An example of this is given in Fig. 2.9.

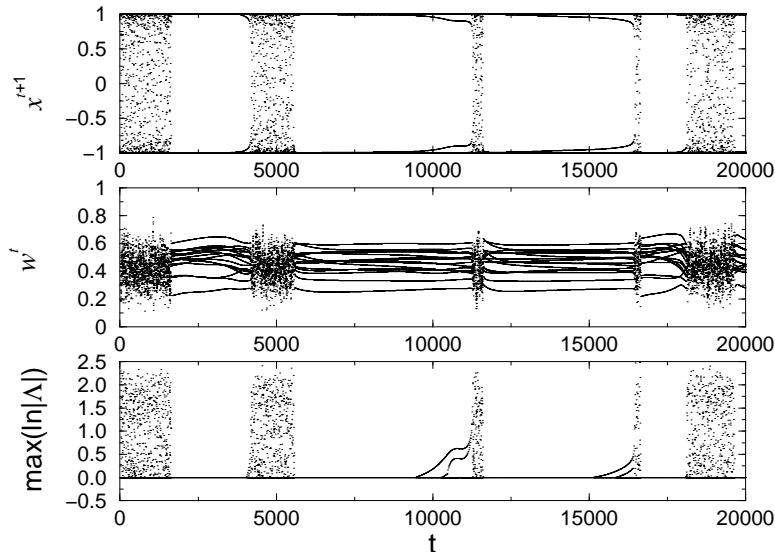


Figure 2.9: Example of intermittent behavior for $M = 6$, $\gamma = 8$. From top to bottom: output x^{t+1} , norm of weights w^t and largest “one-step Lyapunov exponent” $\max(\ln(|\Lambda|))$ (see Section 2.3.5).

2.3.5 Chaotic dynamics and Lyapunov exponents

The term ‘chaotic’ was used in a loose meaning in Sec. 2.3.4 to describe the irregular time series generated by the CBG. However, the system is in fact chaotic in the strict sense, i.e., small deviations in the initial conditions grow exponentially.

Propagation of perturbations in one time step

The sensitivity of trajectories of the map given by Eqs. (2.25) and (2.26) to small changes in the initial conditions can be tested by calculating the eigenvalues of the Jacobi matrix

$$\mathbf{M}^t = \begin{pmatrix} \frac{\partial x_i^{t+1}}{\partial x_j^t} & \frac{\partial x_i^{t+1}}{\partial w_j^t} \\ \frac{\partial w_i^{t+1}}{\partial x_j^t} & \frac{\partial w_i^{t+1}}{\partial w_j^t} \end{pmatrix}. \quad (2.32)$$

This is to be understood as a $2M \times 2M$ matrix with indices i and j running from 1 to M . It describes the evolution of infinitesimal perturbations $\Delta \mathbf{x} \oplus \Delta \mathbf{w}$ during one time step.

The entries of this matrix are of the following form:

$$\begin{aligned}
\frac{\partial x_1^{t+1}}{\partial x_j^t} &= -\beta w_j^t \frac{2}{\sqrt{\pi}} \exp(-\beta^2 h^2); \\
\frac{\partial x_i^{t+1}}{\partial x_j^t} &= \delta_{i-1,j} \text{ for } i = 2, \dots, M; \\
\frac{\partial x_1^{t+1}}{\partial w_j^t} &= -\beta x_j^t \frac{2}{\sqrt{\pi}} \exp(-\beta^2 h^2); \\
\frac{\partial x_i^{t+1}}{\partial w_j^t} &= 0 \text{ for } i = 2, \dots, M; \\
\frac{\partial w_i^{t+1}}{\partial x_j^t} &= -\frac{\eta}{M} \operatorname{erf}(\beta h) \delta_{i,j} - \frac{\eta}{M} \beta w_j^t x_i^t \frac{2}{\sqrt{\pi}} \exp(-\beta^2 h^2); \\
\frac{\partial w_i^{t+1}}{\partial w_j^t} &= \delta_{i,j} - \frac{\eta}{M} \beta x_j^t x_i^t \exp(-\beta^2 h^2).
\end{aligned} \tag{2.33}$$

If $|\beta h|$ is large and the transfer function is saturated, the exponential terms in Eq. (2.33) are negligible. In that case, the upper left section of \mathbf{M} is occupied only on the first lower off-diagonal, and the lower right section is the $M \times M$ unity matrix. Since the upper right section is identically 0, the lower left part does not enter into the calculation of the eigenvalues either. This is not completely obvious, but it follows from the definition of the determinant of a matrix as the sum over permutations of the matrix elements [45]: if one of the factors of a permutation is from the lower left part, at least one factor must be from the upper right part, which is 0, and therefore that permutation gives no contribution to the determinant.

This simplified matrix has M eigenvalues $\Lambda = 0$ and M eigenvalues $\Lambda = 1$. The eigenvectors of the latter span the space of weight vectors, where small changes to \mathbf{w}^t are transferred unmodified to \mathbf{w}^{t+1} . The eigenvalues $\Lambda = 0$ all have the same eigenvector, whose only non-vanishing component is x_M , the component of the sequence vector that is rotated out at $t+1$. This means that the eigenvectors do not span the whole space and that thus the eigenvalues are not a reliable measure of the propagation of a disturbance in the system.

If $|\beta h|$ is small enough for the exponential terms to have an appreciable effect, the effect on the eigenvalues is not easy to calculate. By using values of \mathbf{x} and \mathbf{w} taken from a run of the simulation and numerically calculating the eigenvalues, one finds that typically one of the $\Lambda = 0$ eigenvalues is changed drastically and may have an absolute value $|\Lambda| > 1$. This corresponds to a strong susceptibility of the newly generated sequence component x_1 on small changes in \mathbf{w} or \mathbf{x} . The other eigenvalues only undergo small corrections, corresponding to the feedback of the new component to the weights.

During the regular phases of intermittent behavior, the largest eigenvalues of the one-step matrix are significantly smaller than during the chaotic bursts (see

Fig. 2.9) – corresponding to sequence values that are close to $x = \pm 1$, and thus a nearly saturated transfer function.

Long-time behavior

To find the Lyapunov exponents of the map, which describe the exponential growth or decay of small perturbations of the initial conditions (see e.g. Ref. [46]), it is necessary to consider the development of a small perturbation over a long time, i.e., to calculate the eigenvalues Λ_i^T of $\prod_{t=1}^T \mathbf{M}^t$ (of course, the trajectory is determined using the full nonlinear map). The Lyapunov exponents are then defined as

$$\lambda_i = \lim_{T \rightarrow \infty} (1/T) \ln |\Lambda_i^T|. \quad (2.34)$$

The straightforward calculation of the product of Jacobi matrices brings many numerical problems which can be eliminated by applying a Gram-Schmidt orthonormalization procedure to the columns of the product matrix in regular distances, as described in Ref. [47]. With this procedure, it is possible to average over $T > 100M$ and get numerically stable results. The largest Lyapunov exponent is displayed in Fig. (2.10). Typically, there are $M/2$ positive exponents.

Attractor dimension

The Kaplan-Yorke conjecture [48] states that there is a connection between the dimension D of a attractor of a map and the spectrum of Lyapunov exponents, which are here assumed to be ordered ($\lambda_1 \geq \lambda_2 \geq \dots \geq \lambda_{2M}$):

$$D_{KY} = k + \sum_{i=1}^k \lambda_i / |\lambda_{k+1}|, \quad (2.35)$$

where k is the value for which $\sum_{i=1}^k \lambda_i > 0$ and $\sum_{i=1}^{k+1} \lambda_i < 0$. Applying this to the spectrum of exponents derived from (2.34) gives an average attractor dimension between $1.1M$ and $1.2M$, slightly depending on γ .

The attractor dimension is a measure for the effective number of degrees of freedom of a chaotic system. It cannot be larger than the number of dynamic variables of the system (which, in this case, is $2M$). A much smaller number is possible, as seen in the case of the SGen (Sec. 2.3.1), where the quasi-periodic attractor is one-dimensional. In that case, all components of the sequence vector are strongly correlated. The fact that the Kaplan-Yorke dimension of the CSG is larger than M indicates that its pattern components are more or less independent.

Lyapunov exponents for large M

An alternative method for measuring the largest Lyapunov exponent is to start two trajectories with infinitesimally different initial conditions, and propagate

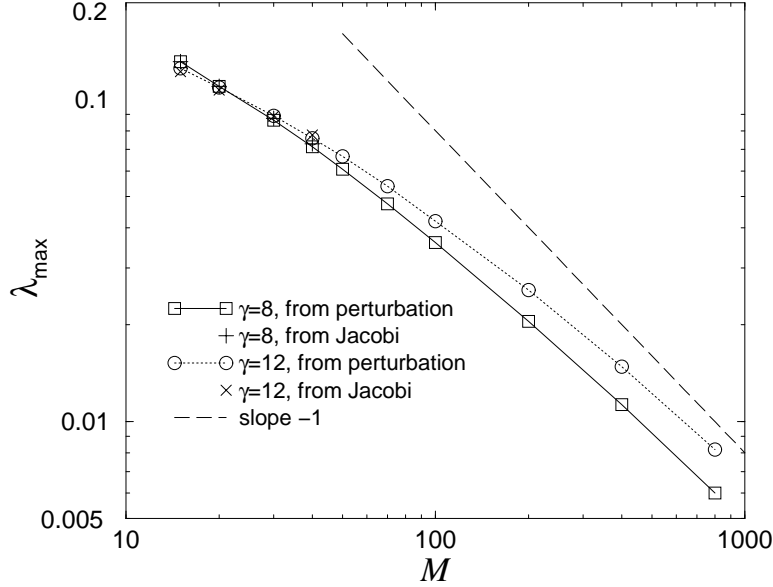


Figure 2.10: Lyapunov exponents measured from the time development of perturbations and from propagating the Jacobi matrix (Eq. (2.34)), for $\gamma = 8$ and $\gamma = 12$.

both of them using the nonlinear map. In regular intervals, measure the distance between the trajectories, store it, and reset the distance to the initial value while keeping the direction of the distance vector.

Since the largest Lyapunov exponent dominates the growth of the perturbation, the contribution of all other Lyapunov exponents can be neglected for sufficiently long times. The advantage of this method is that it requires only $\mathcal{O}(M)$ calculations per time step, rather than $\mathcal{O}(M^2)$ like the previous way, allowing to go to much higher M .

The results for λ_1 are also displayed in Fig. 2.10: the values gained by the two methods agree well within the numerical errors. For large M , λ_{max} decreases with $1/M$, i.e., perturbations grow on the α -timescale of online learning.

This is slightly astonishing, since the matrix Eq. (2.33) has entries that are proportional to $1/M$, but also entries that are of order 1. In the limit of large M , one would expect that it is these entries that are responsible for the growth of deviations. In that simplifying picture, the CSG is similar to the SGen with fixed weights, but is kept in the chaotic transient by the slow movement of weights. However, even in that picture, it takes M time steps for a perturbation to spread throughout all the variables: the matrix entries of order 1 affect the newly generated sequence component, which is then rotated through the M -component pattern vector step-by-step. This would explain the $1/\alpha$ -behavior of the Lyapunov exponents.

2.3.6 Summary of the CSG

Just like for the Confused Bit Generator, the step from fixed to variable weights qualitatively changes the behavior of the system: while the SGen usually generates a quasi-periodic sequence, the CSG is a rather complicated nonlinear mapping that shows many of the trademarks of chaotic systems: high-dimensional chaos, intermittency, the emergence of stable attractors upon variation of the control parameter γ . The existence of an attractive absorbing state makes the study of chaotic behavior difficult for small M . For large M , chaos is stable enough for solid numerical measurements of Lyapunov exponents and other statistical quantities.

The mean square of the norms and outputs can be calculated in a mean-field-like approach, which correctly predicts the saddle-node bifurcation at which a fairly stable chaotic regime becomes possible. Quantitative differences between the calculation and simulations have their origin in temporal correlations between patterns and outputs.

2.4 Decision Tables

2.4.1 Decision tables and DeBruijn graphs

If binary histories are considered, the most general prediction algorithm consists of a Boolean function that has an individual prediction for each possible history. The downside of this generality is that no generalization is possible: since there is no notion of similarity between two histories, one cannot deduce correlations along the lines of “similar histories usually lead to similar consequences”. To make this clearer, and for convenient notation, histories will be denoted by a single number μ , written out as a binary string such as 110010, instead of a vector $\mathbf{x} = (1, 1, -1, -1, 1, -1)$.

There are two convenient ways to visualize a Boolean function: one is a lookup table which contains, in each row, a history μ and a prediction a^μ , as in the example given in Fig. 2.11.

The other representation of the Boolean function takes a graph-theoretical perspective, using directed DeBruijn graphs of order M (see Fig. 2.12 for an example of such a graph). These graphs have one node for each possible pattern μ . Furthermore, each node has two edges entering it, coming from the two possible predecessors, which I denote ${}^0\mu$ and ${}^1\mu$. For example, if $\mu = 1100$, the possible predecessors are ${}^0\mu = 0110$ and ${}^1\mu = 1110$. Each edge also has two outgoing edges, leading to the two possible successors μ^0 and μ^1 (for $\mu = 1100$, the successors are $\mu^0 = 1000$ and $\mu^1 = 1001$). The graph is connected, since one can reach each node from any other node in a maximum of M steps by taking the appropriate exit edges.

μ	a_0^μ
000	0
001	0
010	1
011	1
100	0
101	1
110	1
111	0

Figure 2.11: A Boolean function for $M = 3$, represented as a decision table.

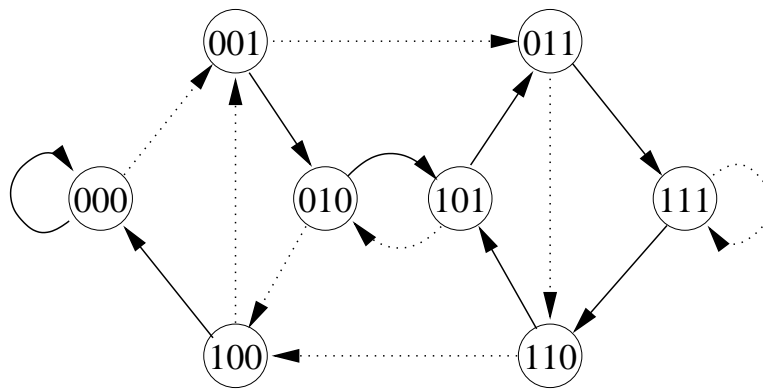


Figure 2.12: The Boolean function from Fig. 2.11 represented as a directed DeBruijn graph of order 3: Nodes represent binary strings of length 3, edges lead to strings that are generated by shifting the current string one position and adding either 0 or 1 as the new least significant bit. Solid lines denote the active exit.

A DeBruijn graph can be modified to represent a Boolean function by labeling only the exit corresponding to a^μ of each node μ “active”. The sequence can then be easily found by going from node to node following the active exits.

2.4.2 Static tables

Each cyclic sequence in which any M -bit pattern appears at most once can be predicted by a suitably prepared M -bit Boolean function. At most, these sequences have length 2^M : namely, if all patterns appear exactly once. These sequences are *Hamiltonian circuits* or *full cycles* on the DeBruijn graph of order M . These cycles have been studied extensively; for a review, see Ref. [49]. One of the central (and oldest) results [50] is the number of different Hamiltonian cycles, which is $2^{2^{M-1}-M}$.

When the system is initialized randomly, there is only a slim chance that the cycle indeed has full length: there are 2^{2^M} possible initial states of the decision table, of which only $2^{2^{M-1}-M}$ correspond to a full cycle – a fraction of $2^{-2^{M-1}-M}$. Most cycles are significantly shorter. The following crude estimate, which ignores much of the structure of the DeBruijn graph, will nevertheless give an approximation of average cycle lengths.

Consider a random graph with the following properties: each of the N nodes has two potential incoming edges and two outgoing edges, of which only one is active. Which node is connected to which is random. You are starting on one node and following the active exits until you come back to a node that you have visited before (i.e., you enter a cycle). Given that you have traveled τ time steps without entering a cycle, the chance of hitting a cycle in the next step is $p_h(\tau) = \tau/2N$ – there are $2N$ possible entrances, but each of the previously visited nodes is weighted only with one entrances, because the other one was already “spent” – it is connected to the node you visited one step earlier.

The probability of entering the cycle for the first time after t steps is

$$P_h(t) = \prod_{\tau=1}^{t-1} (1 - p_h(\tau)) p_h(t). \quad (2.36)$$

Since at that time there are t nodes that can be re-visited (or rather $t - 1$, but this is just an approximation anyway), the cycle that is hit after t steps has an average length $l = t/2$. A further approximation deals with the product in Eq. (2.36):

$$\prod_{\tau=1}^t [1 - \tau/(2N)] \approx [1 - t/(4N)]^t \approx \exp[-t^2/(4N)]. \quad (2.37)$$

The average cycle length is then the sum over all transient times, weighted with

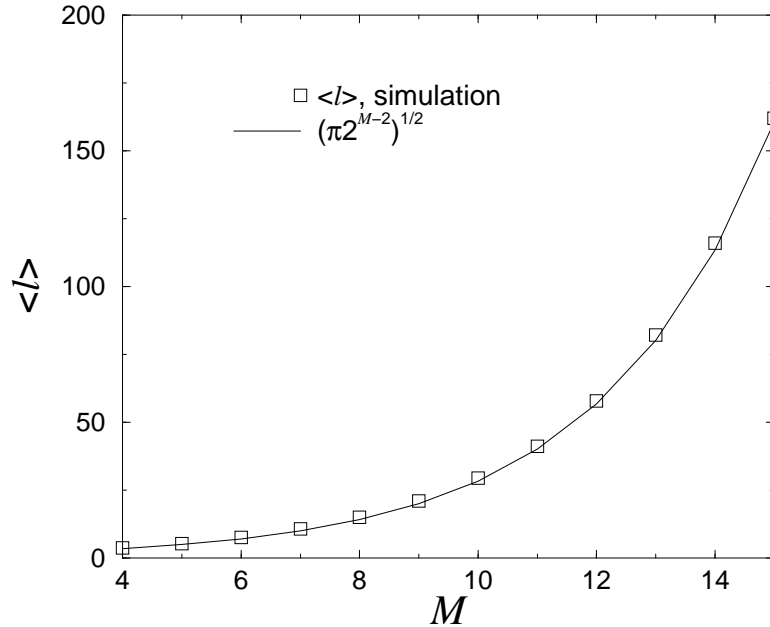


Figure 2.13: Average cycle length of a static Boolean table, starting from random initial conditions: averages over at least 10^4 runs are compared to Eq. (2.38).

the right probability. The sum can be approximated by an integral:

$$\langle l \rangle = \sum_{t=1}^{\infty} P_h(t)t/2 \approx \int_0^{\infty} dt \exp\left(-\frac{t^2}{4N}\right) \frac{t^2}{4N} = \frac{\sqrt{\pi}}{2} \sqrt{N}. \quad (2.38)$$

Using $N = 2^M$ from the DeBruijn graph, the average cycle length scales with $2^{M/2}$. Simulations give a remarkably good fit to the value calculated in Eq. (2.38), as seen in Fig. 2.13.

2.4.3 Dynamic tables: complete antipersistence

As pointed out in the introduction, a prediction algorithm needs a learning rule in order to adapt to a given problem. The simplest learning rule for decision tables is to set the table entry corresponding to the current history to the observed value of the time series.

In order to generate the time series that is completely antipredictable for this prediction algorithm, the entries in the decision table have to be changed at every time step.⁴ To be precise, the algorithm is as follows: At each time step,

⁴The feature that two consecutive appearances of a pattern are likely followed by different outputs was called “antipersistence”, e.g. in Ref. [51]. Usually this term is applied to continuous time series with a Hurst exponent < 0.5 [52]; however, I will use it for binary time series, in the sense mentioned above.

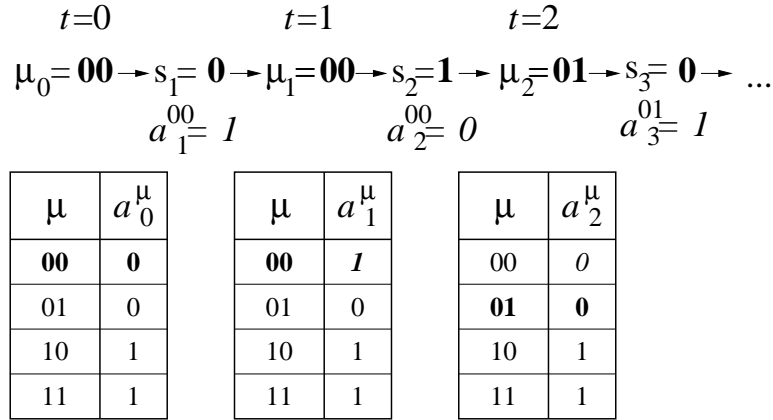


Figure 2.14: An example of a decision table with $M = 2$ and two steps of the dynamics. Boldface numbers indicate the current history and the table entry used for continuing the sequence; italic numbers denote the last table entry that was changed. The sequence generated in this example is 010...

- a new bit is generated by taking the table entry corresponding to the current history μ_t : $s_{t+1} = a_t^{\mu_t}$;
- the history is updated: $\mu_{t+1} = (2\mu_t + s_{t+1}) \bmod 2^M$; i.e., all bits are shifted one position to the left (multiplication with 2), the newly generated bit is added, and the oldest (most significant) bit is dropped (division modulo 2^M);
- the table entry $a_t^{\mu_t}$ that was used for making the decision is changed, such that the sequence will be continued with the opposite decision when the pattern μ_t occurs the next time: $a_{t+1}^{\mu_t} = 1 - a_t^{\mu_t}$. All other entries remain unchanged.

It should be noted this definition of the dynamics is different from the definition as it was used for the CBG: the output of the generator is used for continuing the sequence, rather than the inverse of the output. However, the same time series could be generated by taking always the inverse of the output, but using the inverse of the decision table for initial conditions. I chose the convention presented above to avoid the paradox that one would travel through the graph following the *inactive* exits.

As in the case of the confused perceptron, the internal parameters of the prediction algorithm (in this case, the table entries) become dynamical variables. As an example, three steps of the combined dynamics of sequence and table for $M = 2$ are shown in Fig. 2.14.

In terms of DeBruijn graphs, history moves from one node to the next along the currently active exit. After the move, the exit of the node that was just left is switched, as shown in Fig. 2.15.

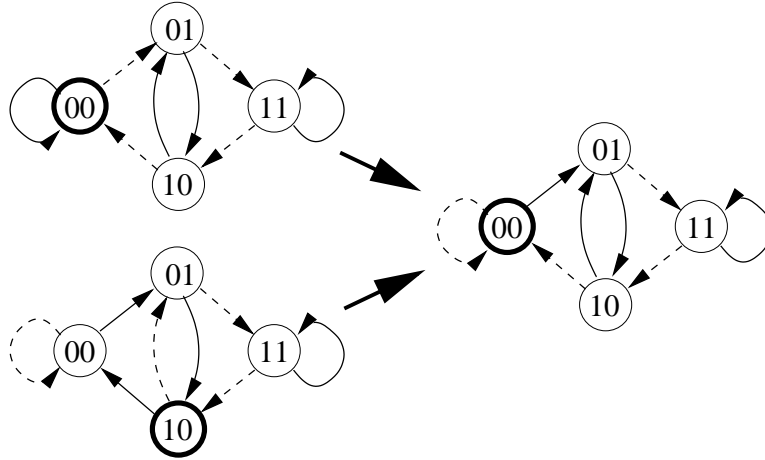


Figure 2.15: Example for a step of the dynamics on a graph of order 2. Active exits are denoted by solid lines, inactive ones by dashed lines. The bold circle indicates the node currently visited. Both the upper left configuration (which happens to be part of a cycle, and corresponds to the example in Fig. 2.14) and the lower one (which is part of a transient) lead to the configuration on the right, which shows that the dynamics is irreversible (see Sec. 2.4.4).

2.4.4 Properties of cycles

The introduced dynamics is deterministic, and the combined system of pattern and table has a finite number $\Omega = 2^M \cdot 2^{(2^M)}$ of different states, so the dynamics necessarily leads into a cycle eventually. The dynamics is irreversible: if a currently visited node has two inactive entrances, it is impossible to tell which path the system took to get to its current state (for an example, see Fig. 2.15). This means that not every state can be part of a cycle, so we will have to consider the necessary conditions for being in a cycle. I will show, step by step, that all cycles are of length $2 \cdot 2^M$ and touch all nodes exactly twice.

Some of the proofs that now follow are redundant; on the other hand, they help to understand the properties of the system, and some of them are applicable to generalizations of the problem, whereas others are not.

Let us assume that at time 0, the system is already moving on a cycle of length l . We count the number of times that a history μ has occurred between time 0 and time t by a visit number v_t^μ . Since the definition of a cycle is that after l steps the system must be in the same state again, it is necessary that v_t^μ is even for all μ , since the table entries a^μ return to their original state only after even numbers of visits.

Also, *all possible nodes are part of the cycle*. Let us prove this by assuming the opposite, namely that there are some nodes that are not touched by the cycle. Since the graph is connected, there must be unused connections between the part of the graph involved in the cycle and the part that is left out. But as

we have seen in the paragraph before, the visit number of each of the nodes that are actually part of the cycle must be at least 2 (larger than 0, and even), so each of its two exits is used, including the one leading to the part of the graph supposedly not included in the cycle. This is a contradiction, so all nodes are involved.

An even stronger statement is possible: the total number of visits to the predecessors ${}^0\mu$ and ${}^1\mu$ of μ must be equal to twice the number of visits to μ , since exactly half of the visits they get are followed by μ , while the other half is followed by the so-called conjugate state $\bar{\mu}$ of μ . (For example, 001 is the conjugate state of 000.) Thus, we have

$$v_i^\mu = (v_i^{0\mu} + v_i^{1\mu})/2 \quad \text{for all } \mu. \quad (2.39)$$

This can be written as a linear equation for an eigenvector with eigenvalue 1 of a matrix \mathbf{M} , with entries $a_{\nu\mu} = 1/2$ if μ is a possible successor of ν and $a_{\nu\mu} = 0$ otherwise. For example, for $M = 2$, the set of Eqs. (2.39) looks as follows:

$$\left[\begin{pmatrix} \frac{1}{2} & 0 & \frac{1}{2} & 0 \\ \frac{1}{2} & 0 & \frac{1}{2} & 0 \\ 0 & \frac{1}{2} & 0 & \frac{1}{2} \\ 0 & \frac{1}{2} & 0 & \frac{1}{2} \end{pmatrix} - \mathbb{1}_4 \right] \begin{pmatrix} v_i^{00} \\ v_i^{01} \\ v_i^{10} \\ v_i^{11} \end{pmatrix} = \begin{pmatrix} 0 \\ 0 \\ 0 \\ 0 \end{pmatrix}. \quad (2.40)$$

Since the sum of columns in matrix \mathbf{M} is always 1, and the individual entries are ≥ 0 , and it describes transitions on a connected graph, we can apply results from the theory of stochastic matrices to state that it has one unique eigenvector with eigenvalue 1 [53], and we easily guess that $v_i^\mu = \text{const}$ fulfills Eq. (2.39). That means that in a cycle, *all states are visited with the same frequency*.

The next step is to show that in a cycle, each node is exactly visited twice, i.e., all cycles of length $4 \cdot 2^M$, $6 \cdot 2^M$, and so on, are in fact two, three or more repetitions of a $2 \cdot 2^M$ -cycle. Again, assume the system is moving on a cycle. If this cycle were truly longer than $2 \cdot 2^M$, there must, at the point $t = 2 \cdot 2^M$, be nodes that have been visited three or more times while others have not been visited for the second time – the visit numbers must add up to $2 \cdot 2^M$, and if all visit numbers were equal to 2, the cycle would be complete. More specifically, there must be an earlier time when all visit numbers v_i^ν are either 0, 1, or 2, and one node is about to be visited for the third time. It suffices to show that this cannot happen to prove that the cycle cannot be longer than $2 \cdot 2^M$.

The third visit to a node μ with $v^\mu = 2$ cannot come from a predecessor (let us say, ${}^0\mu$) with a visit number of $v^{0\mu} = 0$, for the obvious reason that this predecessor has not been visited yet. It also cannot come from a predecessor with $v^{0\mu} = 1$: if $v^\mu = 2$, either it must have been visited before from ${}^0\mu$ (which it cannot – the predecessor has only had one visit so far), or it must have been reached twice from ${}^1\mu$ – this is impossible as well, since it means that $v^{1\mu} \geq 3$. For similar reasons, we can exclude a visit from a node with $v^{0\mu} = 2$: either $v^{1\mu} \geq 3$

as before, or the first visit to ${}^0\mu$ led to μ – then the second cannot. This means that all nodes must receive two visits – thus finishing a cycle – before one of them can be visited for the third time. The question arises why this line of reasoning does not hold true during the transient. The key lies in the observation that the first node to receive three visits is the node where the system was started – it did not get its first visit *from* anywhere on the graph, so the arguments are not applicable.

Using all previous conclusions, the cycles turn out to be of the kind mentioned before: since every combination of M -bit pattern and following bit, i.e., every $M + 1$ -bit pattern, occurs exactly once, the cycles are Hamiltonian paths, or *full cycles*, on the $M + 1$ -graph. Again using results from Ref. [50], we know that there are $2^{2^M - (M+1)}$ distinct Hamiltonian paths.

All possible full cycles on the $M + 1$ -graph can be generated by the antipersistent walk on the M -graph: write down the desired sequence starting at some arbitrary point, look for the first occurrence of each M -bit pattern μ , and set the corresponding table entry to the bit that follows it. Starting the antipersistent walk at the first pattern of the desired sequence, the antipersistent walk will reproduce it.

Since all cycles are of length $2 \cdot 2^M$, a total of $2 \cdot 2^M \times 2^{2^M - (M+1)} = 2^{(2^M)}$ states is part of a cycle. As mentioned before, the total number of possible states is $\Omega = 2^M \cdot 2^{(2^M)}$, which means that a fraction of $2^{(2^M)} / \Omega = 2^{-M}$ of possible states is part of a cycle. It is thus interesting to check how long it takes for the system to reach a cycle, i.e. study the distribution of transient lengths τ . This distribution is not easily accessible to analytical approaches, but easy to measure in computer simulations, either by complete enumeration for small systems or by Monte Carlo simulations for larger ones. The following picture emerges, as shown in Fig. 2.16:

The probability for transient length $\tau = 0$ is just the probability of hitting a cycle right away, and thus the fraction of state space filled with cycles. As mentioned, this is equal to 2^{-M} .

The probability distribution is more or less flat for $1 \leq \tau \leq 2^{M+1}$, the cycle length. From normalization constraints, it follows that $p(\tau) \approx 2^{-(M+1)}$ in that range.

Near $\tau = 2^{M+1}$, there is an exponential drop reminiscent of a phase transition, which gets steeper with increasing M . Even for small M , no transients longer than 2^{M+2} have been observed.

Antipersistence on different timescales

Obviously, a sequence that is antipredictable for one algorithm can be perfectly predictable for another. Is it necessary for that other algorithm to be completely different in its structure, or is it maybe enough to adjust some parameters? To answer this question for this particular algorithm, it suffices to let an observer predict the antipersistent time series using a decision table, and vary the memory

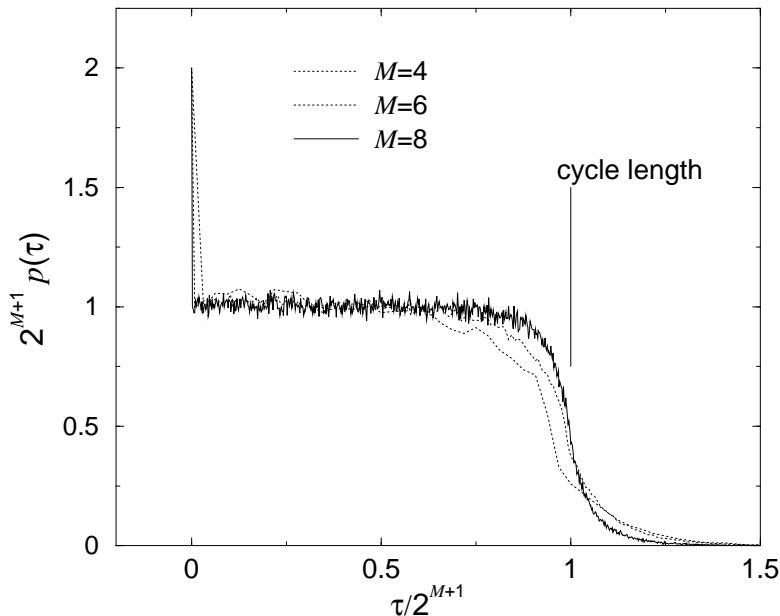


Figure 2.16: Distribution of transient lengths τ , rescaled by the cycle length 2^{M+1} .

length of the observer. For simplicity's sake, we consider the long-time limit, in which both the generator and the observer move on a cycle.

If the observer looks at the same time window as the generator ($M_{obs} = M$), it is obvious that the success rate will be 0 – since each pattern is continued with alternating bits on each visit. For an observer with a slightly larger window, the picture changes: as mentioned above, the antipersistent cycle corresponds to a Hamiltonian cycle on the $M + 1$ -graph, which is completely persistent and predictable with 100% accuracy. For even larger M_{obs} , the antipersistent cycle looks like a closed path which includes only a fraction of $2^{M-(M_{obs}+1)}$ of nodes on the M_{obs} -graph. Prediction is again 100% reliable, and the observer does not even need all of his storage capacity to handle the cases that occur.

If the observer has a shorter time window than the generator, more than one of the generator's patterns will affect the same table entry for the observer. For example, an $M - 1$ -bit pattern ν corresponds to either of the M -bit strings 0ν or 1ν , both of which occur twice in the M -cycle, each time followed by a different successor. The success rate of the predictor depends on the sequence in which these combinations occur; if each permutation of $0\nu0$, $0\nu1$, $1\nu0$ and $1\nu1$ has the same probability, the success rate for all patterns is the average over the different permutations. Fig. 2.17 shows that this average is $1/3$ for $M_{obs} = M - 1$.

For $M_{obs} = M - 2$, all permutations of eight combinations of predecessors and successors have to be taken into account – a task best left to computer algebra programs, which yield $\langle s(M, M - 1) \rangle = 3/7$, in excellent agreement with

permutation				e.r.
0 μ 0	0 μ 1	1 μ 0	1 μ 1	4/4
0 μ 0	0 μ 1	1 μ 1	1 μ 0	2/4
0 μ 0	1 μ 0	0 μ 1	1 μ 1	2/4
0 μ 0	1 μ 0	1 μ 1	0 μ 1	2/4
0 μ 0	1 μ 1	1 μ 0	0 μ 1	4/4
0 μ 0	1 μ 1	0 μ 1	1 μ 0	2/4
total:				16/24

Figure 2.17: Possible permutations of predecessors and successors of a pattern ν on a cycle. The error rate, given in the last column, is the rate of flips between 0 and 1 in the sequence of successors.

simulations (see Fig. 2.18). Larger differences in the time window are beyond even the scope of computer programs; however, it can be argued that for larger $M - M_{obs}$, the visits to the M_{obs} -nodes become more and more random, and $s(M, M_{obs})$ will tend to $1/2$.

To answer the question raised above, it is thus not always necessary to go to structurally completely different algorithms or updating methods to turn a negative overlap into a positive one. However, as the next section shows, increasing the amount of information that is processed does not always improve prediction accuracy.

2.4.5 Stochastic antipersistence

All of the observations from the last sections relied on the fact that the generator is on a cycle with well-known properties. It is thus interesting to ask how stable these results are if the sequence is not completely antipersistent. The simplest generalization is to introduce a probability p for changing the table entry/ exit when visiting a node: $p_{AP} = 1$ reproduces the completely antipersistent walk; $p_{AP} = 0$ is equivalent to using a constant (quenched) decision table, and $p = 1/2$ generates a completely random time series.

A first intuitive guess would be that even a small deviation from deterministic dynamics completely destroys all predictability: after all, on a path of length 2^{M+1} , there are on the average $(1 - p_{AP})2^{M+1}$ occasions where the the sequence is continued persistently, thus leaving the cycle. Indeed, a single “error” is usually enough to move the system from one cycle to another; however, much of the local structure remains untouched. It turns out that the functions $s(M, M_{obs}, p_{AP})$ of prediction rates converge for large M (meaning roughly $M > 12$) to a set of

curves that depend only on p_{AP} and $M - M_{obs}$, which is displayed in Fig. 2.18.

The limit values for $p_{AP} = 1$ have been explained above, and they are approached continuously for $p_{AP} \rightarrow 1$. For $p_{AP} = 0.5$, the curves intersect at $s = 0.5$ – no prediction beyond guessing is possible. For small p_{AP} , all curves converge to 1: the system is dominated by short loops in which only a small fraction of the possible states participate, and those are predicted with high accuracy.

Interestingly, between $p_{AP} = 0.5$ and roughly $p_{AP} = 0.85$, all shown curves are below 0.5, meaning that even observers with longer memory predict the sequence with less than 50% accuracy. I will give an analytical argument why this is the case for $M_{obs} = M + 1$. An $M + 1$ -bit pattern ν is a combination of an M -bit pattern μ and one of its predecessors, let us say ${}^0\mu$, whereas the companion state $\hat{\nu}$ is a combination of μ and the other predecessor ${}^1\mu$. A visit to either ν or $\hat{\nu}$ switches the exit of μ with probability p_{AP} . Consider two subsequent visits to ν , with some number l of visits to $\hat{\nu}$ between them. The probability $s(p_{AP}, M, M + 1)$ of continuing with the same bit after these two visits is a sum of two probabilities: either the exit of μ was switched upon leaving ν the first time and then switched an odd number of times during the l visits to $\hat{\nu}$, or it was not switched the first time and switched an even number of times in between. Given p_{AP} and the probability $\pi_l(p_{AP}, M)$ of having l intermediate visits to $\hat{\nu}$, one then obtains by basic combinatorics

$$s(p_{AP}, M, M + 1) = \sum_{l=0}^{\infty} \frac{1}{2} \pi_l(p_{AP}, M) [1 + (1 - 2p_{AP})^{l+1}]. \quad (2.41)$$

Unfortunately, $\pi_l(p_{AP}, M)$ does not seem to be analytically accessible for general p_{AP} . It can be measured in simulations, and the accuracy of Eq. (2.41) can be verified (see Fig. 2.18); also, for $p = 1/2$, since the system does a completely random walk on the graph, one gets the simple distribution $\pi_l(1/2, M) = 2^{-(l+1)}$. Assuming that this distribution does not change discontinuously near $p + AP = 1/2$, Eq. (2.41) yields the approximation $s(1/2 + \delta p, M, M + 1) \approx 1/(2 + 2\delta p) \approx (1/2)(1 - \delta p)$. This is obviously $< 1/2$ for $\delta p > 0$, i.e., $p_{AP} > 1/2$.

Numerical evidence suggests that near the point of random guessing, the approximation $s(1/2 + \delta p, M, M_{obs}) \approx 1/2 + 2^{-|M - M_{obs}|} \delta p$ holds, i.e., the prediction success is below 1/2 for all small $\delta p > 0$, but the deviation from guessing decreases as the difference in time scales increases. As an educated guess, one can extrapolate that as $M_{obs} - M \rightarrow \infty$, the success rate will be close to 1/2 for all values of p_{AP} except very close to $p_{AP} = 0$ and $p_{AP} = 1$, where it will approach 1.

The error rate $1 - s(p_{AP}, M, M_{obs})$ is a measure of the antipersistence of the time series on the scale M_{obs} – for $M_{obs} = M$, $1 - s$ is completely equivalent to the antipersistence parameter p of the underlying dynamics. However, even if $s(p_{AP}, M, M + 1)$ could be calculated, it would not be possible to recursively

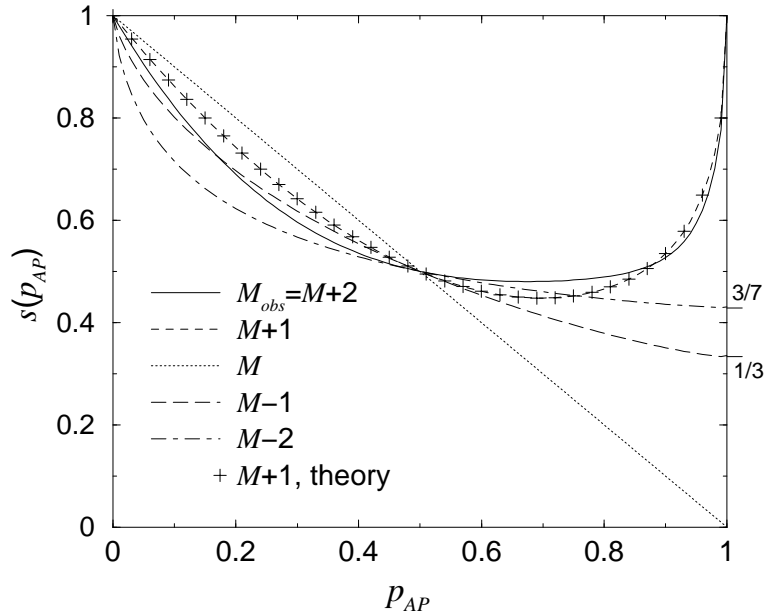


Figure 2.18: Success rate of an observer keeping a table of the recent occurrence of M_{obs} -bit strings and the respective following bit, for $M = 16$. p_{AP} is the probability of flipping the exit in the generating graph. The symbols labeled “theory” were calculated using Eq. (2.41) with approximate probabilities $\pi_l(p_{AP}, M)$ taken from the simulation itself.

apply this function to find the antipersistence on the scales $M + 2, M + 3$ etc. In other words,

$$1 - s(p_{AP}, M, M + 1) \neq 1 - s(\{1 - s(p_{AP}, M, M + 1)\}, M + 1, M + 2). \quad (2.42)$$

It is thus not sufficient to give a single parameter p_{AP} , or $1 - s$, for some M in order to characterize the behavior of a time series completely and to calculate its predictability on other scales of observation. The scale on which the dynamics work is important as well.

2.4.6 Summary of antipersistent time series

Every prediction algorithm is sensitive to specific features in the time series. For the perceptron, this feature was autocorrelations. For decision tables, it is fairly obvious: it is the probability that a given pattern is followed by a certain bit. Apparently, antipredictable sequences suppress the sensitive feature of their corresponding prediction algorithm: in a completely antipersistent time series generated by an M -bit decision table, the probability of continuing an M -bit pattern with 1 is 50%.

This means that all quenched preferences for patterns vanish if antipersistence is introduced: all patterns appear with equal probability. In the deterministic antipersistent time series, it is even possible to prove that all patterns appear exactly twice during one cycle. This is a recurring theme of antipredictable time series: cycles are longer than for predictable algorithms, because the state space of the generating algorithm becomes larger.

I have also shown that observers that keep track of the most recent occurrence of M_{obs} -bit strings can predict the completely antipersistent cycle with 100% accuracy if $M_{obs} > M$, and with less than 50% success rate if $M_{obs} \leq M$. If the stochasticity is introduced by means of a probability p_{AP} of flipping the exit edges, the success rate even of observers with $M_{obs} > M$ can drop below 50%, which shows that larger memory does not necessarily give better results. The rate of antipersistence on one scale is not sufficient to calculate the rate for other scales, which again shows that a time series is antipredictable only for a specific algorithm with specific parameters, including memory length.

Chapter 3

The Minority Game and its variations

3.1 Introduction

In recent years, physicists have applied methods from statistical physics and time series analysis to problems in sociology, biology, and economics [54, 55, 56]. One of the important techniques was the invention and analytical treatment of toy models that still capture essential properties of vastly more complex real-world problems. The Minority Game [13], which has inspired more than 100 publications so far, has become one of the most influential models.

The inspiration for the Minority Game (MG) comes from the El-Farol bar problem brought up by W. B. Arthur [57]: a popular bar has a limited capacity for patrons. If fewer people attend, they have a good time. If the capacity is exceeded, the bar is crowded, and the potential patrons who decided to stay at home that night made the better choice. Arthur's hypothesis was that people have a number of possible prediction algorithms to decide whether to go or stay home, and that they pick the algorithm they use according to their individual success with that algorithm. As a result, attendance fluctuates around the saturation value.

The underlying idea of the El-Farol scenario is competition for limited resources, and can be applied to a large number of different fields. One often-cited example is stock markets, where it pays off to sell if everyone else wants to buy, and to buy if there are many bids to sell. Other possible scenarios include alternative roads between two locations, the specialization of animals on food sources or habitats, a university student's choice of field with a view to job prospects later on, and many more.

One obvious feature of these scenarios is that no "best strategy" can exist: if it did, it would be the same for all players (since there are no a priori differences between them), every player would make the same choice, and all would lose.

The game thus relies on coordination between the players: the aim is to find a niche that few others occupy, and the means cannot be deduction and careful planning, but only inductive thinking – learning from experience and trial and error.

In Arthur’s paper [57], each potential patron has a repertoire of fundamentally different prediction algorithms, which use the time series of previous attendances to predict how crowded the bar will be. He monitors how well each algorithm predicts the actual history, and chooses the most successful one.

This idea was simplified and formalized in the original MG by Challet and Zhang (see Sec. 3.3), where the threshold for overcrowding was set to half the number of players, and the different prediction algorithms were modeled by randomly chosen decision tables (Boolean functions). However, other rules of behavior are conceivable, like fine-tuning the parameters of one prediction algorithm such as a neural network (see Sec. 3.4) or changing individual entries in a decision table if they do not seem to bring success (Sec. 3.6). Another interesting generalization is to allow for more than two different options, as detailed in Sec. 3.7. Again, all sorts of strategies are conceivable in this situation. The following sections give an overview over the different strategies, with plenty of detail on my contributions to the field. Where possible, I will try to point out where the behavior of the players leads to antipredictability in the generated time series.

3.2 Rules of the Minority Game

In all variations of the Minority Game that will be described, the following rules hold:

- there is an (odd) number N of players $i = 1, \dots, N$.
- at each time step t each player makes a decision $\sigma_i^t \in \{+1, -1\}$ (buy/ sell, go/ stay at home, take the highway/ take the country road etc.).
- the minority is determined: $S^t = -\text{sign}(\sum_i \sigma_i^t)$; the players in the minority win ($\sigma_i^t = S^t$), the others lose.
- global efficiency can be measured by

$$\sigma^2 = \left\langle \left(\sum_i \sigma_i^t \right)^2 \right\rangle_t . \quad (3.1)$$

Random guessing would result in $\sigma^2 = N$. Smaller values indicate good coordination, whereas larger values (often of order N^2) indicate herding behavior: finite fractions of the player population correlate their decisions and effectively act as a single agent [58].

- players cannot make contracts or otherwise communicate with each other. The only exchange of information is through the global minority.
- consequently, players can use a window of the global history for making their decision. In many cases, however, very similar or identical results are achieved if the actual history is replaced by an artificial (random) history [59].

3.3 The standard Minority Game

In a series of publications by Challet and Zhang [60, 61] and Challet, Marsili and Zecchina [62], the following model, which became known as the “standard Minority Game”, was introduced and studied numerically and analytically:

Each player is equipped with two decision tables A_+ and A_- , each of which prescribes an action a_+^μ or a_-^μ for each state of the world μ . The state is often taken to be the string of the last M global minority decisions; e.g., if M is set to 3, and in the last three steps the global decision was $-1, -1, 1$, the current state, or “history”, is $\mu = (-1, -1, 1)$. Each decision table thus has 2^M entries, which are determined randomly at the beginning of the game. Of course, each player can only use one decision table at any given time, so he keeps scores for each table and follows the table with the highest score.

The sign of the sum of all players’ choices $A^t = \sum_i \sigma_i^t$ then determines who wins. Those in the minority ($s_i^t = -\text{sign}(A^t)$) gain a point, the others lose. Players also update the scores of their decision tables: Tables that would have predicted the minority sign ($a_\pm^\mu = -\text{sign}(A^t)$) gain a point, regardless of whether this table was used or not. Tables that gave “bad advice” lose a point on their score. Then the game is repeated, and players make choices based on the updated state of the world and possibly use a different decision table than before.

As mentioned above, success or failure of coordination can be measured with the standard deviation of A , usually referred to as $\sigma^2 = \langle A^2 \rangle$ in the literature. Random guessing of all players leads to $\sigma^2 = N$; a value $\sigma^2/N < 1$ therefore indicates successful coordination, whereas $\sigma^2/N > 1$ is a sign of “herd behavior”: agents adapt the same strategies that others are using as well, leading to larger fluctuations.

Closer analysis shows that the relevant parameter in the original MG is the ratio $\alpha = 2^M/N$ of entries in the decision table to the number of players. It is also possible to replace the time series with a random state of the world, with p possible states. The control parameter is then $\alpha = p/N$. For $\alpha > \alpha_c \approx 0.33740$ (i.e., few players, compared to the number of fundamentally different strategy tables available), there is fairly good cooperation ($\sigma^2/N < 1$). However, the frozen disorder in the decision tables causes some preference in the outputs generated by the system: each pattern μ leads to outputs $+1$ or -1 with probabilities

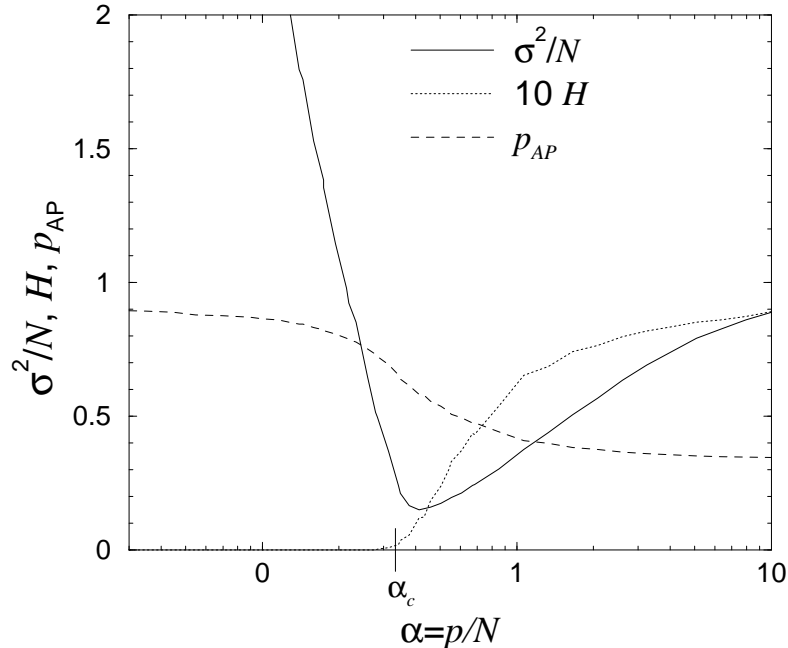


Figure 3.1: Standard minority game: results of simulations for σ^2/N , H and the antipersistence parameter p_{AP} as a function of $\alpha = p/N$. H is multiplied by 1- for better visibility. Simulations use $N = 201$ and random patterns.

$P^\mu(\pm 1) \neq 1/2$. The average deviation of this probability from $1/2$ can be quantified by defining

$$H = \frac{1}{p} \sum_{\mu} p(P^\mu(+) - 1/2)^2. \quad (3.2)$$

At $\alpha = \alpha_c$, the information that can be extracted from the time series in this fashion vanishes in a second-order phase transition. Instead, dynamics become ergodic (i.e., each pattern μ is visited with the same frequency) and increasingly antipersistent (i.e., if a pattern μ results in $\text{sign}(A) = +1$, the probability p_{AP} of getting -1 on the next occurrence of μ is larger than 0.5). The interpretation is that players overreact to occurrences of a pattern, switching to a strategy that prescribes the opposite reaction for the next time that this pattern occurs. This can lead to dramatic crowding, with $\sigma^2 \propto N^2$ as $\alpha \rightarrow 0$. These results are illustrated in Fig. 3.1.

The standard MG can be solved analytically by treating the choice between the two decision tables as a spin variable and applying the replica method to find the ground state of the system [61, 62]. This analysis reveals that the quenched preference for specific outputs is necessary to achieve coordination. If players have two completely opposite decision tables instead of two random (and hence, approximately orthogonal) tables, there is no bias to be exploited, and σ^2/N goes to 1 for all values of η .

Newer studies [63, 64] have shown that the dynamics in the crowded phase depend strongly on initial conditions: if the initial difference between the scores of the two decision tables are drawn randomly from a sufficiently wide distribution, only few players switch from one table to the other in response to one pattern, and coordination becomes better.

3.4 Neural Networks in the MG

An alternative strategy for the Minority Game was first presented in Ref. [21] (although with an erroneous calculation) and published in Refs. [65] and [66]: each player is equipped with a simple neural network (a perceptron, to be precise) that is fed with the vector of past minority decisions.

In a sense, the ensemble of perceptrons is an inverted committee machine: the regular hard committee machine is a two-layer neural network where the output is given by the majority of outputs of the perceptrons that make up the first layer [18, 67, 68], whereas in our case the minority decides who wins. Another difference is that a large number of training algorithms for the committee machine are not compatible with the rules of the MG: since the “members” of the committee machine can communicate and cooperate, it is for example possible to select the perceptron with the smallest hidden field and modify only it – the so-called least-action algorithm. The players in the Minority Game cannot compare notes, and they are assumed to be greedy – foregoing an opportunity to join the winning side in favor of a co-player is not possible in the model.

Therefore, only learning algorithms that include quantities locally available to the neural networks are allowed. The simplest (and the only one for which an analytical solution exists so far) is Hebbian learning of all networks.

The calculation I will now present is a correct, more complete version of that in my Diploma thesis [21]. It is included for the sake of completeness and because it facilitates understanding of the slightly more involved calculation for multi-choice neural networks in Sec. 3.7.2.

3.4.1 Ensembles of vectors

As mentioned, each player in this variation of the MG has a perceptron with an individual weight vector \mathbf{w}_i to make his decision:

$$\sigma_i = \text{sign}(\mathbf{x} \cdot \mathbf{w}_i). \quad (3.3)$$

When considering a population of players, it is helpful to split the weight vectors into a center-of-mass vector

$$\mathbf{C} = \frac{1}{N} \sum_i^N \mathbf{w}_i \quad (3.4)$$

and relative vectors

$$\mathbf{r}_i = \mathbf{w}_i - \mathbf{C}. \quad (3.5)$$

These relative vectors are automatically anti-correlated: if the initial conditions are chosen such that $|\mathbf{r}| = r = 1$, one gets from the condition $\sum \mathbf{r}_i = 0$

$$\langle \mathbf{r}_i \cdot \mathbf{r}_j \rangle_{i \neq j} = \frac{1}{N-1} \sum_{i \neq j} \mathbf{r}_i \cdot \mathbf{r}_j = -\frac{1}{N-1} \quad \text{for } i \neq j. \quad (3.6)$$

A different norm of r can, of course, be included in the calculation by replacing $|\mathbf{C}| = C$ by C/r in the appropriate places. If the initial vectors are chosen at random such that $\langle r \rangle = 1$, it is a fair approximation that each pair of vectors individually is anti-correlated as in Eq. (3.6) if the dimensionality of the space they live in is large enough: the variance $\langle (\mathbf{r}_i \cdot \mathbf{r}_j + 1/(N-1))^2 \rangle$ is of order $1/M$.

The average scalar product between two different weight vectors is now

$$\langle R \rangle_{i,j} = \frac{1}{N(N-1)} \sum_{i,j \neq i} \mathbf{w}_i \cdot \mathbf{w}_j = C^2 - 1/(N-1), \quad (3.7)$$

and their average norm is

$$\langle w \rangle_i = \frac{1}{N} \sum_i \sqrt{\mathbf{w}_i^2} \approx C^2 + 1. \quad (3.8)$$

The correlation between the output of two perceptrons on the same random input pattern \mathbf{x} is

$$\langle \text{sign}(\mathbf{x} \cdot \mathbf{w}_1) \text{sign}(\mathbf{x} \cdot \mathbf{w}_2) \rangle_{\mathbf{x}} = 1 - \frac{2}{\pi} \arccos \left(\frac{\mathbf{w}_1 \cdot \mathbf{w}_2}{w_1 w_2} \right). \quad (3.9)$$

With these relations, the global efficiency $\sigma^2 = (\sum_i \sigma_i)^2$ can be calculated:

$$\begin{aligned} \frac{\sigma^2}{N} &= \frac{1}{N} \left\langle \sum_{i=1}^N 1 + \sum_{i,j \neq i}^N \text{sign}(\mathbf{x} \cdot \mathbf{w}_i) \text{sign}(\mathbf{x} \cdot \mathbf{w}_j) \right\rangle_{\mathbf{x}} \\ &= 1 + (N-1) \left(1 - \frac{2}{\pi} \arccos \left(\frac{C^2 - 1/(N-1)}{C^2 + 1} \right) \right). \end{aligned} \quad (3.10)$$

If C is set to 0 and N is large, a linear expansion of the arccos term in Eq. (3.10) gives $\sigma_{opt}^2/N \approx 1 - 2/\pi \doteq 0.363$. The small anticorrelations (of order $1/K$) between the vectors suffice to change the prefactor in the standard deviation.

If C is much larger than r , there is a strong correlation between the perceptrons. Most perceptrons will agree with the classification by the center of mass $\text{sign}(\mathbf{x} \cdot \mathbf{C})$. As $C \rightarrow \infty$, σ^2/N saturates at N .

What these considerations have shown is that, assuming symmetry between the perceptrons, the system can be described by the number N of players and one order parameter, C (or, strictly speaking, C/r). The next section describes what happens to that order parameter during a simple learning process.

3.4.2 Hebbian Learning

The most remarkable property of neural networks is the ability to adjust their parameters to unknown rules using efficient learning algorithms, and this is what the players in this model do: At each round of the game, each perceptron is trying to learn the decision of the minority according to the Hebbian learning rule. S denotes the minority decision, and the superscript $+$ denotes the updated quantity after the learning step:

$$\mathbf{w}_i^+ = \mathbf{w}_i - \frac{\eta}{M} \mathbf{x} \text{sign}\left(\sum_{j=1}^N \text{sign}(\mathbf{x} \cdot \mathbf{w}_j)\right) = \mathbf{w}_i + \frac{\eta}{M} \mathbf{x} S. \quad (3.11)$$

As the same correction is added to each weight vector, their mutual distances remain unchanged. Only the center of mass is shifted, and a simple equation for its movement can be found:

$$\mathbf{C}^+ = \sum_{i=1}^N \frac{\mathbf{w}_i}{N} + \frac{\eta}{M} \mathbf{x} S. \quad (3.12)$$

$$C^{2+} = C^2 + \frac{2\eta}{M} \mathbf{x} \cdot \mathbf{C} S + \frac{\eta^2}{M}. \quad (3.13)$$

To average over $\mathbf{x} \cdot \mathbf{C} S$ in the thermodynamic limit, it is helpful to split the hidden fields $h_i = \mathbf{x} \cdot \mathbf{w}_i$ into contributions from the center-of-mass, $h^C = \mathbf{x} \cdot \mathbf{C}$, and relative fields $h_i^r = \mathbf{x} \cdot \mathbf{r}_i$. For a given h^C , one can then average over \mathbf{x} :

$$\mathbf{x} \cdot \mathbf{C} S = -|h^C| \text{sign}\left(\sum_{i=1}^N \text{sign}(h^C) \text{sign}(h_i^r + h^C)\right). \quad (3.14)$$

The quantity $\text{sign}(h^C) \text{sign}(h_i^r + h^C)$ is a random variable with mean $\text{erf}(|h^C|/\sqrt{2})$ and variance $1 - \text{erf}(|h^C|/\sqrt{2})^2$. In a linear approximation for small $|h^C|$, I can replace this by mean $\sqrt{2/\pi}|h^C|$ and variance 1. It becomes clear in Eq. (3.15) why this linear approximation is admissible: in the range where it is no longer valid, the effect of h^C has already saturated.

For sufficiently large N , one can use the central limit theorem [69] to show that $\sum_{i=1}^N \text{sign}(h^C) \text{sign}(h_i^r + h^C)$ becomes a Gaussian random variable with mean $\sqrt{2/\pi} N |h^C|$. Since the terms of the sum in (3.14) are anticorrelated rather than independent, the variance turns out to be $(1 - 2/\pi)N$ rather than N , analogously to Eq. (3.10).¹ This yields

$$\left\langle \text{sign}\left(\sum_{i=1}^N \text{sign}(h^C) \text{sign}(h_i^r + h^C)\right) \right\rangle_{h_i^r} = \text{erf}\left(\sqrt{N/(\pi - 2)} |h^C|\right). \quad (3.15)$$

¹This was the source of confusion in Ref. [21]: the anticorrelation was not taken into account properly. In a guessed fit to simulations, the factor $\pi - 2$ that appears in the calculation was then replaced by 1.

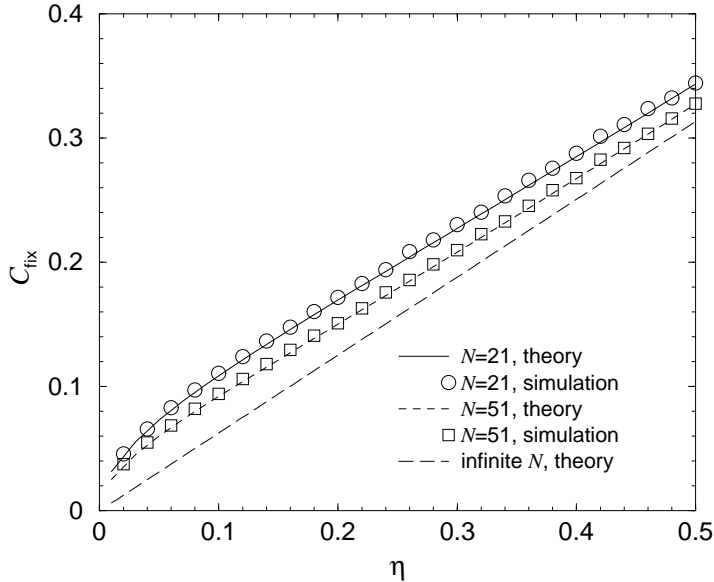


Figure 3.2: Fixed point of C vs. η : simulations with $M = 100$ agree well with Eq. (3.17). The limit for $N \rightarrow \infty$ is $C = \sqrt{2\pi\eta}/4$.

Since h^C is a Gaussian variable with mean 0 and variance C^2 , the average over $h^C S$ can now be evaluated. The following differential equation for the norm of the center of mass results:

$$\frac{dC^2}{d\alpha} = -\frac{4\eta}{\sqrt{2\pi}} \sqrt{\frac{2N/(\pi-2)}{1+2N(\pi-2)C^2}} C^2 + \eta^2. \quad (3.16)$$

The fixed point of C , which can be plugged into Eq. (3.10) to get σ^2/N as a function of η and N , is

$$C_{fix} = \frac{\sqrt{\pi}}{4} \eta \sqrt{1 + \sqrt{1 + \frac{16(\pi-2)}{\pi N \eta^2}}} \quad (3.17)$$

(see Figs. 3.2 and 3.3).

For small C , h^C has only a small influence on the decision of the majority. If the majority disagrees with $\text{sign}(h^C)$, the learning step has a positive overlap with \mathbf{C} . This leads to $C \propto \sqrt{\eta}$ as $\eta \rightarrow 0$.

If C is large, the majority of perceptrons will usually make the same decision as \mathbf{C} , which then behaves like the single confused perceptron: $C \rightarrow \sqrt{2\pi\eta}/4$ if $K\eta^2 \rightarrow \infty$ – compare to Eq. (2.7).

For small C , the majority may not coincide with $\text{sign}(\mathbf{x} \cdot \mathbf{C})$. In that case, the learning step has a positive overlap with \mathbf{C} , leading to $C \propto \sqrt{\eta}$ as $\eta \rightarrow 0$.

The last points are important, since they relate the Minority Game to antipredictability. They are therefore worth a second look. The probability that

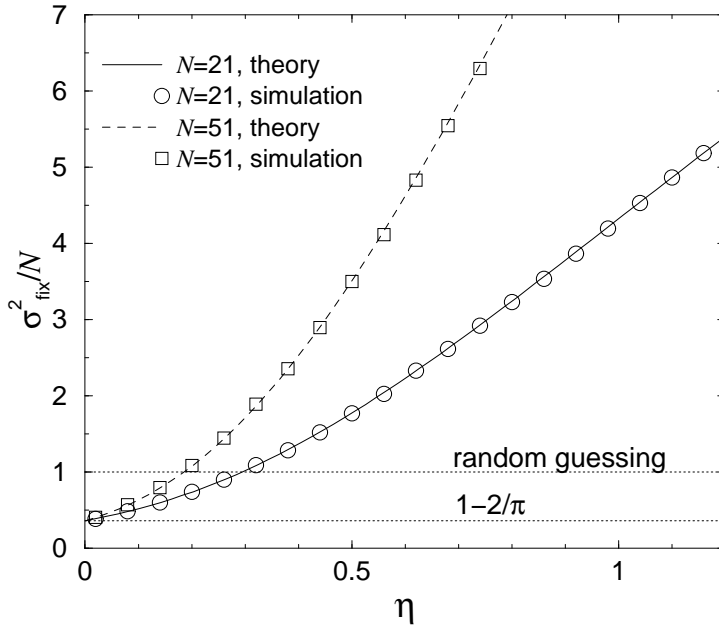


Figure 3.3: Fixed point of σ^2/K vs. η : the combination of Eqs.(3.10) and (3.17) shows that sufficiently small learning rates lead to $\sigma^2/K < 1$.

the majority agrees with the output of the center of mass can be calculated easily. The most important step has already been done, in Eq. (3.15). This can be integrated over the distribution of h^C to get

$$\text{Prob}(\text{sign}(\sum_i \sigma_i) = \text{sign}(\mathbf{x} \cdot \mathbf{C})) = 1 - \frac{1}{\pi} \arctan \left(\sqrt{\frac{\pi - 2}{2NC^2}} \right). \quad (3.18)$$

This result is compared to simulations in Fig. 3.4. It shows the crossover of the time series from essentially random behavior to a high probability of agreeing with the center of mass. In that limit, the ensemble of players could almost be replaced by a single effective player (represented by a confused perceptron) for the purpose to time series generation.

Concludingly, neural networks that learn the output of the minority with Hebbian learning can coordinate well in the Minority Game, reducing the measure of global loss σ^2/N by a factor of up to 0.363. However, if learning rates are not small enough, learning causes a positive overlap between the agents, leading to herding behavior and large global losses. The transition between anti-correlated and correlated behavior is a smooth crossover, not a phase transition.

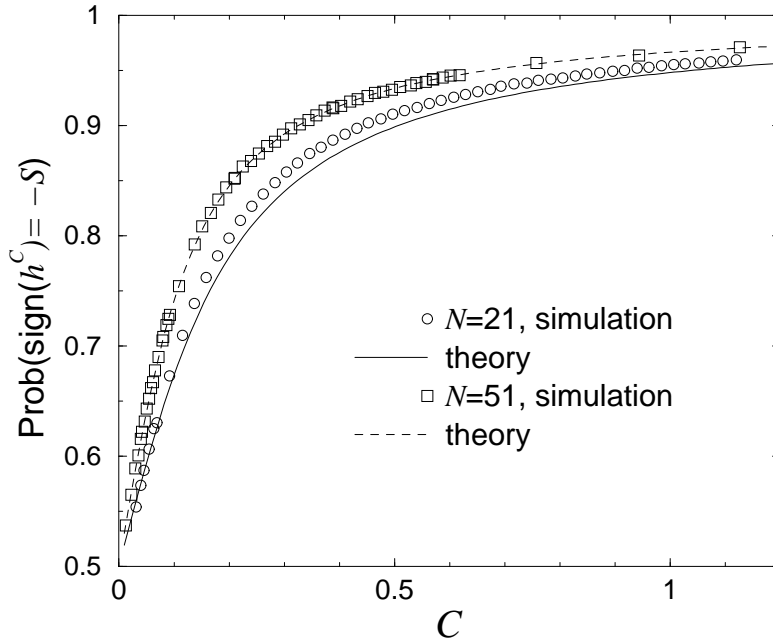


Figure 3.4: Probability that the center of mass determines the decision of the majority: Comparison between Eq. (3.18) and simulations with $M = 100$. Agreement is excellent for $N = 51$, but not so good for $N = 21$.

3.5 Johnson’s evolutionary MG

N. F. Johnson and coworkers introduced another simple set of rules in Ref. [70]: each agent has access to a history table that records the outcome that followed each possible history pattern μ upon the last occurrence of μ . Also, each agent i has an individual probability p_i . In each round, each agent looks at the entry in the history table corresponding to the current pattern μ^t , and chooses this entry with probability p_i ; otherwise, he chooses the opposite of the last “winning option”.

The learning algorithm in Johnson’s scenario is evolutionary: agents who are in the minority gain one point, whereas those in the majority lose one. If an agent’s score falls below a certain threshold $d < 0$, the agent’s strategy is modified, i.e., p_i is changed. The distribution of ps converges to a stationary state where extreme probabilities $p \approx 0$ and $p \approx 1$ are much more likely than intermediate probabilities, as seen in Fig. 3.5.

As Burgos and Ceva pointed out in Ref. [71], the history table is essentially unnecessary in this variation of the game: all players use their individual p_i for each of the possible histories, and there is complete symmetry between $+1$ and -1 . If one is only interested in the distribution of ps and not in the time series generated by the game, one can therefore examine an equivalent game in which

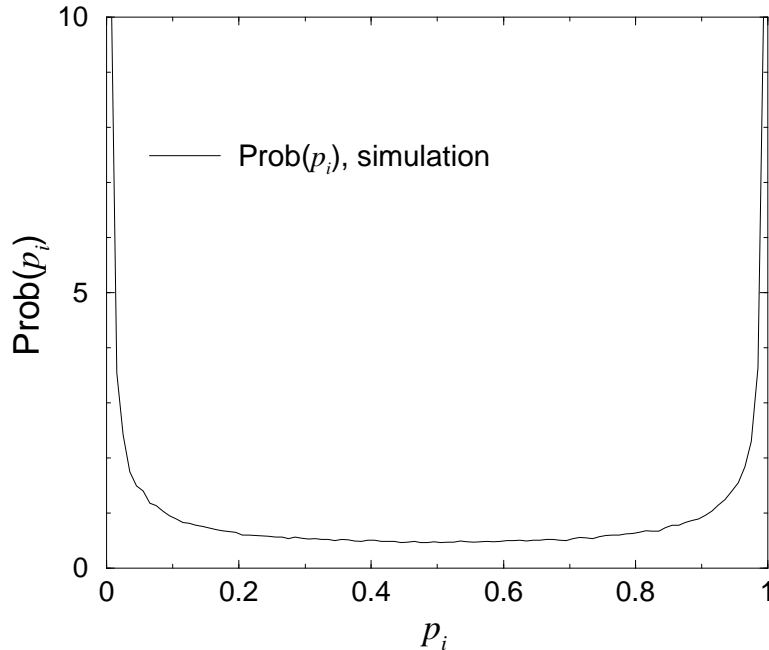


Figure 3.5: Stationary distribution of switch probabilities p in Johnson’s evolutionary MG. Simulations used $N = 1001$ and a threshold $d = -10$; however, results hardly depend on these parameters if $|d|$ is large enough.

each player chooses $+1$ with probability p_i and -1 with $1 - p_i$. One analytical approach was given in Ref. [72]; another theory that models pairs of players whose decisions cancel each other with a given probability was proposed in Ref. [73]. Temporal oscillations were taken into account in a newer study, Ref. [74].

3.6 Reents’ and Metzler’s stochastic MG

Similar in spirit is the strategy suggested by Reents, Metzler and Kinzel in Ref. [75]: players like to stick to the option they chose in the previous round. If a player wins, he has no motivation to change anything, and will choose the same action again. If a player i loses, he will still choose the same action with a probability $1 - p_i$ – after all, times could get better again. However, there is a probability p_i for the player to decide that things have to change – he chooses the opposite action.

Since each player only remembers his current state, the probability of finding the system at a given state at $t + 1$ only depends on the state of the players at t and the parameters p_i and N . The problem is thus a one-step Markov process, and the standard treatment is to calculate the probabilities of finding the game in each possible state.

If each player has the same probability p , the game is fairly easy to describe mathematically: it is unnecessary to keep track of the whole set of $\{\sigma_i\}_{i=1}^N$; instead, one can consider

$$K(t) = \frac{1}{2} \sum_i \sigma_i(t). \quad (3.19)$$

The possible values k that $K(t)$ can take are half-integer and run from $-N/2$ to $N/2$ in steps of 1. This choice of variables may seem awkward, but it is the most convenient. The other possibility, $A = \sum_i \sigma_i$, results in a large number of factors of $1/2$ in the calculation. Furthermore, one player switching sides results in a change in K of one unit, which is easy to remember.

The probabilities to be calculated are

$$\pi_k(t) = \text{prob}(K(t) = k), \quad (3.20)$$

and the dynamics is defined by the transition probabilities

$$W_{k\ell} = \text{prob}(K(t+1) = k \mid K(t) = \ell). \quad (3.21)$$

To shorten notation we consider the probabilities $\pi_k(t)$ as components of the state vector $\boldsymbol{\pi}(t) = (\pi_{-N/2}(t), \dots, \pi_{N/2}(t))^T$. The number of players in the majority at time t is $N/2 + |K(t)|$. Since the individual players perform independent Bernoulli trials, the transition probability $W_{k\ell} = W(\ell \rightarrow k)$ from a state with $K(t) = \ell$ to $K(t+1) = k$ is given by the binomial distribution:

$$\begin{aligned} W_{k\ell} &= \binom{\frac{N}{2} + \ell}{\ell - k} p^{\ell - k} (1 - p)^{\frac{N}{2} + k} \quad \text{for } \ell > 0, \\ W_{k\ell} &= \binom{\frac{N}{2} - \ell}{k - \ell} p^{k - \ell} (1 - p)^{\frac{N}{2} - k} \quad \text{for } \ell < 0. \end{aligned} \quad (3.22)$$

This stochastic process may be considered a random walk in one dimension, where steps of arbitrary size with probability (3.22) are allowed only in the direction of the origin $K = 0$.

Given the initial state $\boldsymbol{\pi}(0)$, the state $\boldsymbol{\pi}(t)$ is updated at each time step by multiplying it by the transition matrix \mathbf{W} :

$$\boldsymbol{\pi}(t+1) = \mathbf{W} \boldsymbol{\pi}(t). \quad (3.23)$$

The mathematical theory dealing with this kind of problems is that of Markov chains with stationary transition probabilities [53]. Since $(\mathbf{W}^2)_{k\ell} > 0$, the chain is irreducible as well as ergodic [76], which implies that regardless of the initial distribution the state $\boldsymbol{\pi}(t)$ converges for $t \rightarrow \infty$ to a unique stationary state $\boldsymbol{\pi}(\infty) \equiv \boldsymbol{\pi}^s$. In view of Eq. (3.23), $\boldsymbol{\pi}^s$ corresponds to an eigenvector of \mathbf{W} with eigenvalue 1:

$$\mathbf{W} \boldsymbol{\pi}^s = \boldsymbol{\pi}^s \quad \text{and} \quad \sum_k \pi_k^s = 1. \quad (3.24)$$

This eigenvector, which characterizes the equilibrium state of the system, can, in principle, be calculated analytically for any N . However, the results are generally rational functions in p whose degree is roughly N – they become rather awkward for larger N , and the computational effort to find them is intolerable. Analytical solutions in a more agreeable form can be found in the two limiting cases of small p ($p = 2x/N$, $N \rightarrow \infty$) and large p ($p = \text{const}$, $p \cdot N \gg 1$).

In intermediate regimes, while analytical results are hard to come by, numerical solutions are easy to obtain. The problem can be simplified by exploiting the symmetry $W_{-k,-\ell} = W_{k\ell}$, which implies the symmetry $\pi_{-k}^s = \pi_k^s$ of the stationary state. By rewriting the eigenvalue problem for the independent components of $\boldsymbol{\pi}^s$ and exploiting the knowledge that the largest eigenvalue is 1, the stationary state is the solution of a linear equation with $N/2$ variables. It can be calculated numerically up to $N \approx 1200$ in reasonable time with standard linear algebra packages.

3.6.1 Solution for small p

If p is so small that only $\mathcal{O}(1)$ players switch sides, it is fairly intuitive that the stationary state is localized within $\mathcal{O}(1)$ of the origin; i.e., only states with $|K| = \mathcal{O}(1)$ have an appreciable probability. This suspicion is confirmed by the analytical calculation in the limit $p = 2x/N$, $N \rightarrow \infty$. The following approximation is good as long as $x \ll N$.

In this case the matrix elements $W_{k\ell}$ can be approximated by Poisson probabilities [53]:

$$\begin{aligned} W_{k\ell} &\rightarrow W_{k\ell}^P = e^{-x} \frac{x^{\ell-k}}{(\ell-k)!} \quad \text{for } \ell > 0, \\ W_{k\ell} &\rightarrow W_{k\ell}^P = e^{-x} \frac{x^{k-\ell}}{(k-\ell)!} \quad \text{for } \ell < 0, \end{aligned} \quad (3.25)$$

where, again, $1/m!$ for negative m has to be interpreted as zero. In the limit $N \rightarrow \infty$ the solution of the problem is an infinite component vector $\boldsymbol{\pi}^s$ satisfying the eigenvalue equation together with the proper normalization:

$$\mathbf{W}^P \boldsymbol{\pi}^s = \boldsymbol{\pi}^s \quad \text{and} \quad \sum_k \pi_k^s = 1. \quad (3.26)$$

This problem was solved by G. Reents, who noticed that the moments of the

stationary distribution follow simple rules:

$$\begin{aligned}
\left\langle |k| - \frac{1}{2} \right\rangle &= \frac{x}{2}, \\
\left\langle \left(|k| - \frac{1}{2} \right) \left(|k| - \frac{3}{2} \right) \right\rangle &= \frac{x^2}{3}, \\
\left\langle \left(|k| - \frac{1}{2} \right) \left(|k| - \frac{3}{2} \right) \left(|k| - \frac{5}{2} \right) \right\rangle &= \frac{x^3}{4}, \\
&\text{etc.}
\end{aligned} \tag{3.27}$$

These in turn determine the characteristic function of π_k^s , and a Fourier transform finally leads to

$$\pi_k^s = \frac{1}{2 (|k| - \frac{1}{2})!} \sum_{j=0}^{\infty} \frac{(-1)^j x^{j+|k|-\frac{1}{2}}}{j! (j + |k| + \frac{1}{2})}. \tag{3.28}$$

Ch. Horn proved in a rather lengthy calculation that Eq. (3.28) indeed satisfies the eigenvalue equation (3.26) [73].

π_k^s can also be expressed by the incomplete gamma function:

$$\pi_k^s = \frac{\gamma(|k| + \frac{1}{2}, x)}{2 x (|k| - \frac{1}{2})!}. \tag{3.29}$$

A comparison with numerically determined eigenvectors of the matrix (3.22) for $N = 801$ gives excellent agreement, as seen in Fig. 3.6. The distribution is roughly flat for small $|k|$, has a turning point near $|k| = x$ and falls off exponentially with k for larger values of $|k|$. From Eq. (3.28), the variance $\sigma^2 = \langle (2k)^2 \rangle$ can be calculated:

$$\sigma^2 = 1 + 4x + \frac{4}{3}x^2. \tag{3.30}$$

For small x , this approaches the optimal value $\sigma^2 = 1$ that occurs if the majority is always as narrow as possible, but even for larger x , σ^2 does not increase with N .

3.6.2 Solution for large p

As mentioned before, an (approximate) analytical solution can also be found if p is of order 1 and $pN \gg 1$. To handle this regime, I introduce a rescaled (continuous) coordinate $\kappa = k/N = \sum_i \sigma_i / (2N)$, the range of which is $-1/2 \leq \kappa \leq 1/2$. Multiplied by N , the stationary state π_k^s for large N turns into a probability density function $\pi^s(\kappa)$, and the matrix $W_{k\ell}$ becomes an integral kernel $W(\kappa, \lambda)$; consequently, the eigenvalue equation Eq. (3.24) is transformed into an integral equation:

$$\pi^s(\kappa) = \int W(\kappa, \lambda) \pi^s(\lambda) d\lambda \quad \text{and} \quad \int \pi^s(\kappa) d\kappa = 1. \tag{3.31}$$

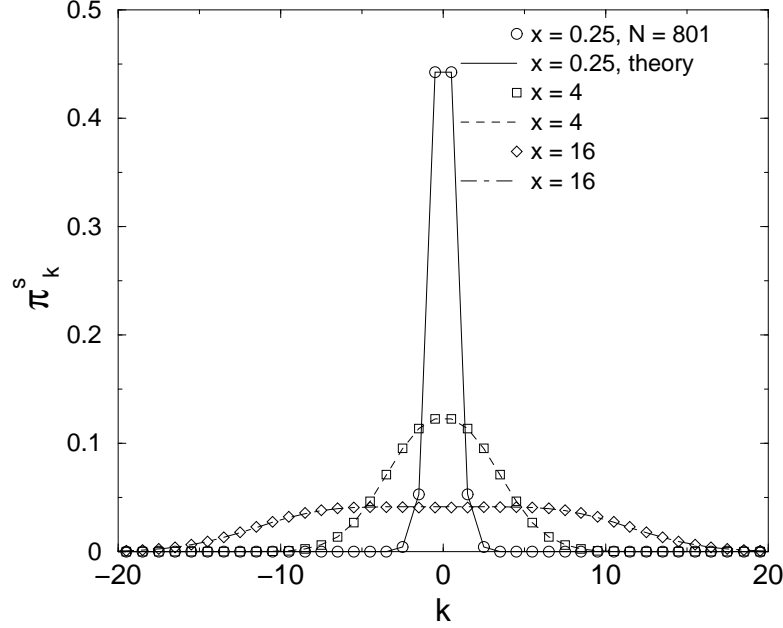


Figure 3.6: Stationary solution π_k^s for $p = x/(N/2)$. The numerical solution for $N = 801$ (symbols) is in very good agreement with the analytical solution for $N \rightarrow \infty$.

Numerical calculations show that the eigenvector $\pi^s(\kappa)$ takes the shape of two Gaussian peaks centered at symmetrical distances $\pm\kappa_0$ from the origin (see Fig. 3.7). The physical interpretation is that the majority switches from one side to the other in every time step. Since approximately $(\kappa_0 + 1/2)pN$ agents switch sides every turn and the distance between the two peaks amounts to a number of $2\kappa_0N$ agents, we get $\kappa_0 = p/(4 - 2p)$.

This reasoning can be made more precise, and also the width of the peaks for large but finite N can be calculated by the following argument: The well known normal approximation for the binomial coefficients in Eq. (3.22) leads to

$$\begin{aligned}
 W(\kappa, \lambda) = N W_{k\ell} &\approx \frac{1}{\sqrt{2\pi} s(\lambda)} \exp\left[-\frac{1}{2} \frac{(\kappa - f(\lambda))^2}{s^2(\lambda)}\right], \\
 \text{where } f(\lambda) &= (1-p)\lambda - \text{sign}(\lambda) \frac{p}{2} \\
 \text{and } s^2(\lambda) &= \frac{p(1-p)(\frac{1}{2} + |\lambda|)}{N}.
 \end{aligned} \tag{3.32}$$

A double Gaussian of the form

$$\pi^s(\kappa) = \frac{1}{2} \frac{1}{\sqrt{2\pi} b} \left[\exp\left(\frac{(\kappa + \kappa_0)^2}{2b^2}\right) + \exp\left(\frac{(\kappa - \kappa_0)^2}{2b^2}\right) \right] \tag{3.33}$$

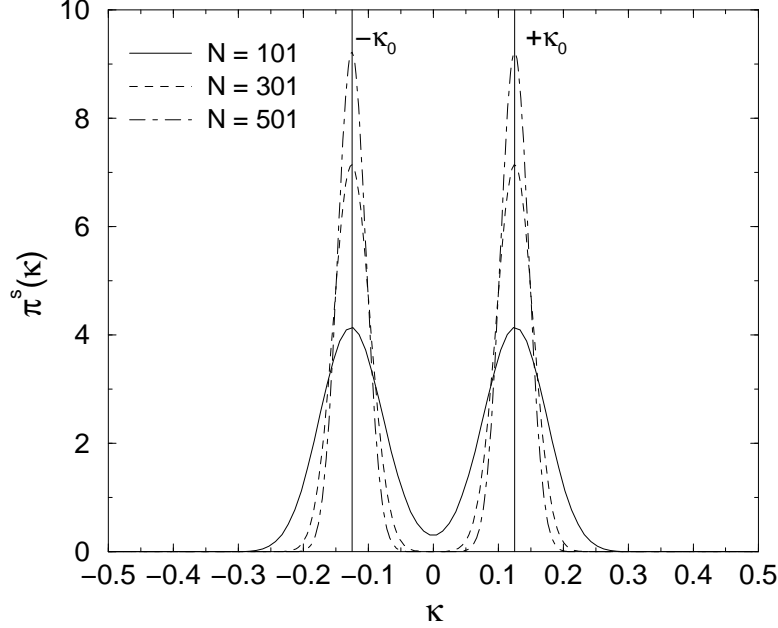


Figure 3.7: Stationary solution $\pi^s(\kappa)$ for $p = 0.4$. With increasing N , the width of the peaks becomes narrower.

is transformed by the integral kernel (3.32) into a double peak of the same type under two approximations:

First, one must approximate $s^2(\lambda)$ of (3.32) by $s^2(\pm\kappa_0)$ in the integral equation. This is justified if the peaks are narrow, i.e., $b^2 \ll 1$.

Second, one must assume that the peaks are well localized on each side of 0, i.e., the tail of the Gaussian on the positive side does not have a significant contribution in the negative range and vice versa. The mathematical condition for this is $b^2 \ll \kappa_0^2$. Also, the peaks should be well separated from $-1/2$ and $+1/2$. If these conditions are fulfilled, one can extend the integral over each peak from $-\infty$ to $+\infty$.

By requiring $\pi^s(\kappa)$ from Eq. (3.33) to satisfy the eigenvalue equation (3.31), one finds

$$\kappa_0 = \frac{p}{2(2-p)} \quad \text{and} \quad b^2 = \frac{1-p}{(2-p)^2 N}. \quad (3.34)$$

The result for κ_0 confirms the simple argument given above, whereas the term for b^2 is slightly surprising: it does not depend on p in the leading order, i.e., it is not simply the number of players who switch sides. Instead, the width of the peaks is the result of two conflicting mechanisms: the variance in the number of players who switch sides makes the peak wider. It is counteracted by a self-focusing mechanism: for example, if the system is at $\kappa = \kappa_0 + b$ at time t , it will on average be at $-\kappa_0 + (1-p)b$ in the next time step, i.e., the average distance from the center $-\kappa_0$ has decreased by a factor $(1-p)$.

Eq. (3.34) also allows to check whether the assumptions made for its derivation are true for a given p and N , i.e., whether the approximation is self-consistent. For example, for $p = x/N$, $\kappa_0^2/b^2 \rightarrow 0$ for $N \rightarrow \infty$ according to (3.34), so one cannot expect the formation of double peaks in this limit. The crossover from single-peak to double-peak distribution occurs for $p \propto 1/\sqrt{N}$.

If the conditions are fulfilled, is easy to integrate over the probability distribution Eq. (3.33) to get an expression for σ^2 :

$$\sigma^2 = \frac{N}{(2-p)^2} (Np^2 + 4(1-p)). \quad (3.35)$$

This agrees well with numerics well if the condition $\kappa_0 \gg b$ is fulfilled, i.e., for sufficiently large p and N , as seen in Fig. 3.8. Numerical evidence shows that

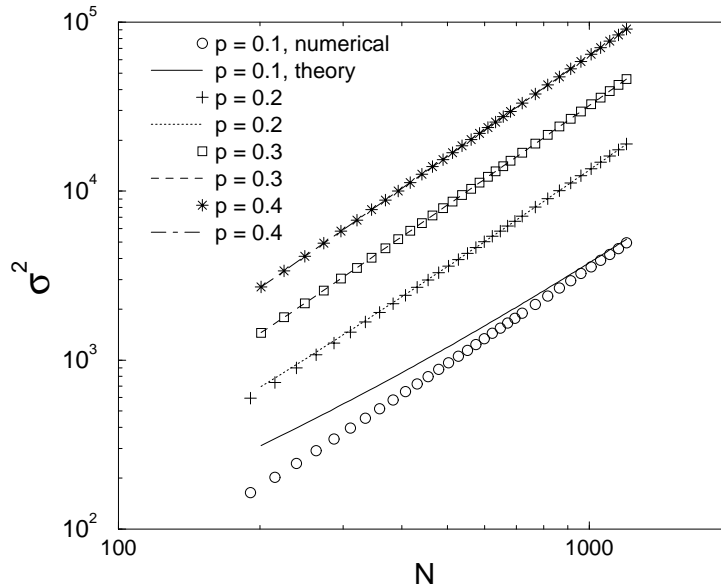


Figure 3.8: σ^2 for several values of p and N , compared to predictions by Eq. (3.35).

σ^2 scales like $\sigma^2 \propto N^2 p^2$ even when the condition $\kappa_0 \gg b$ is not fulfilled, as for $p \propto 1/\sqrt{N}$. In this case we found $\sigma^2 \propto N$, like in the original game of Challet and Zhang and for random guessing. However, the behavior of the system is different: the distribution of κ can have a double peak structure (depending on the proportionality constant) rather than a Gaussian shape, and the minority is still very likely to switch from one side to the other at consecutive time steps.

3.6.3 Mixed strategy populations & susceptibility to noise

In Ch. Horn's diploma thesis [73], computer experiments were presented in which populations with different strategies (decision tables, neural networks, the

stochastic strategy etc.) played in a common minority game, and the success of the strategies depending on the fraction of players that use them was studied. It turned out that in most cases, each of the three mentioned strategies is robust to the presence of a small number of players with other strategies (meaning that the coordination is not completely disrupted by the presence of “strangers”) and that populations that have a large majority of the total population usually score better than the small population using another strategy – the strategies are evolutionarily stable [77].

The susceptibility of a population of players using the stochastic strategy to the presence of other agents can be calculated, provided that the output of these other agents is not strongly correlated to the dynamics of the stochastic players – in other words, the collective output of the alternative-strategy agents can be treated as a random number.

To be more precise, let us assume that among a total on N players, a population of N_S players using the described stochastic strategy competes with $N_R = N - N_S$ players who are simply guessing randomly. The output of guessers can be treated as a random variable K_R , analogous to Eq. (3.19), with a probability distribution

$$\text{Prob}(K_R = k) = \frac{1}{2^{N_R}} \binom{N_R}{k + N_R/2}. \quad (3.36)$$

These guessers only influence the stochastic players’ coordination if they overrule their decision, that is, if $\text{sign}(K_S + K_R) \neq \text{sign}(K_S)$. The probability of that is

$$p_o(K_S) = \frac{1}{2} \text{Prob}(|K_R| > |K_S|) = \frac{1}{2} \sum_{k > |K_S|}^{N_R/2} 2^{-N_R} \binom{N_R}{k + N_R/2}. \quad (3.37)$$

If the decision is overruled, the stochastic players who are on the minority side among their population roll the dice to see whether they change their opinion. In terms of a random walk, there is now a probability $p_o(k)$ that the step from position k leads away from the origin rather than towards it. The entries of the transition matrix have to be changed accordingly:

$$\begin{aligned} W_{k\ell} &= \binom{\frac{N_S}{2} + \ell}{\ell - k} p^{\ell - k} (1 - p)^{\frac{N_S}{2} + k} (1 - p_o(\ell)) \\ &\quad + \binom{\frac{N_S}{2} - \ell}{k - \ell} p^{k - \ell} (1 - p)^{\frac{N_S}{2} - k} p_o(\ell) \quad \text{for } \ell > 0, \\ W_{k\ell} &= \binom{\frac{N_S}{2} - \ell}{k - \ell} p^{k - \ell} (1 - p)^{\frac{N_S}{2} - k} (1 - p_o(\ell)) \\ &\quad + \binom{\frac{N_S}{2} + \ell}{\ell - k} p^{\ell - k} (1 - p)^{\frac{N_S}{2} + k} p_o(\ell) \quad \text{for } \ell < 0. \end{aligned} \quad (3.38)$$

The eigenvalues of this matrix can again be calculated numerically. The agreement with simulations confirms the approach (see Fig. 3.9). In the limit where

$p = 2x/N$ and $N_S \rightarrow \infty$, the distribution depends on the absolute number, not the ratio, of random players.

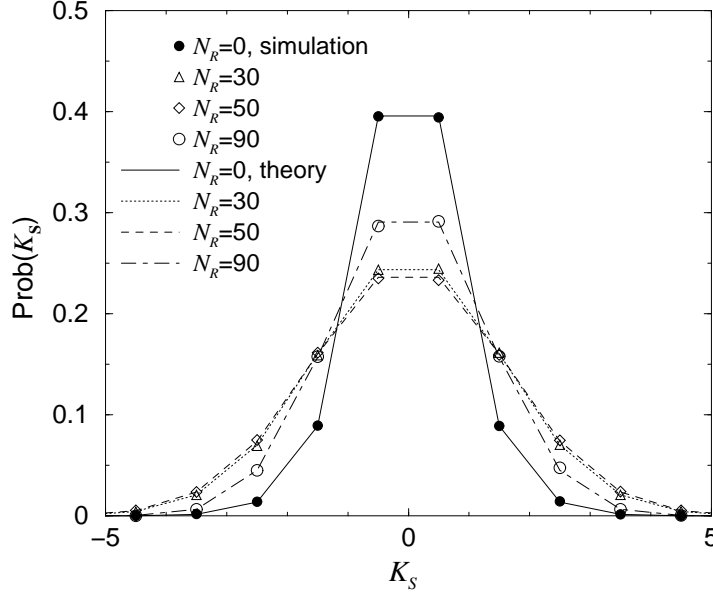


Figure 3.9: Distribution of the output of N_S stochastic players in the presence of $N_R = 101 - N_S$ random players. Simulations are taken from Ref. [73], numerical results are calculated using Eq.(3.38).

Although the width of the distribution of K_S increases slightly from the presence of guessers, this drawback does not have a drastic influence on the average gain (or rather, loss) of the stochastic players: if the guessers overrule the decision made by the stochastic players, that means that the majority of those wins, and they actually increased their population's gain at the expense of the guessers. This argument can easily be quantified: upon averaging the gain using the calculated probability of K_S , the gain is $+2|K_S|$ with probability $p_o(K_S)$ and $-2|K_S|$ otherwise:

$$\langle g_S \rangle = \frac{1}{N} \sum_{K_S} \pi_{K_S}^s [2|K_S|p_o(K_S) - 2|K_S|(1 - p_o(K_S))]. \quad (3.39)$$

Likewise, the gain of the random players can be calculated using the known probability distributions for K_S and K_R . Agreement with simulations is excellent, as seen in Fig. 3.10.

As pointed out in [73], the guessers would be better off in a pure population of N guessers, but worse off if the stochastic players were simply absent, and the N_R guessers made up the whole population. The average loss of isolated random

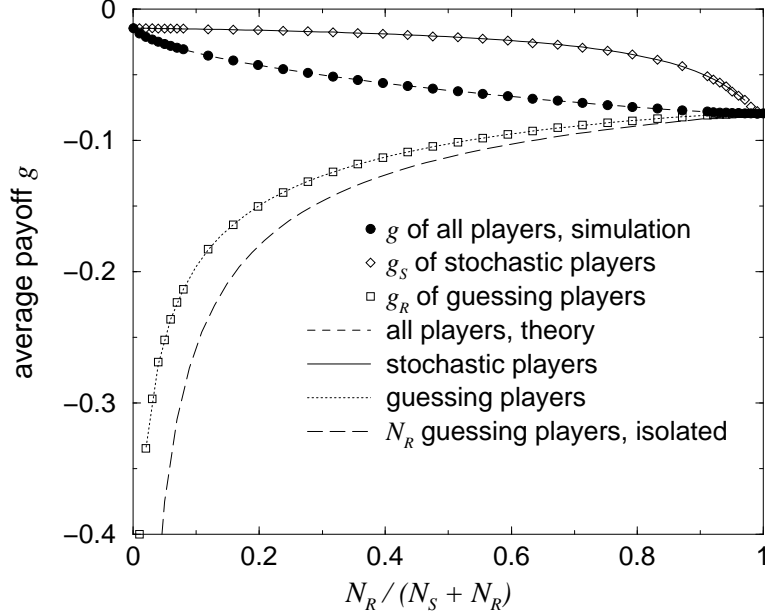


Figure 3.10: Two populations of N_S stochastic players with $p = 1$ and $N_R = 101 - N_S$ random players compete. The numerical results agree excellently with simulations taken from Ref. [73].

players is easy to calculate:

$$\langle g_R \rangle = \frac{1}{N_R} \sum_{K_R=-N_R/2}^{N_R/2} -2|K_R|2^{-N_R} \binom{N_R}{N_R/2 + K_R}, \quad (3.40)$$

and it is worse than that of the mixed population (see Fig. 3.10).

3.6.4 Correlations in the time series

It was mentioned in Sec. 3.6.2 that in the case of fixed p and large N , the majority switches sides at every time step. On the other hand, it is obvious that for $p \ll 2/N$ no player will change his opinion during most time steps, leaving the majority side unchanged. What happens between these extremes?

To answer this question, one can calculate the one-step autocorrelation function $\langle S(t)S(t+1) \rangle$ of the minority sign $S(t)$ from the stationary probability distribution and the transition matrix:

$$\langle S(t)S(t+1) \rangle = \sum_{k,l} \text{sign}(k)\text{sign}(l)\pi_k^s W_{kl}. \quad (3.41)$$

Otherwise, one can simply measure the autocorrelation in a simulation. Figs. 3.11 and 3.12 show the autocorrelation function in the two limits treated in Sec.

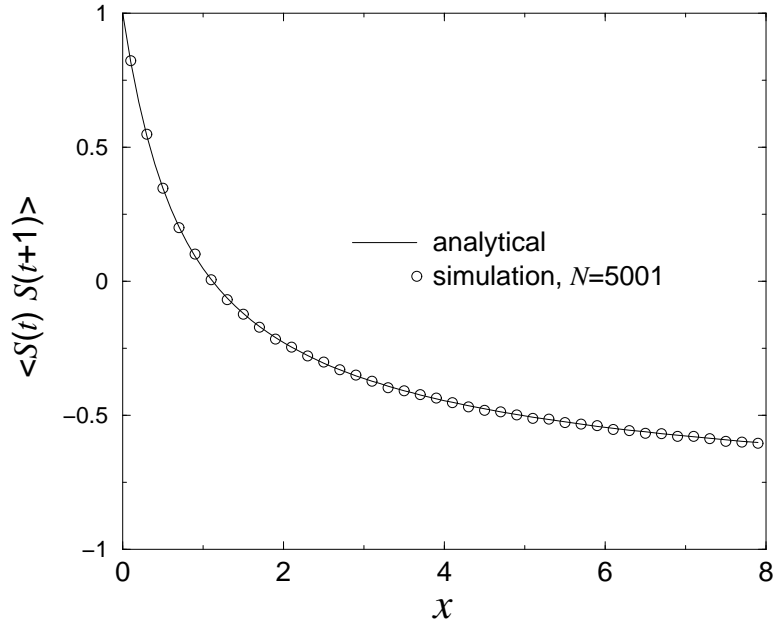


Figure 3.11: One-step autocorrelation of minority signs generated by the stochastic minority game in the limit $p = 2x/N$, $N \rightarrow \infty$.

3.6.1 and 3.6.2, respectively. In the limit of $p = 2x/N$, the correlation is positive for small x , as expected: if fewer than one player change sides on average, the majority is not likely to switch. For $x \approx 1.1$, $\langle S(t)S(t+1) \rangle = 0$. Beyond that point, the autocorrelation function is negative, and it goes to -1 as $x \rightarrow \infty$.

For fixed p , $\langle S(t)S(t+1) \rangle = 0$ goes to -1 rapidly with increasing N . The interpretation in terms of the probability distribution is that an appreciable overlap between the two Gaussian peaks in π^s corresponds to a non-vanishing probability that the minority sign stays the same. As N increases, the peaks get narrower, and the overlap vanishes.

3.6.5 Relation to the original MG

The stochastic MG as it was presented here has only a one-step memory. It is possible (although not necessary) to include a longer history of minority decisions, analogous to the early papers on the evolutionary Minority Game [70]. In that case every player would keep an individual decision table that tells him what to do if a given sequence of minority decisions occurs, similar to the tables that the players in the original Minority Game use. However, instead of changing to an entirely different table, each player changes individual entries in his table with probability p if he loses. It is easy to see – and a similar argument was given in Ref. [71] for the global decision table in Johnson’s variant – that the entries

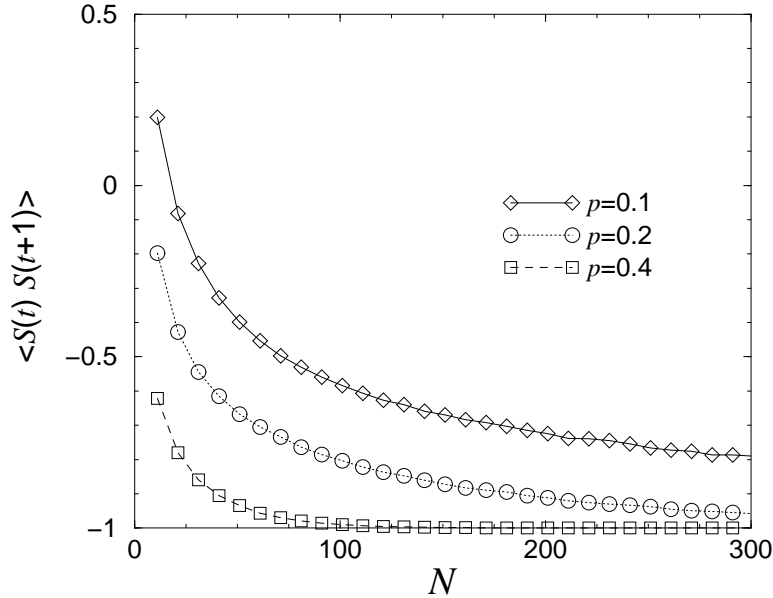


Figure 3.12: For fixed p and increasing N , $\langle S(t)S(t+1) \rangle$ goes to zero as the overlap between the peaks in π^s decreases. See also Fig. 3.7.

for different histories are completely decoupled. Each entry or row in the table corresponds to a one-step Markov process as described above, influenced only by the last time that the same history occurred.

In that sense, introducing a history changes the properties of the time series generated by the decisions, but not the average loss of the players in the stationary state. It might become relevant if one mixes players with different strategies and different memory length, who are susceptible to correlations on different orders of the DeBruijn graph (see Sec. 2.4.4 and 2.4.5). As Sec. 3.6.4 showed, there is a crossover from persistent to antipersistent behavior as the switching probability is increased. If p is constant and N is large enough, the ensemble of players can essentially be replaced by one effective player, who generates a time series with the properties studied in Sec. 2.4.

The presented strategy shows similarities to the behavior of the original minority game in the limit $\alpha \rightarrow 0$, i.e., a small ratio of possible histories compared to the number of players [64]. In the extreme case where each of the two decision tables that each player keeps consists of only one entry (i.e., only the last minority decision counts), the output of roughly 50% of the players is set to either +1 or -1 independent of the history, whereas the other 50% can choose their output depending on their current score. Out of those players, those who chose the minority side will repeat their decision, whereas the update of the scores will cause some of the losers to switch sides. As mentioned before, it has been observed that σ^2 shows a crossover from $\sigma^2 \propto N^2$ to $\sigma^2 \propto 1$ depending on the initial differences

in players' scores [63, 64]; these differences determine the typical number of players who switch sides when they lose. This situation is very much the same for players who use perceptrons with only one input unit [66], where a solution with $\sigma^2 = 1$ is reached if the learning rate η is smaller than the differences between the initial weights of the players. However, in the absence of frozen disorder, the stochastic strategy obviously does not lead to a separation of agents into frozen and oscillating players.

3.7 Multi-choice MGs

A generalization of the MG that was suggested by I. Kanter and studied first by Ein-Dor, Metzler, Kinzel and Kanter in Ref. [78] was to lift the restriction to two alternatives and allowing for Q choices, or "rooms", instead. The choice that is picked by the fewest players wins; in case of a tie, one of the rooms with the lowest attendance is picked at random and declared the winning option. The motivation is clear, since many real-world problems offer more than two choices: an investor has many different stocks to choose from, more than two routes may connect two cities, and a predator may have more than two possible hunting grounds. In a sense, the generalization from the binary MG to a multi-choice MG is analogous to the generalization from an Ising model [79] to a Potts model [80]. However, this analogy does not apply to the mathematical treatment of the standard MG using Ising spin variables [61] – there, the spin variables represented the choice between the two decision tables rather than the two actions.

3.7.1 Random Guessing

The default strategy against which any more sophisticated approaches have to be measured is that of randomly choosing one of the options. It is not as obvious as in the binary MG what numbers come out, or even what quantities one should look at. I will therefore devote a few words to that topic. The following calculations were largely done by Liat Ein-Dor.

The macrostate of the game can be described by the set of numbers $\{N_q\}$ of players who choose each option $q = 1, \dots, Q$. However, the only quantity relevant for global gain or loss is the number $N_{min} = \min_q(\{N_q\})$ of players in the winning room. In analogy to the binary MG, one can define a variance

$$\sigma_{min}^2 = \langle N_{min} - N/Q \rangle_t. \quad (3.42)$$

Analogous to the probability distribution of N_+ in the binary MG, which, for random guessing, follows a binomial distribution, the joint probability distribution

of the N_q s is given by the multinomial distribution:

$$P(\{N_q\}) = Q^{-N} \frac{N!}{N_1! N_2! \dots N_Q!} \delta_{N - \sum N_q}. \quad (3.43)$$

Averages over N_{min} can be evaluated by exploiting the symmetry of the system: I assume that N_1 is the smallest occupation number (which happens with a probability of $1/Q$), include a factor of Q to correct this assumption, and sum over the other N_q with appropriate boundaries. For example, σ_{min}^2 can be calculated as follows:

$$\sigma_{min}^2 = Q \sum_{N_1=0}^N \left(N_1 - \frac{N}{Q} \right)^2 \sum_{N_2, N_3, \dots, N_1}^N P(\{N_q\}). \quad (3.44)$$

Numerics show that for large N , σ_{min}^2 is proportional to N , as expected. To calculate the proportionality constant for $N \rightarrow \infty$, one can introduce new, properly scaled quantities ϵ_q to measure the deviations from equidistribution:

$$N_q = N/Q + \epsilon_q \sqrt{N}, \quad (3.45)$$

and approximate the factorials in Eq. (3.43) using the Stirling approximation

$$N! \approx \left(\frac{N}{e} \right)^N \sqrt{2\pi N}. \quad (3.46)$$

The result

$$P(\{\epsilon_\rho\}) \propto \exp \left(-\frac{Q}{2} \sum_{\rho=1}^K \epsilon_\rho^2 \right) \delta \left(\sum_{q=1}^Q \epsilon_q \right) \quad (3.47)$$

can be used to numerically integrate the continuous expression for $\langle \epsilon_{min}^2 \rangle$:

$$\langle \epsilon_{min}^2 \rangle = \frac{\int_{-\infty}^0 d\epsilon_1 \epsilon_1^2 \int_{\epsilon_1}^{\infty} \left(\prod_{q \geq 2} d\epsilon_q \right) P(\{\epsilon_\rho\})}{\int_{-\infty}^0 d\epsilon_1 \int_{\epsilon_1}^{\infty} \left(\prod_{q \geq 2} d\epsilon_q \right) P(\{\epsilon_q\})}. \quad (3.48)$$

Structurally, this is an integral over the square of the smallest of Q Gaussian random numbers. The only difficulty is the global constraint for the sum of ϵ_q . Results of the numerical integration for $Q = 3, 4, 5$ and 6 are $\sigma_{min}^2/N = \langle \epsilon_{min}^2 \rangle \approx 0.313, 0.322, 0.320, \text{ and } 0.309$, respectively.

Another quantity that is easier to calculate and often just as meaningful as σ_{min}^2 is

$$\sigma^2 = \left\langle \frac{1}{Q} \sum_q \left(N_q - \frac{N}{Q} \right)^2 \right\rangle. \quad (3.49)$$

If there is no systematic preference for one of the options, it is sufficient to look at one of the options, e.g. the option 1. For random guessing, this quantity takes the form

$$\begin{aligned}
\sigma^2 &= \left\langle \left(\sum_{i=1}^N \delta_{\sigma_i,1} - \frac{N}{Q} \right)^2 \right\rangle \\
&= \left\langle \sum_{i,j} \delta_{\sigma_i,1} \delta_{\sigma_j,1} - 2 \frac{N}{Q} \sum_i \delta_{\sigma_i,1} + \frac{N^2}{Q^2} \right\rangle \\
&= \left\langle \sum_i \delta_{\sigma_i,1} + \sum_{i \neq j} \delta_{\sigma_i,1} \delta_{\sigma_i, \sigma_j} - 2 \frac{N}{Q} \sum_i \delta_{\sigma_i,1} + \frac{N^2}{Q^2} \right\rangle \\
&= \frac{N}{Q} + \frac{N(N-1)}{Q} \langle \delta_{\sigma_i, \sigma_j} \rangle - \frac{N^2}{Q^2} \tag{3.50} \\
&= N \left(\frac{Q-1}{Q^2} \right). \tag{3.51}
\end{aligned}$$

The form of the expression in Eq. (3.50) will be useful later on, since it reduces the calculation of σ^2 to the average probability that two agents agree on their output.

3.7.2 Neural Networks

Network architecture

The first scenario for the multi-choice minority game that was studied in detail [78] included an ensemble of neural networks making their choice based on an M -dimensional vector whose components are the most recent minority decisions. Since both the input and the output of the networks are now integer numbers in the range between 1 and Q , the architecture of the networks has to be able to handle this. A simplified version of a Potts perceptron [81] which is introduced in greater detail in Chapter 4, seems appropriate. In this simplification, each player has a weight vector \mathbf{w}_i , from which Q hidden fields are calculated. Each hidden field h_{iq} only gets contributions from components of the weight vector if the corresponding component of the vector is equal to q :

$$h_{iq} = \sum_{j=1}^M w_{ij} \delta_{x_j, q}. \tag{3.52}$$

This architecture is limited compared to the full Potts perceptron: first, there is no interaction between the different input values – the appearance or non-appearance of some q_1 in the pattern does not influence the hidden field for any other q . Second, the options are completely interchangeable: if one would

interchange all occurrences of q_1 and q_2 in the pattern, one would interchange h_{q_1} and h_{q_2} as well. This seems reasonable, given that the options are completely equivalent à priori.

Each agent determines his output σ_i by choosing the option that corresponds to his largest hidden field:

$$\sigma_i = \{k | h_{ik} = \max_q h_{iq}\} \quad (3.53)$$

From these individual outputs, the occupation numbers $N_q = \sum_j \delta_{\sigma_j, q}$ are calculated, and the winning option S is determined:

$$S = \{q | N_q = \min_m N_m\} \quad (3.54)$$

If the learning rule is Hebbian, analogous to Sec. 3.4, an analytical approach is possible. The update rule for the vectors is therefore

$$w_{ij}^{t+1} = w_{ij}^t + \frac{\eta}{M} (Q \delta_{x_j, S} - 1). \quad (3.55)$$

The rule does what one would expect: it increases the hidden field for option S and decreases the fields for the other options. Also, the same update step is applied to all weights, leaving relative vectors unchanged.

Just like in Sec. 3.4, weight vectors can be split into a center of mass $\mathbf{C} = \sum \mathbf{w}_i / N$ and relative vectors $\mathbf{r}_i = \mathbf{w}_i - \mathbf{C}$. The initial conditions are such that vectors have a norm of $|\mathbf{r}_i| = 1$ and symmetrical overlaps of $\mathbf{r}_i \cdot \mathbf{r}_j = -1/(N - 1)$ (the first condition is a choice of length scale, the second is automatically fulfilled approximately if vectors are chosen randomly with a large number M of dimensions). If one sets $C = |\mathbf{C}| = 0$, this is indeed the optimal configuration that can be achieved without breaking the symmetry between the perceptrons.

For random patterns and large N , the hidden fields h_{iq} are Gaussian random numbers. It is convenient to rescale them to variables \hat{h}_{iq} which obey $\langle \hat{h}_{iq} \hat{h}_{ir} \rangle = \delta_{q,r}$ and $\langle \hat{h}_{iq} \hat{h}_{jr} \rangle = R \delta_{q,r}$ for $i \neq j$, where $R = \langle \mathbf{w}_i \cdot \mathbf{w}_j / (w_i w_j) \rangle_{i,j}$ is the overlap between different weight vectors.

The interesting task is calculate σ_{min}^2 for non-vanishing R , i.e., for correlated weight vectors. This is apparently only feasible for small correlations $R = \mathcal{O}(1/N)$, and even there only in a rather convoluted way. The following calculation was basically done by L. Ein-Dor and I. Kanter. However, its presentation in Ref. [78] is somewhat cryptic and slightly wrong, and I will attempt to give an understandable and correct account of it.

Calculating σ^2 and σ_{min}^2

The first step is to calculate the variance σ^2 , which can be broken down to an average over two players, as pointed out in Sec. 3.7.1. The question is thus: what

is the probability that two perceptrons i and j with a small overlap R give the same output, let us say, $\sigma_i = \sigma_j = 1$? Equivalently, what is the probability that $\hat{h}_1^i \geq \hat{h}_q^i \wedge \hat{h}_1^j \geq \hat{h}_q^j$ for all q ? The hidden fields can be combined into one vector $\hat{\mathbf{h}} = (\hat{h}_1^i, \dots, \hat{h}_Q^i, \hat{h}_1^j, \dots, \hat{h}_Q^j)$ of Gaussian variables with the correlation matrix

$$\mathcal{C} = \begin{pmatrix} 1 & \cdots & 0 & R & \cdots & 0 \\ \vdots & \ddots & \vdots & \vdots & \ddots & \vdots \\ 0 & \cdots & 1 & 0 & \cdots & R \\ R & \cdots & 0 & 1 & \cdots & 0 \\ \vdots & \ddots & \vdots & \vdots & \ddots & \vdots \\ 0 & \cdots & R & 0 & \cdots & 1 \end{pmatrix}. \quad (3.56)$$

The joint probability distribution of these variables follows

$$P(\hat{\mathbf{h}}) = \frac{1}{\sqrt{(2\pi)^{2Q} \text{Det}(\mathcal{C})}} \exp\left(-\frac{1}{2} \hat{\mathbf{h}}^T \mathcal{C}^{-1} \hat{\mathbf{h}}\right). \quad (3.57)$$

For general R and Q , this expression is fairly complicated. We simplify it by approximating \mathcal{C}^{-1} to the first order in R . It turns out that

$$\mathcal{C}^{-1} \approx \mathcal{C}_{app}^{-1} = \begin{pmatrix} 1 & \cdots & 0 & -R & \cdots & 0 \\ \vdots & \ddots & \vdots & \vdots & \ddots & \vdots \\ 0 & \cdots & 1 & 0 & \cdots & -R \\ -R & \cdots & 0 & 1 & \cdots & 0 \\ \vdots & \ddots & \vdots & \vdots & \ddots & \vdots \\ 0 & \cdots & -R & 0 & \cdots & 1 \end{pmatrix}, \quad (3.58)$$

which can be verified by checking that $\mathcal{C} \cdot \mathcal{C}_{app}^{-1}$ yields the identity matrix multiplied with $1 - R^2$.

In that approximation, the probability distribution from Eq. (3.57) looks more amiable:

$$P(\hat{\mathbf{h}}) \approx \frac{1}{\sqrt{(2\pi)^{2Q}}} \exp\left(-\frac{1}{2} \sum_q \left((\hat{h}_q^i)^2 + (\hat{h}_q^j)^2 - 2R\hat{h}_q^i \hat{h}_q^j\right)\right). \quad (3.59)$$

Now the probability that both networks give an output of 1 can be calculated,

again in a consequent approximation to first order in R :

$$\begin{aligned}
& \text{Prob}(\sigma_i = \sigma_j = 1) \\
&= \int_{-\infty}^{\infty} d\hat{h}_1^i \int_{-\infty}^{\infty} d\hat{h}_1^j \int_{-\infty}^{\hat{h}_1^i} \prod_{q=2}^Q d\hat{h}_q^i \int_{-\infty}^{\hat{h}_1^j} \prod_{q=2}^Q d\hat{h}_q^j \times \\
&\quad \frac{1}{(2\pi)^Q} \exp\left(-\frac{1}{2} \sum_{q'} (q\hat{h}_{q'}^i{}^2 + \hat{h}_{q'}^j{}^2 - 2R\hat{h}_{q'}^i \hat{h}_{q'}^j)\right) \\
&= \int_{-\infty}^{\infty} d\hat{h}_1^i \int_{-\infty}^{\infty} d\hat{h}_1^j \frac{1}{2\pi} \exp\left(-\frac{1}{2}(\hat{h}_1^i{}^2 + \hat{h}_1^j{}^2 - 2R\hat{h}_1^i \hat{h}_1^j)\right) \times \\
&\quad \left[\int_{-\infty}^{\hat{h}_1^i} \int_{-\infty}^{\hat{h}_1^j} d\hat{h}^i d\hat{h}^j \frac{1}{2\pi} \exp\left(-\frac{1}{2}(\hat{h}^i{}^2 + \hat{h}^j{}^2 - 2R\hat{h}^i \hat{h}^j)\right) \right]^{Q-1} \\
&= \int \dots \left[\int_{-\infty}^{\hat{h}_1^i} \frac{1}{\sqrt{2\pi}} \exp\left(-\frac{\hat{h}^i{}^2}{2}(1-R^2)\right) \Phi(\hat{h}_1^j - R\hat{h}^i) \right]^{Q-1} \\
&\approx \int \dots \left[\int_{-\infty}^{\hat{h}_1^i} \frac{1}{\sqrt{2\pi}} \exp\left(-\frac{\hat{h}^i{}^2}{2}\right) \left(\Phi(\hat{h}_1^j) - \frac{R\hat{h}^i}{\sqrt{2\pi}} \exp\left(-\frac{\hat{h}^j{}^2}{2}\right) \right) \right]^{Q-1} \\
&= \int \dots \left[\Phi(\hat{h}_1^j) \Phi(\hat{h}_1^j) + \frac{R}{2\pi} \exp\left(-\frac{1}{2}(\hat{h}_1^i{}^2 + \hat{h}_1^j{}^2)\right) \right]^{Q-1} \\
&\approx \int_{-\infty}^{\infty} d\hat{h}_1^i \int_{-\infty}^{\infty} d\hat{h}_1^j \frac{1}{2\pi} \exp\left(-\frac{1}{2}(\hat{h}_1^i{}^2 + \hat{h}_1^j{}^2)\right) \left(1 + 2R\hat{h}_1^i \hat{h}_1^j\right) \times \\
&\quad \left[(\phi(\hat{h}_1^i) \phi(\hat{h}_1^j))^{Q-1} + \frac{R(Q-1)}{2\pi} \exp\left(-\frac{1}{2}(\hat{h}_1^i{}^2 + \hat{h}_1^j{}^2)\right) (\phi(\hat{h}_1^i) \phi(\hat{h}_1^j))^{Q-2} \right] \\
&\approx \frac{1}{Q^2} + R \left(\left[\int_{-\infty}^{\infty} dh \frac{h}{\sqrt{2\pi}} \exp(-h^2/2) \Phi(h)^{Q-1} \right]^2 \right. \\
&\quad \left. + (Q-1) \left[\int_{-\infty}^{\infty} dh \frac{1}{2\pi} \exp(-h^2) \Phi(h)^{Q-2} \right]^2 \right). \tag{3.60}
\end{aligned}$$

The first term in Eq. (3.60) is the default result for uncorrelated vectors. The second term is due to the correlations between h_1^i and h_1^j , and the third term represents correlations between h_q^i and h_q^j for $q \geq 2$. For some reason, Ref. [78] only lists the first and third term.

Using this result, σ^2 can be calculated according to Eq. (3.50):

$$\sigma^2(R)/N = \frac{Q-1}{Q^2} + (N-1)RI, \tag{3.61}$$

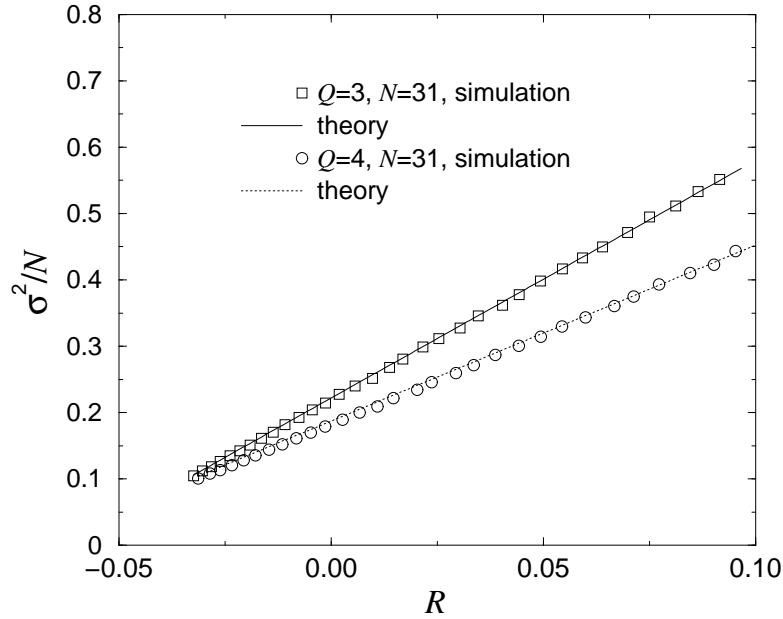


Figure 3.13: Variance σ^2/N as a function of R in the multi-choice minority game with neural networks. Eq. (3.61) agrees well with simulations using $M = 200$. All simulations in this section use random patterns.

where I stands for the two integrals in Eq. (3.60). Plugging in the optimal value $R = -1/(N - 1)$, one gets an optimal σ^2/N which is independent of N , just like in the binary-choice MG.

Considering that Eq. (3.61) is a first-order approximation, it agrees surprisingly well with simulations, as seen in Fig. 3.13.

What is still left to do is to deduce σ_{min}^2 from σ^2 . This can be done in a surprisingly easy way: for large N , the occupation numbers N_q are still Gaussian random numbers whose variance is now given by Eq. (3.61) instead of (3.51). Therefore, the integral necessary to calculate $\sigma_{min}^2/N = \langle \epsilon_{min} \rangle$ has the exact form of Eq. (3.48), and if ϵ is rescaled properly, one can reuse the integrals evaluated to get σ_{min}^2 in the random case:

$$\frac{\sigma^2(R)}{\sigma_{min}^2(R)} = \frac{\sigma^2(R = 0)}{\sigma_{min}^2(R = 0)}. \quad (3.62)$$

The values on the right hand side can be taken from Eqs. (3.51) and (3.48), while the enumerator on the left hand side is given by Eq. (3.61).

Just how good is perfect coordination ($R = -1/(N - 1)$) compared to random guessing? As the calculations have shown, this depends only on Q . The ratio $\sigma^2(R = -1/(N - 1))/\sigma^2(R = 0)$ is shown in Fig. 3.14. For $Q = 2$, one gets the ratio $1 - 2/\pi$, as calculated in Sec. 3.4. For larger Q , the ration slowly converges to 1: the benefit from coordination decreases with Q .

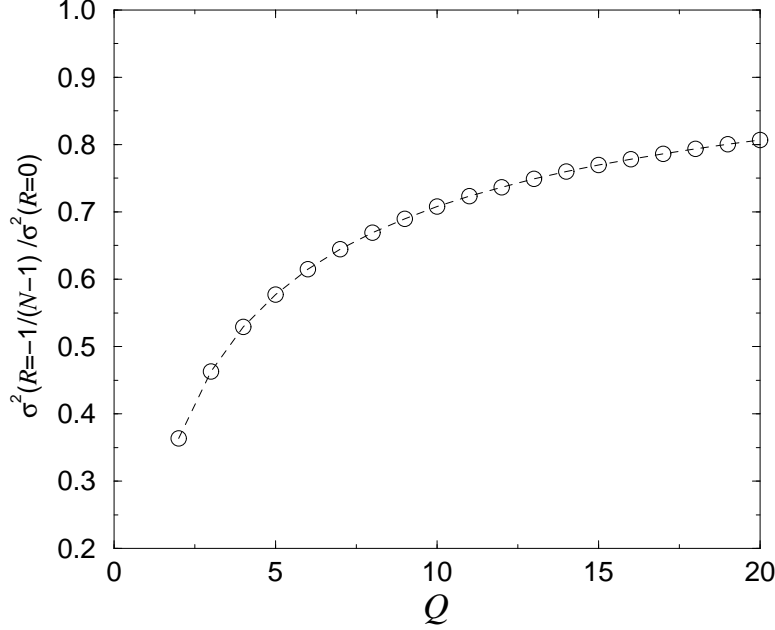


Figure 3.14: Improvement by coordination: $\sigma^2(R = -1/(N - 1))/\sigma^2(R = 0)$ as calculated from Eq. (3.61). For larger Q , the benefit gained from learning decreases.

Learning Dynamics

The preceding paragraphs showed how σ^2 depends on R , and that R depends on the norm of the center-of-mass vector \mathbf{C} . To finish the argument, one can show that the proposed learning rules leads to $C \rightarrow 0$, and thus optimal coordination, for $\eta \rightarrow 0$. The calculation, which is again by L. Ein-Dor, is roughly analogous to that for the binary-choice MG, but takes a shortcut at a convenient spot.

To find C in dependence on η , K , and Q , one starts with the update rule for \mathbf{C} , which is analogous to Eq. (3.55):

$$C_j^{t+1} = C_j^t + \frac{\eta}{M}(Q\delta_{x_j,S} - 1), \quad (3.63)$$

takes the square of it, averages over random patterns, and sums over j :

$$(C^{t+1})^2 = (C^t)^2 + 2Q\frac{\eta}{M} \left\langle \sum_j^M C_j \delta_{x_j,S} \right\rangle + \frac{\eta^2}{M^2} \sum_j^M \langle (Q\delta_{x_j,S} - 1)^2 \rangle. \quad (3.64)$$

For $M \rightarrow \infty$, this turns into a differential equation for C , where one infinitesimal time step $d\alpha = 1/M$ corresponds to one learning step:

$$\frac{dC^2}{d\alpha} = 2\eta Q \left\langle \sum_j C_j \delta_{x_j,S} \right\rangle + \eta^2(K - 1). \quad (3.65)$$

At this point, Ref. [78] makes a convenient approximation: it is assumed that the output of the ensemble of networks always follows the output of the center-of-mass. While possibly true for large N and large η , this is certainly not correct for small η – the range we are interested in! However, I will first try to explain the approximation, and then follow it to the end to see if it makes a difference in the final result.

The hidden fields h_{iq} of each player can again be split into two contributions, one from the random vector and one from the center-of-mass:

$$h_{iq} = \sum_m^M \delta_{x_m,q} r_{im} + \sum_m^M \delta_{x_m,q} C_m. \quad (3.66)$$

The fields induced by the center-of-mass, $h_q^C = \sum_m \delta_{x_m,q} C_m$, thus act as a bias on the random decision of the relative vectors. If C is of order 1, the center-of-mass heavily influences the decision of each individual. However, to influence the decision of the minority, it only has to tip the decision of $\mathcal{O}(\sqrt{N}/Q)$ players.

It is messy to calculate the probability that the output of a single player follows the smallest hidden field of the center-of-mass, not to mention the probability that the ensemble joins this decision. The probability can be measured in simulations, though, and results are shown in Fig. 3.15 for $Q = 4$. As expected, the probability that the room with the largest occupation corresponds to the largest h_q^C goes to 1 as the overlap between weight vectors increases. However, the probability that the smallest occupation is given by the smallest hidden field takes high values for intermediate $\cos(\theta)$ and then decreases again. The reason for this is not yet clear.

If one nevertheless assumes that the option with the smallest h_q^C is the minority decision S of the ensemble, $\sum_j C_j \delta_{x_j,S}$ is simply the smallest of Q uncorrelated Gaussian random numbers with zero mean and variance C^2/Q , and the average over it can be calculated. Again, let us assume that the winning option is 1, and correct the assumption by a factor of Q :

$$\begin{aligned} \left\langle \sum_j C_j \delta_{x_j,S} \right\rangle &\approx Q \int_{-\infty}^{\infty} dh_1^C \frac{h_1^C}{\sqrt{2\pi C^2/Q}} \exp\left(-\frac{h_1^{C^2}}{2C^2/Q}\right) \times \\ &\quad \int_{h_1^C}^{\infty} \prod_{q \geq 2} dh_q^C \frac{1}{\sqrt{2\pi C^2/Q}} \exp\left(-\frac{h_q^{C^2}}{2C^2/Q}\right) \\ &= C\sqrt{Q} \int_{-\infty}^{\infty} dh \frac{h}{\sqrt{2\pi}} \exp(-h^2/2) (1 - \Phi(h))^{Q-1}. \end{aligned} \quad (3.67)$$

This is proportional to C , and together with Eq. (3.65) one gets for the fixed point

$$C_{fix} \approx \eta \frac{Q-1}{2\sqrt{Q^3} J}, \quad (3.68)$$

where J is the integral expression in Eq. (3.67).

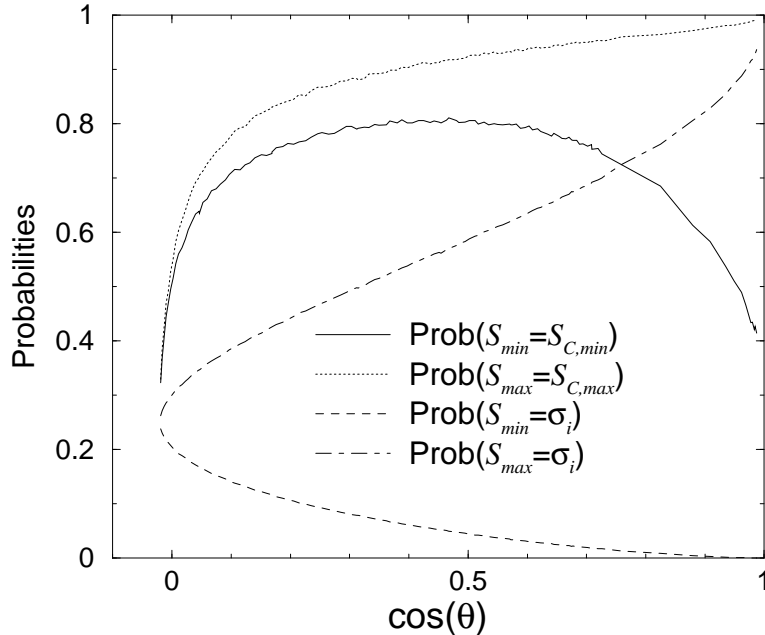


Figure 3.15: Perceptrons in the multi-choice MG: probabilities that the least occupied room S_{min} corresponds to the option $S_{C,min}$ with the smallest bias h_q^C , that the most occupied room S_{max} corresponds to the largest bias $S_{C,max}$, and that the individual decisions σ_i correspond to the respective largest and smallest bias, as a function of the weight vectors' mutual angle $\cos(\theta)$. Simulations used $Q = 4$, $N = 41$ and $M = 100$.

As mentioned before, this approximation is never truly valid. It is the same approximation that replaces the center-of-mass vector in the binary-choice perceptron with a single confused perceptron (see Sec. 3.4.2), but the existence of more than two alternatives complicates the situation.

Nevertheless, simulations indicate that C indeed goes to 0 as $\eta \rightarrow \infty$ for small N , although not linearly. This is again analogous to the binary-choice-perceptron, where $C \propto \sqrt{\eta}$ was found for small η . It does not change the conclusion that σ^2 takes its optimal value for very small learning rates.

3.7.3 Decision tables

The possibility of applying other rules of behavior (such as Challet and Zhang's decision tables) to the multi-choice minority game was only hinted at in Ref. [78]. I will present a straightforward generalization of the standard MG and some simulations which indicate that the behavior of the multi-choice MG is very similar to the two-choice MG. A more thorough analysis based on a slightly modified generalization was presented by Chow and Chau in Ref. [82].

The simplest generalization from the standard MG [60, 61, 62] is to give each player two decision tables with entries $a^\mu \in \{1, \dots, Q\}$ for each of the Q^M possible histories μ . Scoring does not have to be modified: a table receives a point if it would have predicted the correct minority room, and loses a point for an incorrect prediction. The table with the highest score is used.

Since the number of table entries Q^M increases rather drastically, it simplifies simulations to substitute the time series/ history scheme by a number of p possible patterns μ that are picked at random at each time step. In the conventional MG, this alters results only very little [59].

Result can be seen in Fig. 3.16: curves for σ^2/N look qualitatively similar for $Q = 2$ (the binary case, apart from a factor of 4 that comes from different definitions of σ^2), $Q = 3$ and $Q = 4$. For $\alpha \rightarrow \infty$, the values of σ^2 approach those of random guessing ($\sigma^2/N = (Q - 1)/Q^2$), whereas at small α there is a crowded phase.

As in the case of $Q = 2$, a preference for a certain response to each pattern μ appears at α_c and increases with α . This preference can be expressed as an information H in the following way: if c_q^μ is the probability that following a given pattern μ , the minority chooses option q , one defines

$$H = \frac{1}{p} \sum_{\mu=1}^p \sum_{q=1}^Q \left(c_q^\mu - \frac{1}{Q} \right)^2. \quad (3.69)$$

The phase transition can be located by estimating where H becomes 0 for $N \rightarrow \infty$. As seen in Fig. 3.16, the critical value α_c of the phase transition decreases with Q .

3.7.4 Johnson's evolutionary MG

The evolutionary Minority Game suggested in Ref. [70] and briefly described in Sec. 3.5 has several possible generalizations to Q options. In the first, players have a probability p to choose the option that was successful the last time. Otherwise, they choose one of the remaining options at random. In the second, players i have a set of probabilities $\{p_i^q\}$ to visit each of the possible rooms $q = 1, \dots, Q$. If their score drops below a certain threshold, they discard their probabilities and choose a new combination of p_i^q .

Let us first consider the first generalization. It is fairly obvious that this prescription can do very little to improve coordination. Even in the extreme case where exactly N/Q players choose the last winning option with probability 1 and $N(1 - 1/Q)$ roll the dice with probability 1, the standard deviation is that of $N(1 - 1/Q)$ players choosing between $Q - 1$ options. The best thing that can happen is that the number of guessers is effectively reduced by a factor of $1 - 1/Q$.

Simulations show that, compared to the case of $Q = 2$, the self-organization is less pronounced for $Q > 2$. The probability density distribution $P(p_i)$ decreases

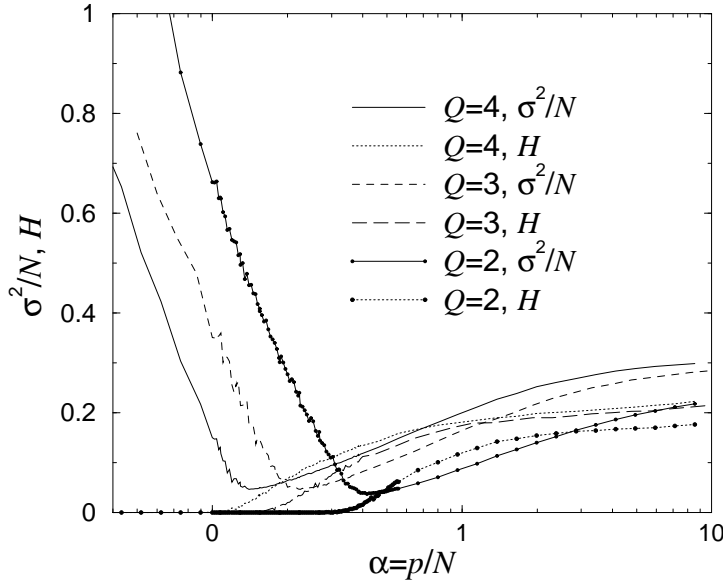


Figure 3.16: Standard Minority Game with $Q \geq 2$ options. Curves for σ^2/N and H look qualitatively similar, whereas the value α_c of the phase transition depends on Q . Simulations use $N = 101$ and $N = 201$.

monotonically towards higher p_i ; there is no double-peak structure (see Fig. 3.17). There is, in the stationary state, a chance of $1/Q$ for the most recent option to win again, i.e., probabilities p_i distribute themselves to arbitrage away any systematic advantage:

$$\int_0^1 P(p_i) p_i dp_i = 1/Q. \quad (3.70)$$

Furthermore, coordination is slightly improved, compared to completely random guessing.

What is the cause of the relatively bad coordination in this evolutionary game? As pointed out in Ref. [73], the stationary distribution $P(p_i)$ is determined by two processes: the removal of agents with a given p_i , i.e., the mean lifetime of an agent with p_i in an environment with a given distribution $P(p_i)$, and the addition of new agents, i.e., the rules according to which the p_i s of removed players are replaced. In a dynamics in which new p s are chosen at random, the stationary distribution $P(p_i)$ is proportional to the mean lifetime $L(p_i)$ of a player with probability p_i . In an environment with a wide distribution $P(p_i)$, having an extreme position apparently does not provide enough advantage to bring about a strong polarization of opinions.

This can be remedied by a small change in the dynamics: a removed player is replaced by a (possibly slightly modified) copy of one of the other players. This ensures, in the spirit of evolutionary biology, that “fitter” strategies spread more quickly than less successful ones. In simulations, it proves essential to add a small

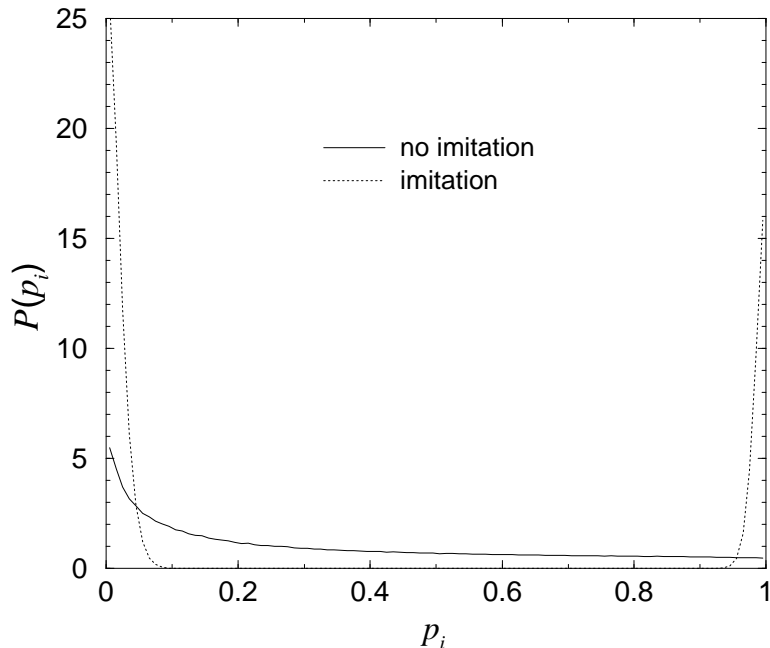


Figure 3.17: Johnson’s Evolutionary Minority Game with $Q = 3$ options and one probability p_i of choosing the last winning option: if new players pick their p_i at random, specialization is weak (solid line). If they imitate an existing player, the population segregates into two crowds (dotted line).

“mutation” (a random number) to the value of p that is being copied, to allow the population to reach advantageous p -values even if the agents that held them initially died out due to fluctuations. In Fig. 3.17, this mutation is a Gaussian random number with mean 0 and $\sigma = 0.005$ that is added to p_i with reflecting boundary conditions.

For $Q = 2$ (binary decision), this leads to a split of the population into two groups: one with $p \approx 0$ and roughly $N/2$ members, the other with $p \approx 1$ and again $N/2$ members. This even leads to $\sigma^2 = \mathcal{O}(1)$. One can argue that this situation is analogous to Reents’ and Metzler’s stochastic strategy, with evaluation of one’s strategy stretched out over a longer time: let us exploit the symmetry of the problem again and say that p_i is the probability of choosing +1. If the population is already separated into two peaks at $p \approx 1$ and $p \approx 0$, these correspond to different populations that say +1 or –1, respectively. Players who have lost a certain amount pick a new p_i – either they rejoin their previous side, or they switch sides. If few enough players die per round, this can lead to $\sigma^2 \approx 1$.

For $Q > 2$, the population again segregates into two factions with extreme opinions ($p_i \approx 0$ or 1). As explained above, even this split cannot do more than reduce the number of guessers, and hence σ^2/N , by a factor of $(Q - 1)/Q$. Numerical evidence shows that this is exactly what happens.

The second generalization, in which each player i has an individual preference p_i^q for each room q , offers (at least in theory) a configuration of perfect coordination: for each option, there is a fraction of $1/Q$ players who choose it with certainty. Analogous to the case of binary decisions, where probabilities close to 0 or 1 are favorable, the preferred probability combinations would be in the edges of the simplex. A suitable order parameter is therefore the average self-overlap of agents' strategy vectors:

$$R = \left\langle \sum_q p_i^{q2} \right\rangle_i, \quad (3.71)$$

which takes values from $1/Q$ if each option is equally likely, to 1 if there is complete specialization. The average of this quantity can be determined analytically for random vectors. The simplest way to generate a random vector on a simplex is to take q random number r_q , equidistributed between 0 and 1, and normalize them $p_k = r_k / \sum_q r_q$. The average of R is then

$$\langle R_Q \rangle = \int_0^1 \prod_q dr_q \frac{\sum_k r_k^2}{(\sum_k r_k)^2}. \quad (3.72)$$

This yields $R_2 = 2 + 12 \log(2) - 9 \log(3) \approx 0.43026$, $R_3 = 2 - 88 \log(2) + 54 \log(3) \approx 0.32812$ etc.. These results, which can be well approximated by $R_Q \approx 1.31/Q$, are the baseline against which a coordination by evolution has to be measured.

Simulations of the evolution process show that if a deceased player is replaced by one with a randomly updated strategy vector, coordination is and stays bad. The probability distribution of R is almost indistinguishable from that of random vectors, and $\langle R_3 \rangle$ merely increases to ≈ 0.445 , compared to 0.43026 for random vectors. In a noisy environment, players who attempt to specialize in one of the options to not have a significant advantage.

Again, the picture changes if new players are allowed to copy (with modifications) the strategy of a randomly chosen other player. The imitation mechanism allows players to explore areas of parameter space that have a slim probability of being chosen at random, like the edges of the simplex. In fact, a strong specialization takes place: in the stationary state, each player has a decided preference for one of the rooms, leading to high average R .

The exact distribution of R depend on the details and parameters of the mutation mechanism. In Fig. 3.18, the following mode was chosen: a Gaussian random number with $\sigma = 0.005$ is added to each component, with reflective boundary conditions at 0 and 1. The resulting vector is normalized to $\sum p_i^q = 1$.

As I have shown, the mechanism of imitation improves coordination among agents, at least for the instances discussed in the last paragraphs. However, strictly speaking, it violates the assumptions made about the rules of the game: Although copying another player's strategy is not the same thing as making an explicit contract stating "Each round, I play this and that, and you play such and

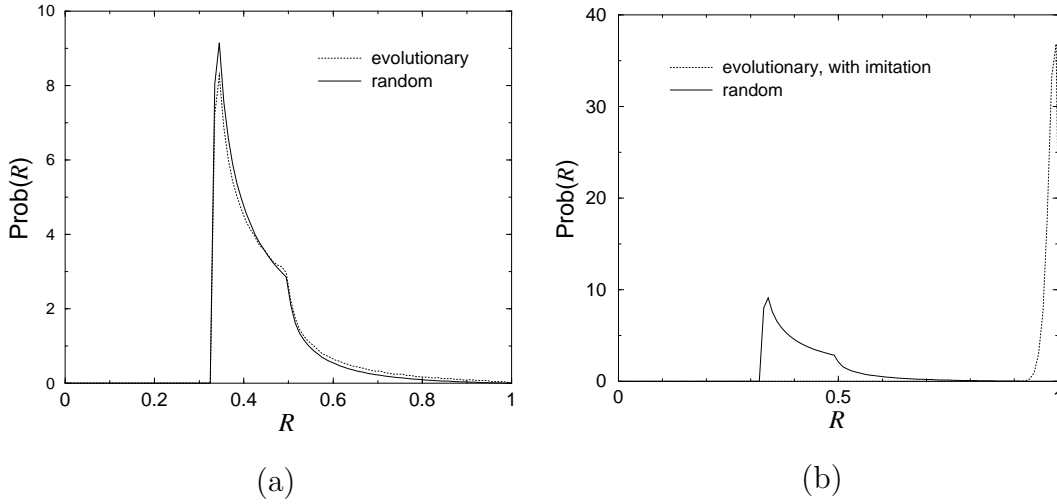


Figure 3.18: Johnson’s Evolutionary Minority Game with $Q = 3$ options and individual preferences: if new players’ strategies are picked at random (a), the stationary distribution of self-overlaps R shows no specialization. This changes if new players imitate existing players with slight modifications (b). Simulations used $N = 1001$.

such”, it amounts to the same thing if a player’s strategy has a strong preference for one of the options.

Interestingly, the “contracts” made by the agents by imitation do not follow the lines of “I play +1 each time you play -1 , and one of us wins for sure” as one would expect. To the contrary, players “agree” to make the same statement most of the time! That this still leads to good coordination is a consequence of the slow adaption brought about by the evolutionary process with sufficiently large thresholds and correspondingly small death rates. If the threshold is very small, such that each round a significant proportion of the population dies, one might expect something like in Reents’ and Metzler’s stochastic strategy to happen.

However, even if the threshold is set to -0.5 , i.e., new players are replaced immediately if they make a mistake, only a small fraction of the population dies each round. This is because those players that survive their first few round typically accumulate ≈ 100 points. As outlined in [73], the score of each player is a random walk with a drift that is proportional to the loss of the player. If a player is very firm in his opinion and gives the same output every time, and there is no systematic preference for either output, the mean loss of that player is 0, and the average time for that player to die is actually infinite (this is a well-known result for random walks with one absorbing edge). Since this limit is not realized completely, players do die eventually, but at a very small rate. Simulations show that the time series generated by the evolutionary MG for $Q = 2$ displays very weak antipersistence ($p_{AP} \approx 0.52$) for a threshold of -0.5 , and significant persistence ($p_{AP} \approx 0.35$) for large negative thresholds.

3.7.5 Reents' and Metzler's stochastic strategy

The stochastic strategy for the MG described in Sec. 3.6 can be adapted to accommodate several options as well. Again, two generalizations suggest themselves:

- 1) Players are informed about which option won the last round. If they won, they repeat their decision; otherwise they move to the last winning room with probability p .
- 2) Players only know if they lost or won. If they lost, they choose, with probability p , to try one of the other options at random.

In both cases, the system can still be considered a one-step Markov process. However, the state of the system must now be characterized by $Q - 1$ values N_1, \dots, N_{Q-1} , which give number of players in each room (the remaining value N_Q can be calculated from normalization constraints: $\sum_q N_q = N$), and the joint probability distribution is a $Q - 1$ -dimensional tensor, or a function living in \mathbb{R}^{Q-1} if one wants to go to continuous variables. Transition probabilities look even worse, taking the form of $2(Q - 1)$ -dimensional tensors or integral kernels. Put briefly, this problem is only accessible to simulations and very crude approximations.

Large p

In the limit of $p = \mathcal{O}(1)$, $N \rightarrow \infty$, the behavior is analogous that detailed in Sec. 3.6.2: finite fractions of players move from room to room, and the minority option changes at every time step. Suitable variables are $n_i = N_i/N$, the fractions of players who chose option i . Occupation probabilities $\pi^s(n_i)$ are a superposition of Q Gaussian peaks whose widths decrease with N . Self-consistent values for the centers of the peaks can be found analytically, as the following example will show:

Let us take $Q = 3$, and the players are not informed about which option was successful, i.e., if they lose and decide to switch, they choose one of the remaining options at random. At any given step, there are three occupation numbers, which we order $n_1 < n_2 < n_3$. Room 1 will now receive players from rooms 2 and 3, whereas rooms 2 and 3 gain players from the respective other room and lose players to all other rooms. Neglecting fluctuations, the rate equations for the occupations n_i^+ at the next time step look like this:

$$\begin{aligned} n_1^+ &= n_1 + (p/2)(n_2 + n_3); \\ n_2^+ &= n_2 - pn_2 + (p/2)n_3; \\ n_3^+ &= n_3 - pn_3 + (p/2)n_2. \end{aligned} \tag{3.73}$$

If one can find a permutation of n_i such that each n_i is equal to n_j^+ with some $j \neq i$, one has a solution. In the present case, the solution for Eq. (3.73) is

$n_1^+ = n_3$, $n_2^+ = n_1$ and $n_3^+ = n_2$ for $0 < p \leq 2/3$, and $n_1^+ = n_3$, $n_2^+ = n_2$ and $n_3^+ = n_1$ for $2/3 \leq p < 1$. The corresponding equations are

$$\begin{aligned}
 n_1 &= \frac{4 - 6p + 3p^2}{3(2-p)^2} \text{ for } p \leq 2/3, 1 - \frac{6}{10-3p} \text{ for } p > 2/3; \\
 n_2 &= \frac{4(1-p)}{3(2-p)^2} \text{ for } p \leq 2/3, \frac{2}{10-3p} \text{ for } p > 2/3; \\
 n_3 &= \frac{2}{3(2-p)} \text{ for } p \leq 2/3, \frac{4}{10-3p} \text{ for } p > 2/3.
 \end{aligned} \tag{3.74}$$

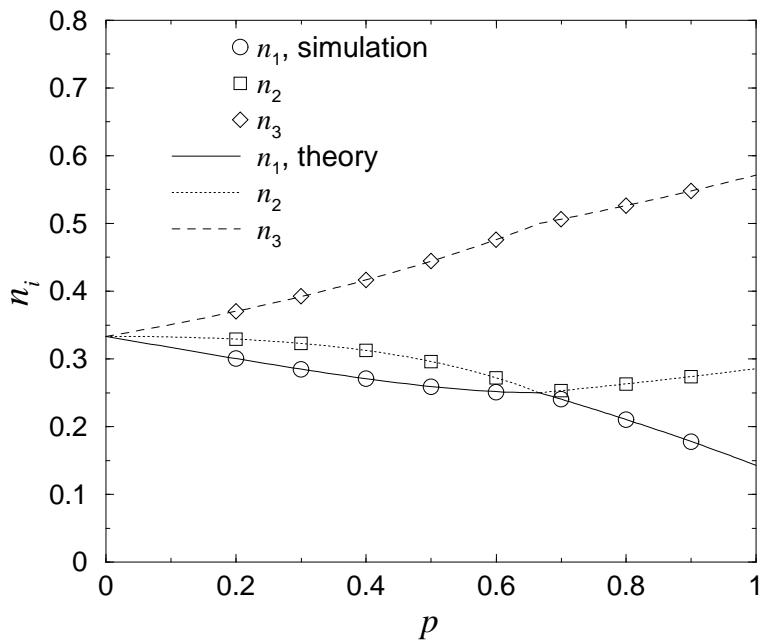


Figure 3.19: Centers of the peaks of $\pi(n)$ in the stochastic MG with $Q = 3$. Simulations with $N = 4001$ agree well with Eqs. (3.74).

Fig. 3.19 shows the results of Eqs. (3.74) compared to simulations. Data collection from the simulations is tedious, because the centers of each peak have to be fitted individually for each p ; however, even the few points give a good impression of the accuracy.

Small p

The case of small $p \propto 1/N$ is even less accessible to analytics. I will therefore only present results from simulations. The probability distribution for the deviation from the optimal configuration, $\pi^s(N_i - N/Q)$, depends less and less on the order of magnitude of N as $N \rightarrow \infty$. However, it does depend on $N \bmod Q$ – this is less relevant for larger p , but it becomes clear that very close to the optimal state,

it makes a difference whether the optimal state has a net gain of 0, $-1/Q$, or $-(Q-1)/Q$.

It also turns out that, if players are not informed about which option won, the probability distribution does not converge to an optimal state, regardless how small p is chosen: even if at most one agent per time step switches sides, there is a chance of $(Q-2)/(Q-1)$ of choosing the wrong room, making matters worse.

A different mechanism prevents perfect coordination if agents are informed about the last minority option, even if $N \bmod Q = 0$, i.e., equidistribution among the rooms is possible: according to the rules outlined above, only one room is declared winner. Even if perfect coordination is achieved at some point, agents from the rooms that are tied with the winner but lost the coin toss will move to the winning room, ruining equidistribution.

The symmetry between $N_i - N/Q < 0$ and $N_i - N/Q > 0$ that was still present for $Q = 2$ is broken, resulting in an increasingly skewed distribution for increasing Q .

Although details are more complex, the broad features of the stochastic MG remain the same: for large p , the ensemble of players can be treated as Q effective players who switch rooms, and strong herd behavior is observed. For $p = \mathcal{O}(1/N)$, there is good, although not perfect, coordination.

3.8 Summary and remarks on the Minority Game

This chapter has provided an overview over different strategies for the Minority Game, with different approaches: the standard MG provides the players with elaborate strategies, but little freedom to change them. The quenched randomness inherent in the model is the source of most of the interesting behavior.

The neural networks approach presented in Sec. 3.4 also includes quenched randomness in the differences between weight vectors. However, this randomness is irrelevant for all practical purposes, and a calculation that assumes a perfectly symmetrical state gives good results. The idea here is to give players a fairly sophisticated prediction algorithm and a learning algorithm that can, in principle, completely alter the parameters of this algorithm. The rate at which this modification takes place determines whether the agents can find an anti-correlated state or whether they over-compensate and show herd behavior. Adaption has to be slower with increasing population size, and there is a smooth crossover from negative to positive correlations between players.

Johnson's evolutionary MG (Sec. 3.5) models each player in a very simplistic way, with only one parameter, and an evolutionary learning algorithm. Nevertheless, it is almost intractable analytically. The evolutionary algorithm suggested in the original publications induces significant self-organization. However, if newly generated players are allowed to copy the strategy from existing players, almost total coordination results (see Sec. 3.7.4).

Reents' and Metzler's stochastic strategy is also very simple. In the treatment given in Sec. 3.6, the whole population is described by a single parameter! Still, my feeling is that the suggested strategy is close to what people do in real-life situations where little information is available. It would be interesting to check this in psychological experiments.

As in the case of the neural networks, coordination becomes better as learning becomes slower, and the rate of change has to be proportional to $1/N$ to achieve optimal coordination. Between this regime and the regime of herding behavior ($p = \text{const}$), there is again a smooth crossover.

It can be shown in simulations and calculations that the stochastic strategy (at least in the small- p regime) is robust to the presence of noise (i.e., other players playing different strategies), and evolutionarily stable.

The section on the multi-choice Minority Game showed that one can find suitable generalizations of all presented strategies to scenarios where players have to choose between more than two different options. With the exception of neural networks, an analytical solution seems too involved to be a realistic option; however, simulations show that the general behavior of the strategies is similar to that for $Q = 2$, with respect to the presence or absence of phase transitions, the scaling regimes for parameters, and so forth. The evolutionary MG is an exception: the original update rule suggested by Johnson et al. yields no specialization; however, a strategy-copying mechanism again leads to self-organization.

Of the presented strategies, only the standard MG shows a phase transition. This has drawn significant attraction [51]; however, I attribute this more to the general fondness of statistical physicists for phase transitions than to good evidence that minority-like settings in real life have a phase transition. Admittedly, it is an established fact that time series from financial markets display power-law probability distributions typical for critical behavior [56]. With sufficient tweaking, it is possible to find a variation of the standard MG (the so-called Grand-canonical MG [83, 84]) which replicates these properties, or "stylized facts". It might be worthwhile to explore if this is possible with any of the other strategies as well.

This chapter has highlighted some connections between the Minority Game and the concept of anti-predictability. All presented strategies show (very pronounced in some cases, and weakly in others) a transition to antipredictability in the time series generated by the ensemble of players.

If players adapt slowly, they can find a well-coordinated state where the next minority decision is either very random (neural networks) or so narrow that even though it can be predicted, it cannot be exploited (stochastic strategy, evolutionary MG with imitation). If quenched randomness is present, however, even slow adaptation is sometimes not sufficient to remove preferences for certain outputs (standard MG).

If players adapt quickly (large learning rates in neural networks, large p in the stochastic strategy, small initial differences in the crowded regime of the standard

MG), they overcompensate: large numbers of players change their opinions at the same time, defeating their own prediction. The Minority Game is thus a well-motivated framework in which antipredictability emerges naturally in some limits, and it allows to study the circumstances that lead to failure of prediction algorithms.

Chapter 4

Neural Networks in Two-Player Games

The Minority Game that was introduced in Chapter 3 and related to the concept of antipredictability is only one example out of a large number of game-theoretical scenarios. Neural networks have been applied to some of these scenarios; however, there seems to be little work on very basic, concrete questions concerning simple neural networks playing simple two-player games.

This chapter will present a short overview over the different areas of game theory, introduce some basic concepts, and then go into details on how and to what extent a simple neural network can be used to learn strategies in two-player games.

4.1 An overview over game theory

The field of game theory can be divided into several distinct areas. Although the mathematical treatment of pure games of chance triggered important research on probability theory [85, 86], game theory in the modern sense often does not include randomness as a necessary ingredient. The usual scenario consists of two or more players who have a choice between a set of *options* or *strategies*.¹ The payoff that each player receives depends on the choices he makes and the choices of the other player(s), which he cannot influence. The aim of each player is to maximize his personal payoff². The difference between the fields lies in the

¹The usual convention in game theory is to call each possible choice a strategy. However, to avoid confusion between strategies, pure strategies, and mixed strategies, I will continue to call them options, and use the term strategy for the set of probabilities of choosing each option.

²Newcomers to game theory often feel that this approach oversimplifies the motivations and emotions of players. Game theorists usually answer that any motivation can, in principle, be quantified and accounted for by modifying the payoffs. Whether this is indeed the case can be argued; however, to allow for an analytical approach, a quantification of preferences seems necessary.

rules of the game, and in the way that the players change or don't change during repetitions of the game:

4.1.1 Combinatorial game theory

In *combinatorial game theory*, players take alternating turns and usually have full information about the state of the game and all possible future combinations of moves. A simple example of this type of game is Nim: the game starts with several heaps of matches, and each player can take an arbitrary number ≥ 1 of matches from one of the heaps. The last player to take a match wins. Many combinatorial games can be reduced to Nim and studied using a generalization of rational numbers called Nimbers (see “Winning Ways” by Berlekamp et al. [87] for details on Nim, an introduction to Nimbers, and lots of information on other combinatorial games).

More complex cases of combinatorial games are Four-in-a-Row, Dots-and-Boxes, Go and Chess. Although it is in principle possible to tell in advance how the game will end if all players play optimally and which moves are optimal in a given situation, one can argue that all “interesting” real-life games require too much computational effort for a human player to go through the complete analysis (in fact, some games have been proven to be NP-complete, i.e., the computational effort increases exponentially with the size of the board [88]). A case in point is TicTacToe, which is simple enough to grasp completely and considered boring by most people beyond the age of 10. On the other hand, a complete analysis of chess is beyond the capacities of even the most advanced computers.

Thus, players of such games rely on heuristics (or experience and “intuition”, which amounts to the same thing) to evaluate the quality of moves in games like Chess [89]. If moves seem equivalent to players, they pick among them more or less randomly, which allows for stochastic treatments of games that are, in principle, deterministic (see e.g. Ref. [90]).

4.1.2 Economic game theory

In *economic game theory* [91], uncertainty is an essential ingredient, since players make their choices simultaneously, and none of the players know what choices the other(s) will make. The simplest scenario considered in economic game theory is that of two-player zero-sum games [12]. Here, each of the two players has a finite number of options. Each combination of options is assigned a number (an entry in the payoff matrix \mathcal{C}) which the first player has to pay to the second if that combination is chosen, such that the gain of one player is always the loss of the other. A popular example is Rock-Paper-Scissors. Zero-sum games always have a unique combination of strategies for the two players where the strategy of each player is optimal if the respective other player does not deviate from his

strategy. Such a combination is called a *Nash equilibrium*. More details on zero-sum games, as well as a formal explanation of Nash equilibria, will follow in Sec. 4.2.

In contrast, non-zero-sum games can have different payoff tables for each player. This makes the situation more complicated, allowing for cases in which there are several equilibria or in which the solution that maximizes “global good” (the sum of average gains) is not stable because options exist that increase one player’s payoff, but decrease the sum of payoffs. The most infamous scenario is the Prisoner’s Dilemma [92].

Some non-zero-sum games involve a large number of players and a fairly simple payoff scheme. For example, the Minority Game described in Chap. 3 is a negative-sum game with an arbitrarily large number of participants.

Games are also classified as complete information games if all players know all entries of all payoff matrices, and as incomplete information games if each participant only knows part of the payoffs (usually at least his own).

4.1.3 Evolutionary game theory

This branch may be considered a spin-off of economic game theory which is concerned with the mechanisms by which equilibria can be reached [77, 93]. Typical models include populations of players with individual strategies that repeatedly play against each other. Successful players generate offspring with the same or at least similar strategies, whereas less successful strategies can become extinct.

Evolutionary game theory has become a testing ground for simple models of interpersonal interactions, allowing to study under which circumstances cooperation among players can exist, when cheating is to be expected, and what ways of behavior favor which response. As the name suggests, it has become extremely important in evolutionary biology, where it is used to model animal behavior and has shed light on many aspects of mating behavior, cooperation within herds, and so forth.

Interestingly, many popular games do not easily fit into the categories of either theory. For example, card games like Poker, Romm e or Magic:The Gathering® and board games like Monopoly® or Siedler von Catan® mix combinatorial elements with a strong stochastic component (rolling the dice, drawing cards) and/or incomplete information (what cards are the other players holding?). In principle, they can be formulated as matrix games if the realization of randomness is included as the choice of a “dummy player”, and picking an option actually means deciding, in advance, what move to make for each conceivable situation during the course of the game. The number of different options is usually exponential in the number of cards and/or die rolls, and the formulation as a matrix game serves purposes of theoretical analysis rather than practical guidelines how to play.

4.2 Zero-sum games

Zero-sum games, in which the gain of one player always corresponds an equivalent loss of the other player, can be treated with a fairly elegant mathematical apparatus introduced by John von Neumann [12]. Let us call one player A and the other B. In each round, A chooses one among K options. In the following analysis, the option that is actually chosen will be denoted by i , $1 \leq i \leq K$. At the same time, B picks an option j from his repertoire of L options. They then consult the entry c_{ij} of the payoff matrix \mathcal{C} , and A receives c_{ij} from B. Accordingly, A will try to play strategies where large c_{ij} are picked, and B will try to keep c_{ij} small (negative, if possible).

In some realizations of \mathcal{C} , it may be optimal for A to keep choosing one option which is better than the alternatives, no matter what B plays, like in this example:

$$\mathcal{C} = \begin{pmatrix} 10 & 2 & 5 \\ 3 & -2 & 1 \\ -5 & 1 & 4 \end{pmatrix}. \quad (4.1)$$

Here, all entries in row 1 are higher than the corresponding entries in rows 2 and 3 – row 1 is said to *strictly dominate* rows 2 and 3, and picking it is a no-brainer, so to speak. Player A is said to play a *pure strategy* if he chooses the same option all the time. If B knows that A is going to repeatedly pick row 1, all that is left to do is minimize the losses and pick column 2 every time as well.

For random payoff matrices, the probability that one pure strategy dominates all other strategies decreases exponentially with increasing K . Even for small payoff matrices, the interesting cases are the ones without dominating strategies, such as Penny-Matching:

$$\mathcal{C} = \begin{pmatrix} 1 & -1 \\ -1 & 1 \end{pmatrix}. \quad (4.2)$$

In this game, player A tries to play the same option as player B, who in turn tries to play the opposite option of player A. The only way for a player to avoid being exploited is to choose at random between the two options – in this case, with 50% probability for each.

Generally, the behavior of players A and B at a given time can be defined by the vectors \mathbf{a} and \mathbf{b} of probabilities a_k and b_l for playing options l and m , respectively. These vectors follow the normalization constraint $\sum_k a_k = 1$ and $\sum_l b_l = 1$, i.e., they lie on the K - and L -dimensional simplex. If a player is playing a pure strategy, his strategy vector only has one nonvanishing component.

The expected payoff λ_k^A for A of one of his strategies k depends only on B's strategy:

$$\lambda_k^A = \sum_l b_l c_{kl}. \quad (4.3)$$

Player A will prefer strategies with higher λ_k^A . In the language of game theory,

a *strictly rational* agent will *always* prefer the option with the highest λ_k , thus playing a pure strategy every time, unless the the expected payoffs of several strategies are exactly tied. This almost never happens in models where the player estimates the opponent’s strategy from experience, rather than calculating the opponent’s equilibrium strategy and assuming he will play it [15]. A more tolerant approach, and one that emerges automatically in the neural network learning model discussed later, is to give higher probabilities to options with higher payoffs, and gradually eliminate those that promise significantly lower payoffs completely.

4.2.1 Nash equilibria

A *Nash equilibrium* is a combination of strategies \mathbf{a}^* and \mathbf{b}^* such that no player can improve his average payoff by unilaterally deviating from his equilibrium strategy. The average payoff for player A is

$$\lambda^A = \sum_{i,j} a_i c_{ij} b_j. \quad (4.4)$$

He will try to maximize the payoff he receives if B makes life as difficult as possible for him, and will choose

$$\max_{\mathbf{a}} \min_{\mathbf{b}} \sum_{i,j} a_i c_{ij} b_j. \quad (4.5)$$

On the other hand, player B, who is trying to minimize the amount he pays to A, will choose

$$\min_{\mathbf{b}} \max_{\mathbf{a}} \sum_{i,j} a_i c_{ij} b_j. \quad (4.6)$$

The Nash equilibrium fulfills both conditions at the same time. As von Neumann proved [12], in zero-sum games, there is exactly one Nash equilibrium. If it is a mixed strategy, all options that are played with non-zero probability (the *support* of the strategy) yield the exact same average payoff, also called the value of the game ν . The necessary and sufficient conditions for \mathbf{a}^* and \mathbf{b}^* can be written in a very concise way:

$$\lambda_i^A = \sum_j c_{ij} b_j^* \leq \nu \quad \text{for all } i; \quad (4.7)$$

$$\lambda_j^B = \sum_i a_i^* c_{ij} \geq \nu \quad \text{for all } j. \quad (4.8)$$

The minimax theorem guarantees that the smallest value for which a solution to Eq. (4.7) can be found is the largest value that yields a solution to Eq. (4.8). For a given payoff matrix, the equilibrium strategies can be calculated using linear optimization. For details, consult Ref. [94] and [95].

The interpretation of the Nash equilibrium is not very intuitive and worth spending a few words on. If player A plays the “optimal” strategy \mathbf{a}^* , he is

guaranteed the average payoff ν . There is no way for B to exploit A. However, there are usually several options for B that are precisely equivalent – each one makes B pay ν to A on average. In that sense, it is not a big challenge to play against a player who sticks to \mathbf{a}^* and does not respond to his opponent’s actions – B has to find one of the strategies in the support of \mathbf{b}^* and play it. ³ Doing this opens up player B to exploitation from A, which in turn would allow B to exploit A. On the other hand, it means that a learning algorithm of player B cannot be expected to converge to the minimal-optimal solution \mathbf{b}^* if A always plays \mathbf{a}^* .

In a game with a finite number of options, a small deviation from \mathbf{a}^* or \mathbf{b}^* only causes a small difference in the λ_i^A , which can only be empirically detected through many repetitions of the game. A pair of learning algorithms that rely only on observing the opponent’s actions will therefore converge to equilibrium very slowly (if they converge at all).

4.3 Multi-Choice Perceptrons

Economic game theory often assumes perfectly rational players with unlimited computational resources and a perfect grasp of the situation: both players study the game thoroughly before they start playing, find the Nash equilibrium and play the corresponding strategy, thus fulfilling the expectations of the opponent, who likewise plays his optimal strategy. Since this rarely applies to real-world situations, the question of *learning* in games has received much attention (see Ref.[96] and references herein): how can a player who is not familiar with the behavior of the opponent find a strategy, based on his knowledge of the payoff matrix and the observed behavior of the opponent?

Even in learning scenarios, there is a concept of a *rational* player: it means a player who, based on some prediction algorithm, calculates the expected payoff for each of his options and *always* chooses the one that promises the highest payoff. However, it was shown in Ref. [15] that under rather general circumstances, a rational player has no chance of learning to play the correct equilibrium strategy.

It is therefore interesting to search for strategies that are not rational, but that will converge to the Nash equilibrium, at least under some circumstances. One obvious candidate are neural networks, whose most interesting property is the ability to learn from examples. If each player has only two choices, a simple perceptron could be used to make the decision. This has been studied in some detail in Ref. [66] for some simple games like “Matching Pennies”. That case was also examined in Ref. [30]. However, even in the case of $K = 2$, a more complex network may be appropriate: a simple perceptron with random unbiased patterns will pick each option with 50% probability – this is generally not the optimal mixed strategy. If a larger number of options is available, a different architecture

³This can be readily verified using the corresponding program in Ref. [94].

is needed in any case. The obvious choice is the Potts perceptron, also known as Multi-Class perceptron [81].

A simplified version of the Potts perceptron was introduced in Section 3.7.2; here, we need the full architecture. This is still the simplest neural network that can handle inputs and outputs of the required form – quite possible, more elaborate networks could give better results; however, their behavior becomes mathematically less tractable.

To be able to choose one of K output options, the network of player A consists of K hidden units that generate K hidden fields h_i .

The output σ is usually taken to be the option with the highest hidden field:

$$\sigma = \{i | h_i = \max_l (h_l)\}. \quad (4.9)$$

This rule is the reason why this architecture is also called “Winner-takes-all perceptron” (WTAP, for the sake of brevity). For reasons explained below, it can be helpful to take as output the option with the highest absolute value of the hidden field:

$$\sigma = \{i | |h_i| = \max_l |h_l|\}. \quad (4.10)$$

For real-valued input vectors \mathbf{x} , each hidden unit is a linear perceptron:

$$h_l = \mathbf{w}_l \cdot \mathbf{x}. \quad (4.11)$$

If the input vectors consist of integers between 1 and Q (for example, a time series of the opponent’s decision), a more elaborate scheme is needed: each hidden unit has a set of Q weight vectors \mathbf{w}_l^q with entries w_{ln}^q . The hidden field for output l is

$$h_l = \sum_q \sum_n w_{ln}^q (Q\delta_{x_n,q} - 1). \quad (4.12)$$

This can be written as

$$h_l = \sum_q h_l^q \text{ with } h_l^q = \mathbf{w}_l^q \cdot \mathbf{x}^q, \quad (4.13)$$

where the \mathbf{x}^q are vectors with components $x_n^q = Q\delta_{x_n,q} - 1$. Thus each of the possible input values generates a separate contribution to the total hidden field.

In the following sections, I will assume real-valued inputs, which are easier to treat and to imagine. As usual, the variance of one component of the input is taken to be $\langle x_n^2 \rangle = 1$. Later on, the learning rules will be generalized to multi-value inputs.

What can and should we expect the neural network to do? If the inputs are completely random, the network should at least be able to use these patterns as seeds to generate a probability distribution of outputs and to adapt this distribution such that it gradually improves the perceptron’s average payoff. If the

inputs indeed contain some information on the opponent's action, the network might be able to capitalize on this. However, if the opponent is also a network of similar capabilities, there is no a priori reason why one should be able to outplay the other.

It turns out that learning has to follow different principles depending on whether the input pattern has a bias (a preferred direction) or whether it is an isotropic random vector. Note that it is not important whether this bias carries any information about the opponent or not. If the aim were to create a good, applicable learning algorithm, one could artificially add a bias vector. However, my first aim is to see what happens for a rather naïve approach to learning in different scenarios.

4.4 Learning from unbiased patterns

4.4.1 Generating a probability distribution

As mentioned in Section 4.3, one of the feats that a neural network in a two-player game should be capable of is to generate any probability distribution of outputs when fed with random patterns. The first step is therefore to check whether this is feasible.

If the weight vectors of the network's hidden units are mutually perpendicular ($\mathbf{w}_i \cdot \mathbf{w}_j = w_i^2 \delta_{ij}$), the hidden fields are uncorrelated Gaussian random numbers with variances $\langle h_i^2 \rangle = w_i^2$.⁴ The probability a_i that option i is chosen is then

$$\begin{aligned} a_i &= \int_{-\infty}^{\infty} \frac{dh_i}{\sqrt{2\pi w_i^2}} \exp\left(-\frac{1}{2} \frac{h_i^2}{w_i^2}\right) \prod_{j \neq i} \int_{-\infty}^{h_i} \frac{dh_j}{\sqrt{2\pi w_j^2}} \exp\left(-\frac{1}{2} \frac{h_j^2}{w_j^2}\right) \\ &= \int_{-\infty}^{\infty} \frac{d\hat{h}_i}{\sqrt{2\pi}} \exp\left(-\frac{\hat{h}_i^2}{2}\right) \prod_{j \neq i} \Phi\left(\frac{\hat{h}_i w_i}{w_j}\right). \end{aligned} \quad (4.14)$$

It is clear that under these circumstances, no probability larger than 1/2 can be achieved: even if all other weights are set to 0 (and correspondingly their hidden fields are 0), there is only a 50% chance that the hidden field of the nonzero vector is larger than 0.

It is also clear that no probability can be smaller than 2^{-K+1} : if one weight is set to 0 while all others have a finite value, there is still a chance of 2^{-K+1} that all others are negative, and thus the field with a value of 0 wins. The function (4.14) interpolates between these two extremes.

A small variation of the decision rule removes these limitations: if the output is determined by the largest absolute field, as suggested in Eq. (4.10), a_i is given

⁴The assumption of perpendicular vectors simplifies things immensely. Of course, it must be justified later, when learning algorithms are considered.

by

$$\begin{aligned}
a_i &= \int_0^\infty \frac{2dh_i}{\sqrt{2\pi w_i^2}} \exp\left(-\frac{1}{2} \frac{h_i^2}{w_i^2}\right) \prod_{j \neq i} \int_0^{h_i} \frac{2dh_j}{\sqrt{2\pi w_j^2}} \exp\left(-\frac{1}{2} \frac{h_j^2}{w_j^2}\right) \\
&= \int_0^\infty \frac{2dh_i}{\sqrt{2\pi}} \exp(-h_i^2/2) \prod_{j \neq i} \hat{H}\left(\frac{w_i h_i}{w_j}\right), \text{ where} \\
\hat{H}(x) &= \int_0^x \frac{2dh}{\sqrt{2\pi}} \exp(-h^2/2). \tag{4.15}
\end{aligned}$$

This rule allows for probabilities a_i between 0 and 1 – however, the interpretation of Eq. (4.10) is admittedly dubious if the pattern has any meaning beyond being a random number seed: The invariance of Eq. (4.10) to the sign of h essentially states, “If the situation is such-and-such, do this, and if the situation is exactly the opposite, do the same.”

In the simplest case of $K = 2$, Equation (4.15) can be evaluated analytically, and we obtain

$$a_1 = (2/\pi) \arctan(w_1/w_2) \text{ and } a_2 = 1 - a_1. \tag{4.16}$$

4.4.2 Learning rule

If we assume that the patterns are random and the strategy is only determined by the set of weight norms $\{w_i\}$, we need a learning rule that adapts the norms accordingly. The following rule employs the mechanisms of the Confused Bit Generator: if a perceptron learns the opposite of its own output, its norm converges to a finite value. If it reinforces its output, the norm grows linearly with α . A plausible first attempt at a learning rule is therefore

$$\mathbf{w}_l^{t+1} = \mathbf{w}_l^t + \frac{\eta}{M} \mathbf{x} \text{sign}(\mathbf{x} \cdot \mathbf{w}_l) c_{lj}. \tag{4.17}$$

The row player updates each of its weights using the column j of the payoff matrix that his opponent chose. Weights with a high payoff get positive feedback, while weights with a negative payoff are suppressed. Averaging over many outputs j and patterns \mathbf{x} , Eq. (4.17) becomes

$$\langle \mathbf{w}_l^{t+1} - \mathbf{w}_l^t \rangle_{j,\mathbf{x}} = \frac{\eta}{M} \langle \mathbf{x} \text{sign}(\mathbf{x} \cdot \mathbf{w}_l) \rangle_{\mathbf{x}} \sum_j b_j c_{lj}. \tag{4.18}$$

That means that the feedback term on the right hand side is proportional to the expected payoff $\lambda_l^A = \sum_j b_j c_{lj}$ for that option. A positive value of λ_l^A leads to linear growth, a negative value leads to a finite value, and a vanishing value $\lambda_l^A = 0$ gives $w_l \propto \sqrt{\alpha}$.

This may be problematic since the value of the game ν may be different from 0, leading to a suppression of all options for $\nu < 0$ or enhancement of non-optimal

options for $\nu > 0$. An even better learning rule incorporates this and estimates the value of the game by subtracting the current payoff c_{ij} from the potential payoff of the updated option, c_{lj} :

$$\mathbf{w}_l^{t+1} = \mathbf{w}_l^t + \frac{\eta}{M} \mathbf{x} \text{sign}(\mathbf{x} \cdot \mathbf{w}_l)(c_{lj} - c_{ij}). \quad (4.19)$$

This rule is somewhat more difficult to treat, since the update for each option explicitly depends on what option was chosen by the player, i.e., it depends on all other w_i as well. For large K , one can ignore this effect, but for small K it turns out to be important. Thus I will first look closer at the textbook case of $K = L = 2$ for specific matrices (called generalized penny-matching in the literature) and then go to the limit of large K for random matrix entries.

4.4.3 The case of $K = 2$

As mentioned above, for small K , the output of the WTAP has to follow the largest absolute value of the inner field $|h_i| = |\mathbf{w}_i \cdot \mathbf{x}|$ – otherwise both options would be chosen with 50% probability each. Using absolute fields, the strategy for two options is given by Eq. (4.16). In the spirit of on-line learning, we can take the square of Eq. (4.19) and use the limit $M \rightarrow \infty$ to transform the update equations it into a set of differential equations for the w_i . For example, for option 1 of player A, one obtains (with $\mathbf{x} \cdot \mathbf{x} = M$):

$$w_1^{t+1^2} = w_1^{t^2} + \frac{\eta}{M} |h_1| (c_{1j} - c_{ij}) + \frac{\eta^2}{M} (c_{1j} - c_{ij})^2. \quad (4.20)$$

The second and third term on the right hand side vanishes if $|h_1| > |h_2|$, which has to be taken into account when averaging:

$$\begin{aligned} \langle |h_1| (c_{1j} - c_{ij}) \rangle_{h_1, h_2} &= \left(\int_0^\infty Dh_1 2w_1 h_1 \int_0^{h_1 w_1 / w_2} 2Dh_2 \right) (\lambda_1^A - \lambda_2^A) \\ &= \sqrt{\frac{2}{\pi}} w_1 \left(1 - \frac{w_1}{\sqrt{w_1^2 + w_2^2}} \right) (\lambda_1^A - \lambda_2^A); \end{aligned} \quad (4.21)$$

$$\langle (c_{1j} - c_{ij})^2 \rangle = x_2 (b_1 (c_{11} - c_{21})^2 + b_2 (c_{12} - c_{22})^2). \quad (4.22)$$

In this special case, λ_i^A is an abbreviation for $b_1 c_{i1} + b_2 c_{i2}$. Using the chain rule, a differential equation for w_1 can be derived:

$$\begin{aligned} \frac{dw_1}{d\alpha} &= \sqrt{\frac{2}{\pi}} \eta \left(1 - \frac{w_1}{\sqrt{w_1^2 + w_2^2}} \right) (\lambda_1^A - \lambda_2^A) + \\ &\quad \eta^2 a_2 [b_1 (c_{11} - c_{21})^2 + b_2 (c_{12} - c_{22})^2] / (2w_1). \end{aligned} \quad (4.23)$$

A similar equation can be derived for w_2 . If player B is using a neural network with the same learning rule (whose vectors I will denote as \mathbf{v}_j with norms v_j to

avoid confusion), the differential equations for its weight vectors norms v_1 and v_2 can be written down as well:

$$\begin{aligned} \frac{dw_2}{d\alpha} &= \sqrt{\frac{2}{\pi}}\eta \left(1 - \frac{w_2}{\sqrt{w_1^2 + w_2^2}} \right) (\lambda_2^A - \lambda_1^A) + \\ &\quad \eta^2 a_1 [b_1(c_{11} - c_{21})^2 + b_2(c_{12} - c_{22})^2] / (2w_2). \end{aligned} \quad (4.24)$$

$$\begin{aligned} \frac{dv_1}{d\alpha} &= \sqrt{\frac{2}{\pi}}\eta \left(1 - \frac{v_1}{\sqrt{v_1^2 + v_2^2}} \right) (\lambda_2^B - \lambda_1^B) + \\ &\quad \eta^2 x_2 [b_1(c_{11} - c_{12})^2 + a_2(c_{21} - c_{22})^2] / (2v_1). \end{aligned} \quad (4.25)$$

$$\begin{aligned} \frac{dv_2}{d\alpha} &= \sqrt{\frac{2}{\pi}}\eta \left(1 - \frac{v_2}{\sqrt{v_1^2 + v_2^2}} \right) (\lambda_1^B - \lambda_2^B) + \\ &\quad \eta^2 b_1 [a_1(c_{11} - c_{12})^2 + a_2(c_{21} - c_{22})^2] / (2v_2). \end{aligned} \quad (4.26)$$

The symbol λ_j^B stands for the expected payoffs of B's options $a_1c_{1j} + a_2c_{2j}$, and player B favors strategies j with minimal λ_j^B . This set of ODEs can now be solved numerically for any 2×2 payoff matrix. In simple cases, the asymptotics can be calculated analytically. For example, take the payoff matrix

$$c = \begin{pmatrix} 1 & 0 \\ 1 & 1 \end{pmatrix}. \quad (4.27)$$

In this case, $\lambda_1^A = b_1$, $\lambda_2^A = 1$, $\lambda_1^B = 1$, and $\lambda_2^B = a_2$. One can assume that for large α , $w_1 \ll w_2$ and $v_1 \ll v_2$, and correspondingly make the expansions $a_1 \approx (2/\pi)w_1/w_2$, $b_1 \approx (2/\pi)v_1/v_2$, $w_2/\sqrt{w_1^2 + w_2^2} \approx 1 - (w_1/w_2)^2/2$, and $v_2/\sqrt{v_1^2 + v_2^2} \approx 1 - (v_1/v_2)^2$, a short calculation leads to the asymptotic value for w_1 and v_2 : $w_1, v_2 \rightarrow \sqrt{\pi/8}\eta$; for w_2 one gets $w_2 \propto \alpha^{1/3}$, corresponding to $a_1 \propto \alpha^{-1/3}$. With this result, the exponent for v_2 and b_1 can be calculated; it is $v_2 \propto \alpha^{2/9}$ and $b_1 \propto \alpha^{-2/9}$. The complete numerical solution of Eqs. (4.23–4.26) agrees excellently with simulations and also confirms the calculated asymptotic exponents, as seen in Fig. 4.1.

It turns out that the minimax-optimal solution for this problem is $\mathbf{a}^* = (0, 1)$, $\mathbf{b}^* = (1, 0)$; i.e., \mathbf{b} converges to the wrong solution. However, if $\mathbf{a} = \mathbf{a}^*$, the payoff is indifferent to the choice of \mathbf{b} , and as long as $\mathbf{a} \neq \mathbf{a}^*$, $\mathbf{b} = (0, 1)$ is the best response of player B.

In this example, the proposed learning algorithm converges to a strategy that gives the same payoff as the equilibrium strategy, but the rate of convergence is slow (power-law convergence with small negative exponents) and depends on the realization of the matrix. A look at Eqs. (4.23–4.26) shows that the Nash equilibrium (which is characterized by $\lambda_1^A = \lambda_2^A$ and $\lambda_1^B = \lambda_2^B$) is a stationary point of the update equations only in the long-time limit where $1/w_i$ and $1/v_j$ are negligible. This is better than no convergence at all, but can hardly be considered

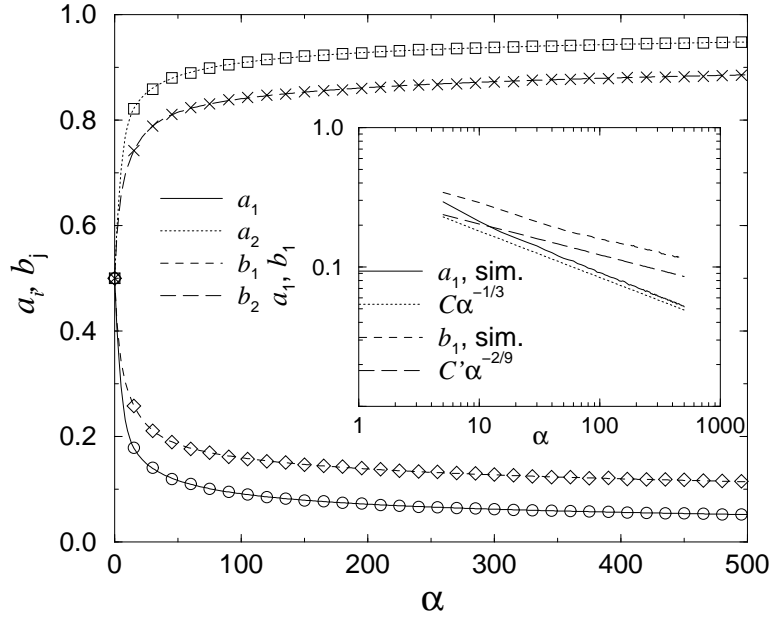


Figure 4.1: Development of strategies in a zero-sum game with payoffs according to Eq. (4.27), under learning rule Eq. (4.19). Symbols in the large plot denote simulations with $M = 2000$.

good in a situation where a few round should be enough to clarify what is the best thing to do. However, a learning algorithm, even a slow one, may be more useful in situations where the optimal behavior is not as obvious, such as for large payoff matrices.

4.4.4 Large K

Let us now turn to the case of large payoff matrices. To make statements that are valid for fairly generic cases, I will also assume that the entries are random and uncorrelated – to be specific, they are random Gaussian numbers of variance $\langle c_{ij}^2 \rangle = K$. The statistics of the minimax-optimal solution for this scenario were studied by J. Berg and A. Engel [97, 98, 99]. Combining these results with simulations and calculations that I did, the following picture emerges:

If player A picks a random strategy \mathbf{a}_r , the expected payoffs λ_j^B of player B's options are again Gaussian random numbers with zero mean and a variance of roughly 1 (the exact value depends on the self-overlap of the random strategy vector).

If both players are playing the minimax-optimal strategies \mathbf{a}^* and \mathbf{b}^* , and $K = L$, on average 50% of each player's options are in the support of this strategy, i.e., they are played with non-zero probability. Each of these yields an average payoff of ν , which is 0 for $K \rightarrow \infty$ and a Gaussian random number of mean 0

and variance $\langle \nu^2 \rangle \propto 1/K$ for finite K . The strategies which are not played give a payoff that is lower than ν and follows a Gaussian probability distribution.

In order to see how a WTAP that learns according to Eq. (4.19) behaves, it is necessary to assume that the entries in the payoff matrix are not correlated to the strategies of the players. This may seem counter-intuitive at first: after all, player A ought to prefer strategies with above-average entries. However, if player B can avoid being exploited completely (by a learning algorithm or other clever strategy), player A will have to put up with taking strategies with below-average entries as well, at least for large K , where dominating strategies are exceedingly unlikely.

The mentioned assumption leads to $\langle c_{ij}^2 \rangle_{i,j} = \langle c_{ij}^2 \rangle_{i,j} K$ and $\langle c_{lj} c_{ij} \rangle_{i,j} = K a_l$. It is easy to calculate that $\langle \mathbf{x} \cdot \mathbf{w}_l \text{sign}(\mathbf{x} \cdot \mathbf{w}_l) \rangle = \sqrt{2/\pi} w_l$, and to combine these results into

$$\frac{dw_l^2}{d\alpha} = \sqrt{8/\pi} \eta \left(\lambda_l - \sum_i a_i \lambda_i \right) w_l + 2\eta^2 K (1 - a_l). \quad (4.28)$$

The second term on the right hand side is a random walk term. The factor $(1 - a_l)$ can be explained by a look at Eq. (4.19): the weight that belongs to the currently chosen option is not updated. More important, however, is the first term, which causes the weights with above-average success to grow and those with below-average success to shrink. This term is proportional to w_l , so it will dominate for large α and correspondingly large w_l .

If both players play their optimal strategies \mathbf{a}^* and \mathbf{b}^* , $\sum_i a_i \lambda_i$ is equal to the value of the game ν , and the first term in Eq. (4.28) goes to 0 for those options l that are part of the optimal strategy, and stays negative for those that are not. Neglecting the second term, this would be an indication that the optimal strategies are a fixed point of the considered learning rule.

To be sure that the assumption of perpendicular vectors underlying Eq. (4.14) holds, we must examine the time development, and hence the fixed point, of angles $\theta_{lm} = \arccos(\mathbf{w}_l \cdot \mathbf{w}_m / (w_l w_m))$ between the vectors. A calculation similar to the one above yields for the unnormalized overlap $R_{lm} = \mathbf{w}_l \cdot \mathbf{w}_m$:

$$\begin{aligned} \frac{dR_{lm}}{d\alpha} &= \eta \sqrt{\frac{2}{\pi}} \cos(\theta_{lm}) \left[w_l \left(l_m - \sum_i \lambda_i a_i \right) + w_m \left(\lambda_l - \sum_i \lambda_i a_i \right) \right] \\ &\quad + \eta^2 \left(1 - \frac{2\theta_{lm}}{\pi} \right) K (1 - a_l - a_m). \end{aligned} \quad (4.29)$$

Using the chain rule, an expression for the development of $\cos(\theta)_{lm}$ can be derived. Interestingly, all terms proportional to η vanish:

$$\begin{aligned} \frac{d \cos(\theta_{lm})}{d\alpha} &= \eta^2 K \left(\frac{1 - 2\theta_{lm}/\pi}{w_l w_m} (1 - a_l - a_m) \right. \\ &\quad \left. - \frac{\cos(\theta_{lm})}{w_l^2} (1 - a_l) - \frac{\cos(\theta_{lm})}{w_m^2} (1 - a_m) \right). \end{aligned} \quad (4.30)$$

Of the remaining terms, the ones proportional to $\cos(\theta)_{lm}$ dominate: the prefactor $1/(w_l w_m)$ is smaller or equal to $1/w_l^2 + 1/w_m^2$, $1 - a_l - a_m$ is smaller or equal to $1 - a_l$ and $1 - a_m$, and near the fixed point $\theta = \pi/2 + \Delta\theta$, an expansion gives $1 - 2\theta/\pi \approx -2\Delta\theta/\pi$, whereas $\cos(\pi/2 + \Delta\theta) \approx -\Delta\theta$. Hence, for small $\Delta\theta$ the right hand side is proportional to $-\Delta\theta$, and $\theta = \pi/2$ is a stable fixed point. This is reassuring and tells us that the use of Eq. (4.14) is at least a good approximation.

The approximation can be tested in simulations, which show that angles between different weight vectors fluctuate around 0, with a variance that depends on M . Therefore, Eq. (4.14) agrees well ($\sim 1\%$ accuracy for $M = 100$) with the output probabilities measured in the simulations. This allows to calculate the mixed strategy, and hence the learning success, at any point in the simulations with reasonable computational effort.

Playing against an opponent with a fixed strategy

The first test case is playing a simplified matrix game against an opponent who follows a pre-determined strategy, i.e. chooses columns j with constant probabilities b_j .

If this fixed strategy is chosen at random, the distribution of expected average payoffs λ_i will be Gaussian with a variance near 1, as mentioned above. Without loss of generality, we can rename options such that $\lambda_1 > \lambda_2 > \dots > \lambda_K$.⁵ The best strategy for player A is then $a_i = \delta_{i,1}$. A WTAP that uses Eq. (4.10) and is updated according to Eq. (4.19) should converge to the optimal solution: The weight belonging to the most profitable option always grows at least like $\sqrt{\alpha}$:

$$\begin{aligned} \frac{dw_1}{d\alpha} &= \frac{1}{2w_1} \left[\sqrt{\frac{8}{\pi}} \eta \left(\lambda_1 - \sum_i a_i \lambda_i \right) w_1 + 2\eta^2 K (1 - a_1) \right] \\ &> \sqrt{\frac{2}{\pi}} \eta (\lambda_1 - \lambda_2) (1 - a_1). \end{aligned} \quad (4.31)$$

Pure strategies that give below-average payoff (compared to the current average, i.e., to $\sum a_i \lambda_i$) have a negative growth term in their update equation, i.e., their weight stays bounded, and their probability a_i of being played goes to zero, removing them from the competition. Gradually, the average payoff increases, eliminating one non-optimal choice after the other. This is what happens in simulations as well, as seen in Fig. 4.2.

As pointed out previously, if B is constantly playing the optimal strategy \mathbf{b}^* , the best thing that A can do is to eliminate the strategies with $\lambda_i < \nu$ that are not in the support of \mathbf{a}^* . As Fig. 4.3 shows, the neural network succeeds in doing this: after a learning time of $\alpha = 100$, the suboptimal options are strongly suppressed (only the option with the payoff closest to ν still has an appreciable

⁵The case that two expected payoffs are exactly equal occurs with probability 0.

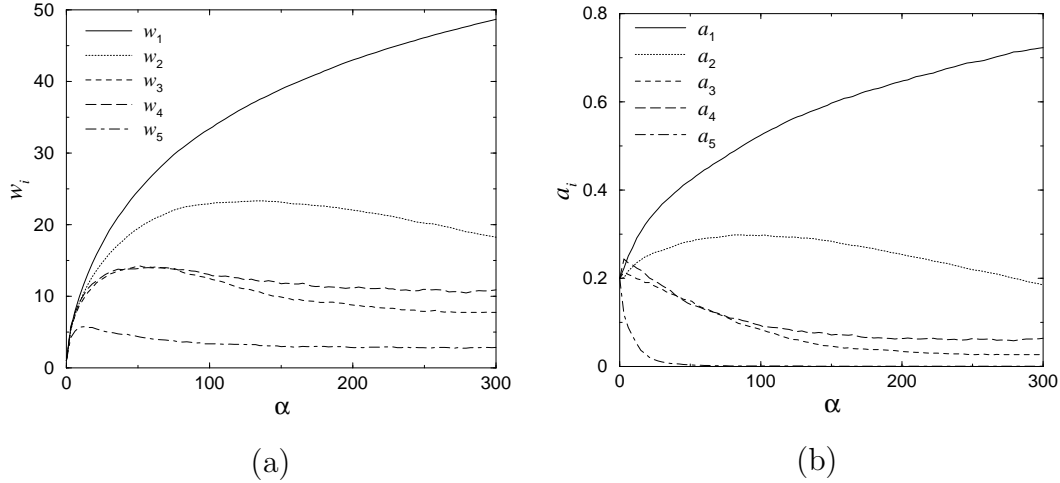


Figure 4.2: Playing against a non-adaptive opponent with a random strategy: the weight of the most advantageous strategy 1 grows fastest, whereas the weights of below-average strategies shrink (Plot (a)). Correspondingly, the most profitable strategy is used increasingly (Plot (b)). Simulations used a random matrix with $K = L = 5$ and $M = 100$.

probability), whereas the strategies in the support of \mathbf{a}^* are played with random positive probabilities.

Playing against adaptive opponents - Fictitious Play

One of the standard learning algorithms in game theory is *Fictitious Play* [96]: the adaptive player (in this case, player B) keeps a histogram of his opponent's decisions i^τ up to a time t , which he uses to estimate A's strategy \mathbf{a} by $\tilde{\mathbf{a}}$:

$$\tilde{a}_k = \frac{1}{t} \sum_{\tau} \delta_{k, i^\tau}. \quad (4.32)$$

Player B then estimates the average payoffs of his available strategies assuming that A will continue playing as he did before:

$$\tilde{\lambda}_j^B = \sum_k c_{kj} \tilde{a}_k, \quad (4.33)$$

and chooses the output with minimal $\tilde{\lambda}_j^B$. This updating rule has been proven to converge to the optimal strategy if both players use it, in the sense that the empirical estimate $\tilde{\mathbf{a}}$ converges to \mathbf{a}^* , and $\tilde{\mathbf{b}}$ to \mathbf{b}^* , as $t \rightarrow \infty$ [96].

However, in a different sense, it does not converge: at any given time, the output of the ‘‘Fictitious Play’’-player is deterministic, and he often repeats the same output for several time steps, so he never plays the optimal mixed strategy.

Simulations show that in the long run, when Fictitious Play and the proposed neural network algorithm play against each other, they converge to the Nash

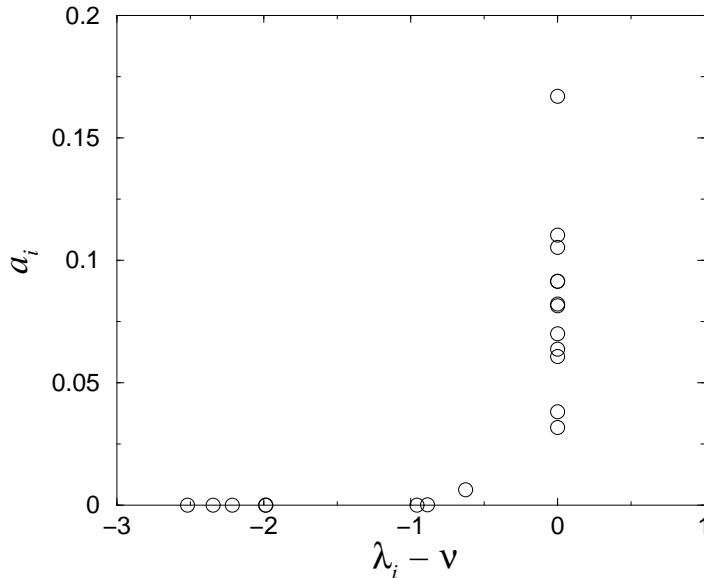


Figure 4.3: Components a_i of the strategy vector versus expected payoff λ_i , against an opponent using the equilibrium strategy \mathbf{b}^* . The figure shows the state after 10^4 learning steps with $K = 20$, $M = 100$.

equilibrium in the long-time average sense. At any given moment, the output distribution of A is significantly different from \mathbf{a}^* . However, just as the histogram of outputs of two players doing Fictitious Play converges to \mathbf{a}^* and \mathbf{b}^* , so does the output of the Neural Network player. Fig. 4.4 shows the components of $\tilde{\mathbf{a}}$ and $\tilde{\mathbf{b}}$ (the empirical long-time averages) versus the components of \mathbf{a}^* and \mathbf{b}^* after 10^6 steps in a simulation with $K = 20$. Perfect convergence to equilibrium would result in all points lying on the diagonal. The figure also shows the current strategy \mathbf{a} of the Neural Network at the moment when the simulation ended. One can see that the deviation of the current \mathbf{a} (empty squares) from the equilibrium strategy is larger than that of $\tilde{\mathbf{a}}$ (empty circles), which agrees reasonably well with \mathbf{a}^* .

The fluctuations of \mathbf{a} around the optimal strategy can be quantified by introducing an overlap $R = \mathbf{a} \cdot \mathbf{a}^* / |\mathbf{a}| |\mathbf{a}^*|$ and an expected payoff $\bar{\lambda}^A = \langle \sum_i \lambda_i^A \rangle$ averaged over times short compared to the total learning process. R is observed to fluctuate around high values ≈ 0.9 , but never converges to 1, whereas $\bar{\lambda}^A$ fluctuates around the value of the game, as seen in Fig. 4.5. The figure also shows the overlap of $\tilde{\mathbf{a}}$ with \mathbf{a}^* (dotted line), which seems to converge to 1. However, the rate of convergence depends on the realization of the payoff matrix.

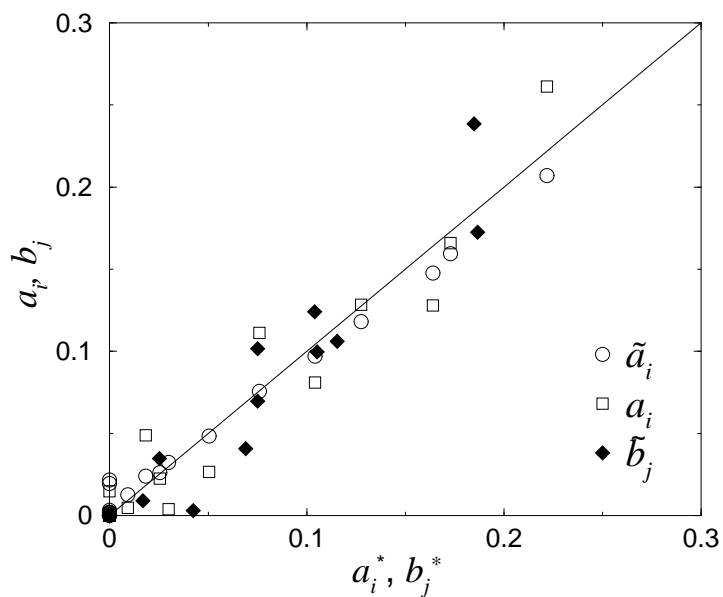


Figure 4.4: Averaged empirical and current strategies $\tilde{\mathbf{a}}$ and \mathbf{a} of a neural network playing against Fictitious Play (empty symbols) and empirical strategy $\tilde{\mathbf{b}}$ of the opponent (filled symbols) after 10^6 learning steps with $K = 20$, $M = 100$, compared to the equilibrium strategies \mathbf{a}^* and \mathbf{b}^* . Perfect agreement with the equilibrium strategies would result in all points lying on the diagonal.

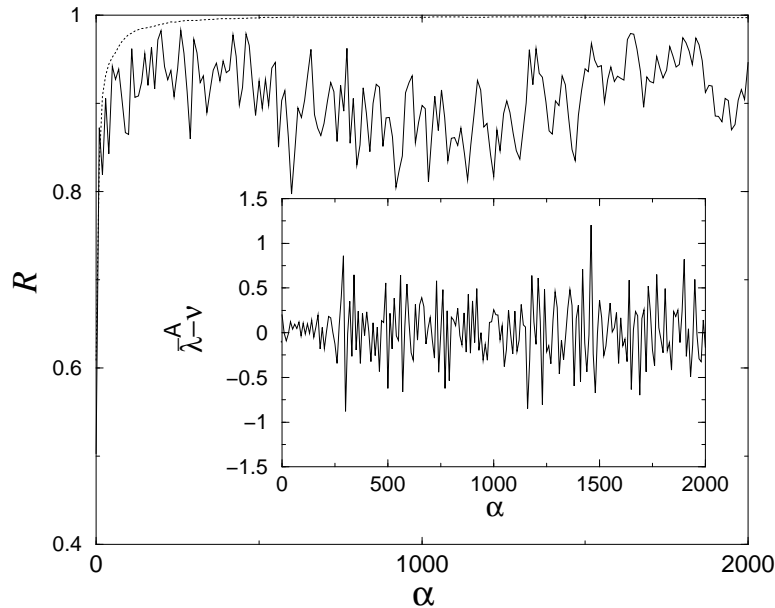


Figure 4.5: Dynamics of the overlap R between \mathbf{a} and \mathbf{a}^* (solid line) and between $\tilde{\mathbf{a}}$ and \mathbf{a}^* (dotted line) of a neural network playing against Fictitious Play. The inset shows the payoff $\bar{\lambda}^A$ for A, averaged over 1000 round of play. The simulation used $M = 100$ and $K = 20$.

Playing against an equivalent opponent

One rather obvious question is how the proposed learning algorithm fares against an opponent who is using the same architecture and the same update rule. The answer is, quite good, with some exceptions. Generally, the principles of the algorithm work fine: options that give above-average payoffs are strengthened, the others are suppressed. If equilibrium is reached, the weight vectors continue to grow slowly due to the random walk term in Eq. (4.28), which gradually slows down the dynamics. Simulations show that the strategies of the two players usually reach a high overlap with the Nash equilibrium. Fluctuations around the optimal strategy decrease with increasing M and decreasing η .

The mentioned exceptions concern two possible problems: for one, there is again the possibility that an option that is not in the support of the optimal strategy has a payoff that is only negligibly below the value of the game. This option is very hard to tell apart from a “good” one, i.e., one that is in the support, by looking at average payoffs, and may stay in the strategy mix for a long time. From the point of view of optimization, such an option corresponds to a very shallow valley whose minimum has to be found.

The second problem can occur if the networks of both players are fed with the same pattern. If two weight vectors of the two networks have an angle other

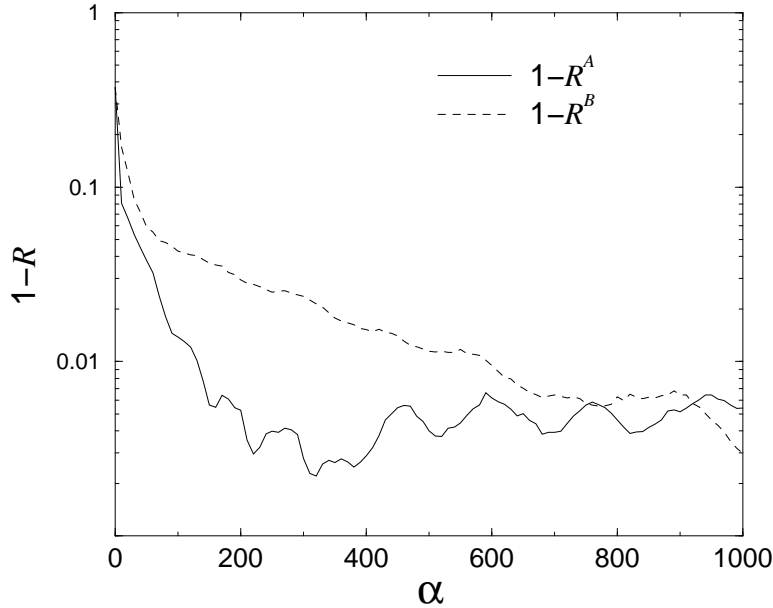


Figure 4.6: Two neural networks with $M = 1000$ playing a zero-sum game: the plot shows how the overlaps with the equilibrium strategy increase during learning, then saturate at some value that depends on M and η .

than $\pi/2$, the output of the players is mutually correlated. Although a calculation similar to that leading to Eq. (4.30) shows that the overlaps between the different weight vectors of the two players, $\mathbf{w}_l \cdot \mathbf{v}_k / (w_l v_k)$, should have a stable fixed point at 0, simulations show that a significant overlap (on the order of 0.9) can develop. If one network can predict the output of the other beyond the point of knowing the probability distribution \mathbf{a} , the concept of an equilibrium mixed strategy breaks down. It appears, however, that this irregularity appears less frequently with increasing M .

A remark on efficiency and more general schemes

The proposed learning algorithm essentially uses the patterns as random number seeds, without drawing any further information from them. The only relevant property of the weight vectors was their norm. If the task is to find an algorithm that learns to play a two-player game, would it not be more efficient to reduce the problem from updating and multiplying vectors to rolling Gaussian random numbers and updating their variance according to Eq. (4.28)? Indeed it would. This abstraction also opens the way to all sorts of fiddling with the learning rule: the noise term (the term proportional to η^2 in Eq. (4.28) can be made larger or smaller, the learning rate can be made time-dependent, the variance can be increased linearly, polynomially or exponentially. . . possibilities are limitless.

This opens the door to a more general class of learning algorithms for two-player games: adjusting the variances of random numbers, the largest of which determines the output, is one way of updating the probability vector. However, it is not trivial to find one that even comes close to the Nash equilibrium.

A remark on time scales

The analysis of the learning algorithm tacitly assumed the usual limit $M \rightarrow \infty$, which allows to replace $\langle c_{lj} \rangle$ with $\sum_j b_j c_{lj}$ – as long as K is finite, each option j that is played at all is played an infinite number of times during a short time interval $\Delta\alpha$. In reality, M is always finite – and as the remark above showed, M is not really relevant as the dimensionality of a vector space. However, a certain number of rounds have to be played to get a good estimate of the expected payoff of an option. Let us assume that strategies are fixed for a moment. If a large number t of rounds are played, player A played option i $t(a_i + \Delta_i)$ times, where Δ_i is a Gaussian random number of mean 0 and variance $\langle \Delta_i^2 \rangle = a_i(1 - a_i)/t$. The mean square deviation between the observed and the expected payoff for one of B's options j is then

$$\begin{aligned}
\langle (\lambda_j^B - \tilde{\lambda}_j^B)^2 \rangle &= \left\langle \left(\sum_i \Delta_i c_{ij} \right)^2 \right\rangle \\
&= \left\langle \sum_i \Delta_i^2 \right\rangle + \left\langle \sum_{i,l \neq i} \Delta_i \Delta_l c_{ij} c_{lj} \right\rangle \\
&= \sum_i c_{ij}^2 a_i (1 - a_i) / t \\
&\sim \frac{K}{t}.
\end{aligned} \tag{4.34}$$

To decide which one of two options with payoffs λ_1^B and λ_2^B is better, player B has to wait roughly $t > K/(\lambda_1^B - \lambda_2^B)^2$ time steps.

Learning in two-payer games is, as is often the case in learning scenarios, a tradeoff between accuracy (exact judgment which option is the best) and speed (to avoid being exploited by insisting on a suboptimal strategy for a long time). Things become even trickier near equilibrium, since the difference in expected payoffs decreases the closer the opponent comes to his optimal strategy, and vanish if he reaches it. At that point, any drift term in a learning algorithm vanishes. Since the noise term remains, fluctuations are inevitable.

An optimized learning algorithm might take this into account and adapt quickly as long as differences in the expected payoffs are large, while it reduces both the rate of adaption and, if possible, additional noise terms when it is near an equilibrium. However, it is not obvious how proximity to equilibrium can be detected unambiguously.

Learning from time series

So far, the patterns that the neural networks used had no meaning in themselves and contained no information on the opponent's actions. This could be considered the worst case, and it is good to know that the networks responded reasonably if the update rule was chosen accordingly. If the patterns now represent real information – e.g., they contain the time series of the opponent's output – should not the networks perform much better?

To check this, we have to leave the simplicity of real-valued patterns behind and use Q -state patterns, as described in Sec. 4.3: the components of A's patterns can take $Q^A = L$ values, whereas B's patterns consist of $Q^B = K$ values. The first update rule to try is the generalization of Eq. (4.19):

$$\mathbf{w}_l^{qt+1} = \mathbf{w}_l^{qt} + \frac{\eta}{M} \mathbf{x}^q \text{sign}(h_l)(c_{lj} - c_{ij}). \quad (4.35)$$

The output is determined by the hidden field with the highest absolute value, and the patterns that each network sees are the time series of the other player's output.

The outcome is disillusioning: the output probabilities have no similarity with the optimal strategy. A closer look reveals that both perceptrons lock into long stretches of repeated outputs, similar to a single Bit Generator with fixed weights. Since weights are not exactly fixed in this case, cycles do not continue forever, but nevertheless, no convergence to an equilibrium is observed.

Could the network possibly draw useful information from the patterns and at the same time avoid falling into cycles if the components of the patterns had no temporal correlation? For example, one can feed the networks an artificial time series of an opponent playing his optimal strategy with true random numbers. The results are again surprising: while the strategy of the networks at any given time is not very close to equilibrium, the long-time average of outputs converges to equilibrium fairly quickly, similar to two players playing Fictitious Play against each other.

One more detail shows that some new mechanisms are at work: if the output is determined by the largest hidden field h_i instead of $|h_i|$, there is no convergence to equilibrium in any sense. That points to the fact that the sign of h_i is no longer random, which has its reason in an inherent bias in the patterns.

4.5 Learning from biased patterns

A bias in the patterns can easily lead to a bias in the weights (which are, after all, a linear combination of the initial weights and the patterns that are shown during the learning process), which can in turn cause a bias in the hidden fields. To understand these effects systematically, it is easier to go back to real-valued

patterns with a bias, and later make the generalization of the terms introduced there to multi-valued inputs.

To be specific, a biased pattern vector consists of an unbiased random vector $\tilde{\mathbf{x}}$ and a constant vector \mathbf{y} of norm y . The weight vectors can also be split into components parallel and perpendicular to the bias:

$$\begin{aligned}\bar{\mathbf{w}}_i &= \frac{\mathbf{w}_i \cdot \mathbf{y}}{y^2} \mathbf{y}; \\ \tilde{\mathbf{w}}_i &= \mathbf{w}_i - \bar{\mathbf{w}}_i.\end{aligned}\tag{4.36}$$

The appropriate order parameters are $\bar{w}_i = \mathbf{w}_i \cdot \mathbf{y} / y$, which can take positive and negative values, and $\tilde{w}_i = \sqrt{\tilde{\mathbf{w}}_i \cdot \tilde{\mathbf{w}}_i}$, which is positive or zero.

For any pattern \mathbf{x} , the hidden field h_i of strategy i now has three components:

- a stochastic component $\tilde{h}_i = \tilde{\mathbf{w}}_i \cdot \mathbf{x}$ that is assumed to be independent from the \tilde{h}_l of the other options l ;
- a constant component $\bar{\mathbf{w}}_i \cdot \mathbf{y} = \bar{w}_i y$;
- and a stochastic component $\bar{\mathbf{w}}_i \cdot \tilde{\mathbf{x}} = h_c \bar{w}_i$ where the factor h_c is a Gaussian variable of variance 1 that takes the same values for all strategies l for a given x .

The chance that h_i for a given i is the largest now reads (analogous to 4.14):

$$a_i = \int_{-\infty}^{\infty} D\hat{h}_i \int_{-\infty}^{\infty} Dh_c \frac{1}{2\pi} \prod_{l \neq i} \Phi \left[\frac{1}{\tilde{w}_l} \left(\tilde{w}_i \hat{h}_i + (h_c + y)(\bar{w}_i - \bar{w}_l) \right) \right]. \tag{4.37}$$

The integrals can possibly be eliminated by linear transformation of the variables; however, the transformed expression neither becomes prettier nor gives more insight.

If the bias dominates the output, a second look at the update rule is necessary. If Eq. (4.19) is used and the weight of an option has a large negative bias \bar{w}_i , the hidden field will be negative, and the update will tend to make it more negative if the option is favorable. This is not a problem if the output follows the maximal $|h_i|$; however, it is now also possible to let the output follow the maximal h_i (Eq. (4.9)) and drop the $\text{sign}(h_l)$ -term in the update rule:

$$\mathbf{w}_l^{t+1} = \mathbf{w}_l^t + \frac{\eta}{M} \mathbf{x} c_{lj}.\tag{4.38}$$

The normalizing term proportional to $-c_{ij}$ is not needed anymore either – it would result in adding the same update vector to all \mathbf{w}_l , thus shifting all hidden fields by the same amount for a given pattern vector. This no longer has an influence on the decision of the network.

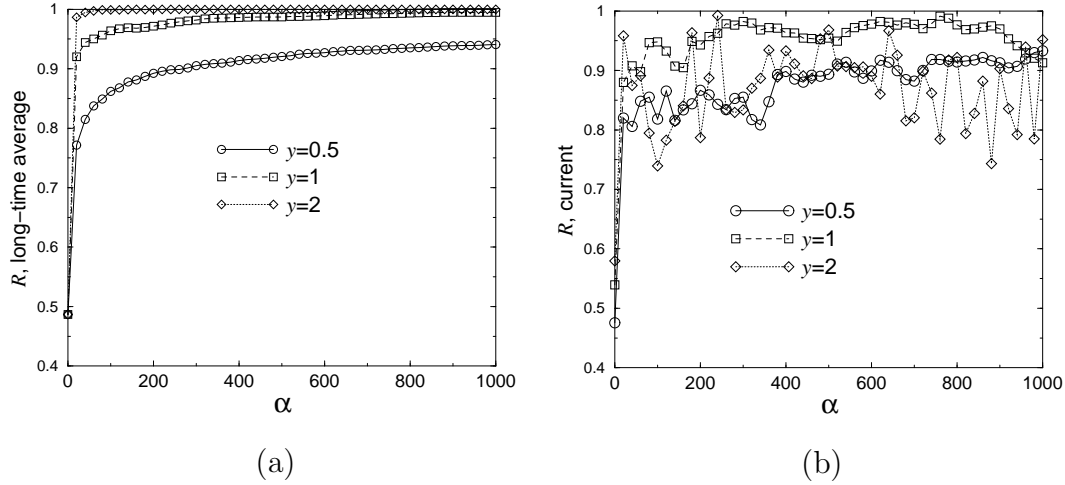


Figure 4.7: Learning from biased patterns: while the long-time averaged strategy converges to \mathbf{a}^* quickly for large bias y (as in Fictitious Play), the current strategy comes closest to \mathbf{a}^* for intermediate y .

The development of the two order parameters w_l and $\bar{w}_l = \bar{h}_l/y$ is straightforward:

$$\frac{dw_l}{d\alpha} = \frac{\eta^2}{2w_l} \sum_j b_j c_{lj}^2; \quad (4.39)$$

$$\frac{d\bar{w}_l}{d\alpha} = \eta y \sum_j b_j c_{lj} = \eta y \lambda_l^A. \quad (4.40)$$

Interestingly, rule (4.38) implements a “soft” fictitious play rule. This can be seen in the limit $y \rightarrow \infty$, where the stochastic component can be neglected completely. At time t , the strategy i^t with the largest \bar{w}_i^t is played, while the opponent plays j^t ; \bar{w}_l^t at time t can be written as

$$\bar{w}_l^t = \sum_{\tau=0}^t \frac{\eta}{N} y l_{j^t} = \frac{\eta}{N} y \sum_j c_{lj} t \tilde{b}_j = \frac{\eta}{N} y t \tilde{\lambda}_l^A, \quad (4.41)$$

where \tilde{b}_j and $\tilde{\lambda}_l^A$ are analogous to Section 4.4.4. By adjusting the range of y between 0 and ∞ , it is possible to interpolate between random guessing and purely deterministic fictitious play. If y takes intermediate values, there is enough stochasticity to get, at any given time, a mixed strategy that is reasonably close to \mathbf{a}^* ; however, the convergence to \mathbf{a}^* in the long-time average is slower than for larger bias y . This is shown in Fig. 4.7.

Multi-state patterns

The same ideas can be generalized to Q -state input patterns and weight vectors. It will become clear how unequal probabilities of the Q inputs amount to a bias.

As mentioned, each output l now has a set of Q weight vectors \mathbf{w}_l^q with entries w_{ln}^q . The hidden field for output l is

$$h_l = \sum_q \sum_n w_{ln}^q (Q\delta_{\xi_n, q} - 1) = \sum_q h_l^q \text{ with } h_l^q = \mathbf{w}_l^q \cdot \mathbf{x}^q, \quad (4.42)$$

where the \mathbf{x}^q are vectors with components $Q\delta_{\xi_n, q} - 1$. One can then assume that the bias in the pattern is the same for all of its components (this is necessarily the case with time series patterns, since each value is shifted through the entire weight vector) and is thus completely defined by the probabilities of encountering the possible inputs q . We then use the deviations δq from the uniform distribution to describe this distribution:

$$\text{prob}(x_n = q) = \frac{1}{Q}(1 + \delta q). \quad (4.43)$$

Note that $\sum_q \delta q = 0$. We then proceed by splitting \mathbf{x}^q into an average and a random component:

$$\mathbf{y}^q = \begin{pmatrix} \delta q \\ \vdots \\ \delta q \end{pmatrix}; \tilde{\mathbf{x}}^q = \mathbf{x}^q - \mathbf{y}^q. \quad (4.44)$$

The hidden field h_l^q can be split into three parts analogous to the case of real-valued input patterns:

$$h_l^q = \bar{h}_l^q + \bar{w}_l^q h_c^q + \tilde{h}_l^q, \quad (4.45)$$

where $\bar{h}_l^q = \bar{\mathbf{w}}_l^q \cdot \mathbf{y}^q = \bar{w}_l^q y^q$ is the constant part, $h_c^q = \bar{\mathbf{w}}_l^q \cdot \tilde{\mathbf{x}}^q / \bar{w}_l^q$ is a random variable that is the same for all l , and $\tilde{h}_l^q = \tilde{\mathbf{w}}_l^q \cdot \tilde{\mathbf{x}}^q$ is random and different for each l (the \tilde{h}_l^q are uncorrelated if the $\tilde{\mathbf{w}}_i$ are pairwise orthogonal, which I assume for simplicity's sake).

The variance $\langle h_c^{q2} \rangle$ of h_c^q can be calculated in a straightforward manner; the result is

$$\langle h_c^{q2} \rangle = Q(1 - (1 + \delta q)/Q)(1 + \delta q). \quad (4.46)$$

Similarly, the variance of \tilde{h}_l^q is

$$\langle \tilde{h}_l^{q2} \rangle = \tilde{w}_l^{q2} Q(1 - (1 + \delta q)/Q)(1 + \delta q). \quad (4.47)$$

The addition of the fields h^q belonging to different q is almost, but not quite straightforward. The total field can be written like this:

$$h_l = \bar{h}_l + z_l h_{ct} + \tilde{h}_l. \quad (4.48)$$

\bar{h}_l is simply the sum of the constant components $\sum_q \bar{h}_l^q$. The second term is based on the assumption that \bar{w}_l^q is approximately proportional to y^q for all q , with a

coefficient characteristic for l : $\bar{w}_l^q = z_l y^q$. This assumption will be justified later. The sum $\sum_q \bar{w}_l^q h_c^q$ can then be written as $z_l h_{ct}$, where h_{ct} is a Gaussian variable with a variance of $\langle h_{ct}^2 \rangle = \sum_q y^{q2} Q(1 - (1 + \delta q)/Q)(1 + \delta Q)$. Again, h_{ct} is the same for all l .

The components of the strategy vector \mathbf{a} can now be calculated in analogy to Eq. (4.37):

$$a_i = \int_{-\infty}^{\infty} D\hat{h}_i \int_{-\infty}^{\infty} Dh_c \prod_{l \neq i} \Phi \left[\frac{1}{\bar{w}_l} (\tilde{w}_l \hat{h}_i + (y^2 + h_c)(z_i - z_l)) \right]. \quad (4.49)$$

Three questions remain: what is z_l ? What is all this splitting of the hidden fields good for? And what relevance does this have for time-series patterns?

The first question can be answered by a look at the learning rule, which, in analogy to Eqs. (4.35) and (4.38), can be taken as

$$\mathbf{w}_l^{q \ t+1} = \mathbf{w}_l^{q \ t} + \frac{\eta}{M} \mathbf{x}^q c_{lj}, \quad (4.50)$$

where j is the opponent's action at time t . The average update of the weight component parallel to the bias is then

$$\langle \bar{\mathbf{w}}_l^{q \ t+1} \rangle_{\mathbf{x}} = \bar{\mathbf{w}}_l^{q \ t} + \left\langle \frac{\eta}{M} \mathbf{y}^q c_{lj} \right\rangle_j. \quad (4.51)$$

The order parameter \bar{w}_l^q then follows the differential equation

$$\frac{d\bar{w}_l^q}{d\alpha} = \eta y^q \sum_j b_j c_{lj} = \eta y^q \lambda_l^A \quad \text{for all } q, \quad (4.52)$$

which can be solved:

$$\bar{w}_l^q = \bar{w}_{l_0}^q + y^q \left(\eta \int_0^\alpha \lambda_l^A(\tau) d\tau \right). \quad (4.53)$$

Neglecting the initial weight $\bar{w}_{l_0}^q$, the characteristic quantities z_l are therefore proportional to the average payoffs of option l , integrated from the beginning of the game.

Regarding the second question, what is this good for? Eq. (4.49) states the following: The bias in the pattern creates a strong preference for those options that have accumulated higher z_l , i.e., higher expected payoffs in the course of the game. This preference can be overruled by either a fluctuation in the pattern (if the total pattern $\mathbf{x} = \tilde{\mathbf{x}} + \mathbf{y}$ has a negative overlap with the bias \mathbf{y} , the bias accumulated in the weights works in the opposite direction) or by the contribution from the weight and pattern perpendicular to the bias. For sufficiently large bias, either case becomes unlikely, and the learning process again reduces to Fictitious Play.

As for time-series patterns, the relevance is this: if the strategy played by the opponent has a significant bias (for example, if the opponent is playing \mathbf{b}^* , where roughly half of the options do not appear at all), some of the δq are of order 1. Since the norm of the bias vectors is $y^q = \sqrt{M}|\delta q|$, that means that there is indeed a strong bias (of order \sqrt{M} rather than 1), and nothing significantly different from Fictitious play can be expected – if the opponent’s output is properly randomized. If two networks with equivalent architecture use each other’s outputs as input patterns, both lock into short cycles for many repetitions, never coming close to anything like equilibrium.

4.6 Summary

The scenarios presented in this chapter have shown that a slightly modified Winner-Takes-All Perceptron with a learning algorithm inspired by the Confused Bit Generator can be used to learn a good strategy in zero-sum games: it concentrates on the optimal pure strategy if there is one, and finds a good mixed strategy even against adaptive opponents. The ingredients for success are a drift term which strengthens options whose payoff is better than the current one, and weakens the others, and a noise term which gradually increases the norms of the weight vectors, decreasing the impact that a single learning step has.

This learning algorithm can be expected to converge to Nash equilibrium in the limit of infinitely slow adaption ($M \rightarrow \infty$) and infinite learning times ($\alpha \rightarrow \infty$), and gives a reasonable approximation of equilibrium for finite M and α . It is not “rational” – on the other hand, it generates a truly mixed strategy, as opposed to algorithms like Fictitious Play, which generate mixed strategies only in the long-time average.

Finding the equilibrium mixed strategy \mathbf{a}^* in a zero-sum game is a nontrivial problem of stochastic optimization: the “energy landscape” becomes increasingly flat as one’s opponent comes closer to his equilibrium strategy \mathbf{b}^* ; however, only then is \mathbf{a}^* the best response. Considering this difficulty, the success of the presented learning algorithm is a pleasant surprise, even if learning is slow.

A different learning algorithm is required if there is a bias in the patterns. This bias leads to a bias in the weight vectors, and the combination of these causes a bias in the hidden fields of the neural network. This can be exploited: it is now the overlap of the weight vector with the bias in the patterns, rather than the norm of the weight vector, which gives the preference for one or the other option. Depending on the strength of the bias, one gets pure guessing in the limit of small bias, fictitious play in the limit of infinite bias, and “soft” fictitious play in intermediate regimes.

So far, no scenario has been found where the neural network could explicitly make use of any actual information encoded in the patterns. If time series of the opponent’s output are used for patterns, and both players use networks, they lock

into short cycles. More work is necessary to decide whether this is a systematic problem of the used network architecture, and whether it can be remedied with a different learning algorithm.

Chapter 5

Conclusion and outlook

The projects presented in this dissertation tried to make some connections between the fields named in its title: neural networks, game theory, and time series generation. Neural networks played games, time series were generated by games, networks learned and generated time series, etc.. The concept that connects these fields is that of prediction: neural networks can be used as prediction algorithms, time series generation and prediction are so closely related that they are almost interchangeable, and, last but not least, economic game theory deals with the attempt to predict an opponent's actions as accurately as possible and not allow him to predict and outplay oneself.

The aim of Chap. 2 was to study the properties of time series that are antipredictable for three selected prediction algorithms, and to find common aspects between them, such as a tendency towards longer cycles than for perfectly predictable series, and a suppression of the features that the algorithm is sensitive to.

Chap. 3 gave an overview over some of the variations of the Minority Game, some of which were introduced first by our research group. It was demonstrated that this game naturally gives rise to antipredictability in the time series of minority decision if agents try to adapt rapidly. I also demonstrated that, with minor adaptations, all conventional strategies can also be generalized to more than two options.

In Chap. 4, a neural network tried to find a suitable strategy for a zero-sum game by learning from experience. A learning algorithm was found that uses random input patterns to generate a mixed strategy that can come close to the equilibrium strategy. This algorithm probably can still be optimized by a more systematic analysis what information can be extracted from watching the opponent's play. However, it is not yet obvious under what circumstances a learning algorithm should play a mixed strategy at all.

By its conception, this work is interdisciplinary, and a reader with a background in physics may have wondered, "Is this physics?". The answer, depending on one's point of view, is no, yes, yes, and maybe.

This dissertation does not deal with the classical subjects of physics, namely, the properties of inanimate matter. In that sense, it is not physics.

A different definition might be, “physics is what physicists do”. In that sense, it is physics: all of the co-workers who collaborated on the various projects were trained as physicists, as are the majority of scientists who have published on the statistical properties of neural networks and on the Minority Game.

The third answer concerns the methods: most of the methods used to achieve results in this work, like averaging over disorder in online learning, the application of Markov chains in the stochastic MG, the analysis of the nonlinear properties of the CSG, and the extensive use of Monte Carlo simulations to check analytical results (or replace them where they are not available), are well-rooted in statistical physics and nonlinear dynamics.

The fourth answer should really be, “who cares, as long as it is interesting?” If methods from one field can help to get insights in other fields, they should be applied, no matter how the result has to be classified.

I hope that this work has shed some light on the problems it treated from unusual angles. What must be kept in mind is that all models presented here are toy problems that may or may not have a strong tie to real life. Many of these toy problems develop a life of their own, intriguing researchers with mathematical subtleties and technical challenges. I have tried to avoid this tendency by presenting and comparing several algorithms and strategies and finding global aspects that connect them.

What remains to be done is to establish which of these models has what relevance to “real life”, i.e., the behavior of humans, or animals, or other entity: what strategies do stock brokers, car drivers, predatory animals use when they make their decisions in Minority Game-like settings? How do humans adapt their strategy in games? This will necessarily require much know-how on sociology, ecology or psychology and much experimental work, such as that begin in Ref. [100]. It may thus not be the answer that a theoretical physicist is well-equipped to answer.

Appendix A

Notation

In a work that deals with a rather large number of projects, concepts and mathematical objects, a certain overloading of symbols like α , λ and N is inevitable. This chart might be helpful to find out what meaning a given symbol has in each chapter.

A, B	players in a zero-sum game
\mathbf{a}, \mathbf{b}	strategy vectors of players A and B
$\mathbf{a}^*, \mathbf{b}^*$	optimal (Nash-equilibrium) strategies
C	Chap. 2: autocorrelation function; Chap. 4: norm of center-of-mass of perceptrons.
\mathcal{C}	Chap. 3: correlation matrix for multi-choice perceptron; Chap. 4: payoff matrix.
h	hidden fields of neural networks.
H	Chap. 2: energy in the Bernasconi Model; Chap. 3: information generated in the standard MG.
K	Sec. 3.6: state of the stochastic MG;
K, L	Chap. 4: number of options available to A and B;
l	Chap. 2: cycle length.
M	memory length of prediction algorithm.
\mathbf{M}	Sec. 2.3.5: Jacobi matrix of the CSG; Sec. 2.4.4: transition probabilities on DeBruijn graph.
N	Chap. 2: number of nodes in a graph; Chap. 3: number of players in the MG.
p	Sec. 3.6: probability of changing sides.
p_{AP}	antipersistence parameter (see Sec. 2.4.5)
p_h, P_h	Sec. 2.4.2: probability of hitting a cycle.
Q	number of options in multi-choice MG; number of different inputs/outputs in multi-choice perceptrons
\mathbf{r}	Sec. 3.4: relative vectors.
R	Sec. 3.4, 3.7.2: overlap of weight vectors;

	Sec. 3.7.4: self-overlap of strategy vector;
	Chap. 4: normalized overlap between \mathbf{a} and \mathbf{a}^* .
s	Sec. 2.4.5: success rate of prediction algorithm;
S	Sec. 2.3.2: r.m.s. output of the CSG.
	Chap. 3: decision of the minority.
\mathbf{w}^t	parameters of a prediction algorithm at time t . specifically: weight vector of a perceptron.
\mathbf{W}, W	Sec. 3.6: transition matrix/ kernel.
x	Sec. 3.6: proportionality constant $p = 2x/N$.
x^t	value of a time series.
\mathbf{x}^t	vector with components $x^{t-M-1}, \dots, x^{t-1}$.
α	neural networks: rescaled learning time: $\alpha = t/M$. Bernasconi problem: ratio p/M between length of sequence and memory; standard MG: ratio p/N between length of decision table. and number of players.
β	amplification of continuous perceptron.
γ	rescaled amplification $\beta\eta$ of continuous perceptron.
η	learning rate.
λ	Chap. 2: Lyapunov exponents of the CSG; Chap. 4: expected payoff.
$\boldsymbol{\pi}, \pi$	Sec. 3.6: state vector/ function.

Bibliography

- [1] W.S. McCulloch and W. Pitts. A logical calculus of ideas immanent in nervous activity. *Bulletin of Mathematical Biophysics*, 5:115–133, 1943.
- [2] Marvin Minsky and Seymour Papert. *Perceptrons: An introduction to Computational Geometry*. MIT Press, Cambridge, MA, 1969.
- [3] J. Hertz, A. Krogh, and R.G. Palmer. *Introduction to the Theory of Neural Computation*. Addison-Wesley, Redwood City, 1991.
- [4] Peter Riegler. Dynamics of on-line learning in neural networks. Dissertation, Universität Würzburg, 1997.
- [5] A. L. Hodgkin and A. F. Huxley. A quantitative description of membrane currents and its application to conduction and excitation in nerve. *J. Physiol. (London)*, 117:500–544, 1952.
- [6] H. C. Tuckwell. *Introduction to Theoretical Neurobiology*. Cambridge University Press, Cambridge, UK, 1988.
- [7] J.J. Hopfield and C.D. Brody. What is a moment? “Cortical” sensory integration over a brief interval. *PNAS*, 97:13919–13924, 2000.
- [8] J.J. Hopfield and C.D. Brody. What is a moment? Transient synchrony as a collective mechanism for spatiotemporal integration. *PNAS*, 98:1283–1287, 2001.
- [9] Andreas S. Weigend and Neil A Gershenfeld, editors. *Time Series Prediction*, Reading, Mass., 1992. Addison-Wesley.
- [10] Ansgar Freking, Wolfgang Kinzel, and Ido Kanter. Learning and predicting time series by neural networks. [cond-mat/0202537](https://arxiv.org/abs/cond-mat/0202537), 2002.
- [11] Huaiyu Zhu and Wolfgang Kinzel. Anti-predictable sequences: Harder to predict than a random sequence. *Neural Computation*, 10:2219–2230, 1998.
- [12] John von Neumann and Oskar Morgenstern. *Theory of Games and Economic Behaviour*. Princeton University Press, Princeton, N.J., 1944.

- [13] Minority game homepage (with extensive bibliography). <http://www.unifr.ch/econophysics/minority>.
- [14] Rainer Schlittgen and Bernd H. J. Streitberg. *Zeitreihenanalyse*. R. Oldenbourg Verlag, München, 1994.
- [15] Dean P. Foster and H. Peyton Young. On the impossibility of predicting the behaviour of rational agents. *Proc. Nat. Acad. Sciences*, 98:12848–12853, 2001.
- [16] Luca Gammaitoni, Peter Hänggi, Peter Jung, and Fabio Marchesoni. Stochastic resonance. *Rev. Mod. Phys.*, 70:223–288, 1998.
- [17] T. Sauer, J. A. Yorke, and M. Casdagli. Embedology. *J. Stat. Phys.*, 65:579–616, 1991.
- [18] T.L.H. Watkin, A. Rau, and M. Biehl. The statistical mechanics of learning a rule. *Rev. Mod. Phys.*, 65:499, 1993.
- [19] Michael Biehl and Peter Riegler. On-line learning with a perceptron. *Europhys. Lett.*, 28:525, 1994.
- [20] Richard Metzler, Wolfgang Kinzel, Liat Ein-Dor, and Ido Kanter. Generation of unpredictable time series by a neural network. *Phys. Rev. E*, 63(5):056126, 2001.
- [21] Richard Metzler. Online-Lernen wechselwirkender neuronaler Netze. Diplomarbeit, Universität Würzburg, 1999.
- [22] Richard Metzler. Antipersistent binary time series. *J. Phys. A*, 35:721–730, 2002.
- [23] Avner Priel and Ido Kanter. Long-term properties of time series generated by a perceptron with various transfer functions. *Phys. Rev. E*, 59(3):3368–3375, 1999.
- [24] E. Eisenstein, I. Kanter, D.A. Kessler, and W. Kinzel. Generation and prediction of time series by a neural network. *Phys. Rev. Letters*, 74(1):6–9, 1995.
- [25] M. Schröder. *Learning, Generation and Generalisation of Time Series with a Perceptron*. Dissertation, Universität Würzburg, 1998.
- [26] M. Schröder and W. Kinzel. Limit cycles of a perceptron. *J. Phys. A*, 31:9131–9147, 1998.
- [27] O. Kinouchi and N. Caticha. Optimal generalization in perceptrons. *J. Phys. A*, 25:6243–6250, 1992.

- [28] J. K. Anlauf and M. Biehl. The AdaTron: An adaptive perceptron algorithm. *Europhys. Lett.*, 10:687, 1989.
- [29] Peter Riegler. Verallgemeinern in neuronalen Netzen beim Einschnitt-Lernen. Diplomarbeit, Universität Würzburg, 1994.
- [30] Inés Samengo and Damián H. Zanette. Competing neural networks: Finding a strategy for the game of matching pennies. *Phys. Rev. E*, 62:4049, 2000.
- [31] David Saad, editor. *On-line Learning in Neural Networks*. Cambridge University Press, Cambridge, 1998.
- [32] M.R. Schroeder. *Number Theory in Science and Communication*. Springer-Verlag, Berlin, 1984.
- [33] J. Bernasconi. Low autocorrelation binary sequences: statistical mechanics and configuration space analysis. *J. Physique*, 48:559–567, 1987.
- [34] Stephan Mertens and Christine Bessenrodt. On the ground states of the Bernasconi model. *J.Phys. A*, 31:3731–3749, 1998.
- [35] M. J. E. Golay. The Merit Factor of long low autocorrelation binary sequences. *IEEE Trans. Inform. Theory*, IT-28:543, 1982.
- [36] Liat Ein-Dor, Ido Kanter, and Wolfgang Kinzel. Low autocorrelated multi-phase sequences. [cond-mat/0103185](https://arxiv.org/abs/cond-mat/0103185), 2001.
- [37] C. de Groot, D. Würtz, and K. H. Hoffmann. Low autocorrelation binary sequences: Exact enumeration and optimization by evolutionary strategies. *Optimization*, 23:369–384, 1992.
- [38] Stephan Mertens. Exhaustive search for low-autocorrelation binary sequences. *J. Phys. A*, 29:L473–L481, 1996.
- [39] G. Reents and R. Urbanczik. Self-Averaging and On-Line Learning. *Phys. Rev. Lett.*, 80(24):5445–5448, 1998.
- [40] <http://itp.nat.uni-magdeburg.de/~mertens/bernasconi/cyclic.shtml>.
- [41] Jorge Kurchan. Elementary constraints on autocorrelation function scalings. *Phys. Rev. E*, 66:017101, 2002.
- [42] I. Kanter, D.A. Kessler, A. Priel, and E. Eisenstein. Analytical study of time series generation by feed-forward networks. *Phys. Rev. Lett.*, 75(13):2614–2617, 1995.

- [43] A. Priel, I. Kanter, and D.A. Kessler. Noisy time series generation by feed-forward networks. *J. Phys. A*, 31:1189–1209, 1998.
- [44] Edward Ott. *Chaos in Dynamical Systems*. Cambridge University Press, Cambridge, 1993.
- [45] Gerhard Berendt and Evelyn Weimar-Woods. *Mathematik für Physiker*. VCH Verlagsgesellschaft, Weinheim, 1990.
- [46] Lui Lam, editor. *Introduction to Nonlinear Physics*. Springer, New York, 1997.
- [47] Alan Wolf, Jack B. Swift, Harry L. Swinney, and John A. Vastano. Determining Lyapunov exponents from a time series. *Physica D*, 16:285–317, 1985.
- [48] J. Kaplan and J. Yorke. *Functional Differential Equations and Approximations of Fixed Points*, page 204. Springer, Heidelberg - New York, 1979.
- [49] Harold Fredricksen. A survey of full length nonlinear shift register cycle algorithms. *SIAM Review*, 24(2):195–221, 1982.
- [50] C. Flye Sainte-Marie. 48. *L'Intermediaire des mathematiciens*, 1:107–110, 1894.
- [51] D. Challet and M. Marsili. Phase transition and symmetry breaking in the minority game. *Phys. Rev. E*, 60(6A):R6271–R6274, 1999.
- [52] Holger Kantz and Thomas Schreiber. *Nonlinear time series analysis*. Cambridge University Press, Cambridge, UK, 1997.
- [53] W. Feller. *An Introduction to Probability Theory and its Applications*, volume 1. John Wiley & Sons, New York, 1970.
- [54] Wolfgang Weidlich. *Sociodynamics: A Systematic Approach to Mathematical Modelling in the Social Sciences*. Harwood Academic Publishers, New York, 2000.
- [55] Yaneer Bar-Yam. *Dynamics of Complex Systems*. Perseus Publishing, Cambridge, MA, 1997.
- [56] J. D. Farmer. Physicists attempt to scale the ivory tower of finance. adap-org/9912002, 1999.
- [57] W. B. Arthur. Inductive reasoning and bounded rationality. *Am. Econ. Assoc. Papers and Proc*, 84:406, 1994.

- [58] M. Hart, P. Jefferies, N.F. Johnson, and P.M. Hui. Crowd-anticrowd model of the Minority Game. cond-mat/0003486, 2000.
- [59] Andrea Cavagna. Irrelevance of memory in the minority game. *Phys. Rev. E*, 59:R3783, 1999.
- [60] D. Challet and Y.-C. Zhang. Emergence of cooperation and organization in an evolutionary game. *Physica A*, 246:407, 1997.
- [61] Damien Challet and Yi-Cheng Zhang. On the minority game: Analytical and numerical studies. *Physica A*, 256:514–532, 1998.
- [62] D. Challet, M. Marsili, and R. Zecchina. Statistical mechanics of systems with heterogeneous agents: Minority games. *Phys. Rev. Lett.*, 84(8):1824–1827, 2000.
- [63] Juan P. Garrahan, Esteban Moro, and David Sherrington. Continuous time dynamics of the Thermal Minority Game. *Phys. Rev. E*, 62:7670, 2000.
- [64] J.A.F. Heimerl and A.C.C. Coolen. Generating functional analysis of the dynamics of the Minority Game with random external information. *Phys. Rev. E*, 63:056121, 2001.
- [65] W. Kinzel, R. Metzler, and I. Kanter. Dynamics of interacting neural networks. *J. Phys. A*, 33:L141–L147, 2000.
- [66] R. Metzler, W. Kinzel, and I. Kanter. Interacting neural networks. *Phys. Rev. E*, 62(2):2555, 2000.
- [67] H. Schwarze and J. Hertz. Generalization in a large committee machine. *Europhys.Lett.*, 20:375–380, 1992.
- [68] A. Engel, H. M. Köhler, F. Tschepe, H. Vollmayr, and A. Zippelius. Storage capacity and learning algorithms for two-layer neural networks. *Phys. Rev. A*, 45:7590–7609, 1992.
- [69] N.G. van Kampen. *Stochastic Processes in Physics and Chemistry*. Elsevier Science B.V., Amsterdam, 1992.
- [70] N. F. Johnson, P. M. Hui., R. Jonson, and T. S. Lo. Self-organized segregation within an evolving population. *Phys. Rev. Lett.*, 82(16):3360, 1999.
- [71] E. Burgos and Horacio Ceva. Self organization in a minority game: the role of memory and a probabilistic approach. cond-mat/0003179, 2000.
- [72] T. S. Lo, P. M. Hui, and N. F. Johnson. Theory of the evolutionary minority game. *Phys. Rev. E*, 62:4393, 2000.

- [73] Christian Horn. Strategien für das Minoritätsspiel. Diplomarbeit, Universität Würzburg, 2001.
- [74] Ehud Nakar and Shahar Hod. Semianalytical approach to the evolutionary minority game. cond-mat/0206056, 2002.
- [75] G. Reents, R. Metzler, and W. Kinzel. A stochastic strategy for the minority game. *Physica A*, 299:253–261, 2001.
- [76] Felix R. Gantmacher. *Application of the Theory of Matrices*. Interscience Publ., New York, 1959.
- [77] John Maynard-Smith. *Evolution and the Theory of Games*. Cambridge University Press, Cambridge, 1982.
- [78] Liat Ein-Dor, Richard Metzler, Ido Kanter, and Wolfgang Kinzel. Multi-choice minority game. *Phys. Rev. E*, 63:066103, 2001.
- [79] Kerson Huang. *Statistical Mechanics*. John Wiley & Sons, New York, 1987.
- [80] F. Y. Wu. The Potts model. *Rev. Mod. Phys.*, 54(1):235–268, 1982.
- [81] Timothy L. H. Watkin, Albrecht Rau, Desiré Bollé, and Jort van Mourik. Learning multi-class classification problems. *J. Phys. I France*, 2:167–180, 1992.
- [82] F. K. Chow and H. F. Chau. Multiple choice minority game. cond-mat/0109166, 2002.
- [83] D. Challet, M. Marsili, and Y.-C. Zhang. Stylized facts of financial markets in minority games. *Physica A*, 294:514, 2001.
- [84] P. Jefferies, M.L. Hart, P.M. Hui, and N.F. Johnson. From market games to real-world markets. cond-mat/0008387, 2000.
- [85] Jakob Bernoulli. *Wahrscheinlichkeitsrechnung (Ars conjectandi)*. Harry Deutsch Verlag, Thun und Frankfurt am Main, 1999. original: 1713, Basel.
- [86] Gerd Girenzer, Zeno Swijrink, Theodore Porter, Lorraine Daston, John Beatty, and Lorenz Krüger. *The Empire of Chance*. Cambridge University Press, Cambridge, UK, 1989.
- [87] Edwyn R. Berlekamp, John H. Conway, and Richard K. Guy. *Winning Ways*. Academic Press, London, 1982.
- [88] Eric D. Demaine. Playing games with algorithms: Algorithmic combinatorial game theory. arXiv:cs.CC/0106019, 2001.

- [89] Daniel King. *Wie man im Schach gewinnt. 10 goldene Regeln.* J. Beyer Verlag, Hollfeld, 1998.
- [90] Richard Metzler and Andreas Engel. Jamming transitions and avalanches in the game of Dots-and-Boxes. *Phys. Rev. E*, 65:066108, 2002.
- [91] Wang Jianhua. *The Theory of Games.* Clarendon Press, Oxford, 1988.
- [92] William Poundstone. *Prisoner's Dilemma.* Oxford University Press, Oxford, 1992.
- [93] Robert Axelrod. *The Evolution of Cooperation.* Basic Books, New York, 1984.
- [94] Wolfgang Kinzel and Georg Reents. *Physics by Computer.* Springer Verlag, Berlin, 1998.
- [95] William H. Press, Saul A. Teukolsky, William T. Vetterling, and Brian P. Flannery. *Numerical Recipes in C.* Cambridge University Press, Cambridge, 1988.
- [96] Drew Fudenberg and David K. Levine. *The theory of learning in games.* MIT Press, Cambridge (MA), London, 1998.
- [97] J. Berg and A. Engel. Matrix games, mixed strategies and statistical mechanics. *Phys. Rev. Lett.*, 81:4999–5002, 1998.
- [98] J. Berg. Statistical mechanics of random two-player games. *Phys. Rev. E*, 61:2327, 2000.
- [99] Johannes Berg. Statistical mechanics of random games. Dissertation, Uni Magdeburg, 1999.
- [100] Peter Ruch, Joseph Wakeling, and Yi-Cheng Zhang. The interactive minority game: Instructions for experts. cond-mat/0208310, 2002.

Acknowledgment

At this point, I wish to express my gratitude to the people and institutions who contributed to this work directly or indirectly. I will start with the Chair for Computational Physics in Würzburg.

First of all, I want to thank my supervisor, Prof. Wolfgang Kinzel, for the ideas and concepts that got this project started, and for his supportive supervision. Special thanks also go to Georg Reents and Christian Horn for the collaboration on the stochastic Minority Game, and to Christoph Bunzmann and Michael Biehl for helpful advice on various problems. Constructive work would have been impossible without the system administrators, especially Ansgar Freking, Andreas Klein, and Alexander Wagner, and the secretaries Uschi Eitelwein, Brigitte Wehner, and Christine Schmeisser.

The second group that contributed greatly to this work is that of Prof. Andreas Engel at the university of Magdeburg, and his students and post-docs Johannes Berg and Stephan Mertens. There, I learned about the basics of game theory and replica calculations and got valuable ideas and constructive criticism.

I am also grateful to Prof. Ido Kanter of Bar-Ilan University, Ramat Gan, Israel, and his students Avner Priel, Liat Ein-Dor, Michal Rosen-Zwi and Hanan Rosemarin for countless ideas and inspirations and for the collaboration on the multi-choice Minority Game. I greatly enjoyed the stays in Israel that Prof. Kanter invited me to.

I acknowledge financial support by the German-Israeli Foundation for Scientific Research and Development (GIF). My graduate student position was financed by the GIF grant No. I-521-8.14/1997.

Last but not least, I wish to thank my dear friend Monika, my parents, my friends, the Phachschaft Physik, the Judo section of the DJK Würzburg, the Weltenwanderer Würzburg e.V., and everyone else who made my private life more pleasant in the last years.

